

**METAPOPULATION THEORY**  
**IN PRACTICE**

---

A thesis  
submitted in partial fulfilment  
of the requirements for the Degree of  
Doctor of Philosophy  
at  
Lincoln University

by  
**J. M. Kean**

---

Lincoln University  
1999



Abstract of a thesis submitted in partial fulfilment of the  
requirements for the Degree of Ph.D.

## **METAPOPULATION THEORY IN PRACTICE**

by J. M. Kean

A metapopulation is defined as a set of potential local populations among which dispersal may occur. Metapopulation theory has grown rapidly in recent years, but much has focused on the mathematical properties of metapopulations rather than their relevance to real systems. Indeed, barring some notable exceptions, metapopulation theory remains largely untested in the field. This thesis investigates the importance of metapopulation structure in the ‘real world’, firstly by building additional realism into metapopulation models, and secondly through a 3-year field study of a real metapopulation system.

The modelling analyses include discrete- and continuous-time models, and cover single species, host-parasitoid, and disease-host systems, with and without stochasticity. In all cases, metapopulation structure enhanced species persistence in time, and often allowed long-term continuance of otherwise non-persistent interactions. Spatial heterogeneity and patterning was evident whenever local populations were stochastic or deterministically unstable in isolation. In metapopulations, the latter case often gave rise to self-organising spatial patterns. These were composed of spiral wave fronts (or ‘arcs of infection’ in disease models) of different sizes, and were related to the stability characteristics of local populations as well as the dispersal rates.

There was no evidence for self-organising spatial patterns in the host-parasitoid system studied in the field (the weevil *Sitona discoideus* and its braconid parasitoid *Microctonus aethiopoidea*), and a new model for the interaction suggested that this is probably due to the strong host density-dependence and stabilising parasitism acting on local populations. Dispersal may be important because of very high mortality in dispersing weevils, which may be related to the scarcity of their host plant in the

landscape. If this is the case, the model suggested that local weevil density may be sensitive to the area of crop grown.

Stochastic models showed that species in suitably large metapopulations may persist for very long times at relatively low overall density and with very low incidence of density-dependence. This suggests that metapopulation processes may explain a general inability to detect density-dependence in many real populations, and may also play an important part in the persistence of rare species. For host-parasitoid metapopulation models, persistence often depended on the way in which they were initialised. Initial conditions corresponding to a biological control release were the least likely to persist, and the maximum host suppression observed in this case was 84%, as compared with 60% for the corresponding non-spatial models and >90% often observed in the field.

Metapopulation structure also allowed persistence of ‘boom-bust’ disease models, although the dynamics of these were particularly dependent on assumptions about what happens to disease classes at very low densities. Models assuming infinitely divisible units of density, models incorporating a non-zero extinction threshold, and individual-based models all gave differing results in terms of disease persistence and rate of spatial spread.

Fitting models to overall metapopulation dynamics often gave misleading results in terms of underlying local dynamics, emphasising the need to sample real populations at an appropriate scale when seeking to understand their behaviour.

**Keywords:** metapopulations, models, host, parasitoid, disease, pest management, biological control, *Sitona discoideus*, *Microctonus aethiopoidea*.

# Table of Contents

<b>Abstract .....</b>	<b>ii</b>
<b>Table of Contents.....</b>	<b>iv</b>
<b>List of Figures .....</b>	<b>viii</b>
<b>List of Tables.....</b>	<b>x</b>
<b>1. Introduction .....</b>	<b>1</b>
<b>1.1 The metapopulation paradigm .....</b>	<b>1</b>
1.1.1 Population regulation and the birth of the ‘metapopulation’.....	1
1.1.2 Classical metapopulations and conservation biology.....	3
1.1.3 Metapopulations in pest management .....	3
1.1.4 Metapopulations, persistence, and stability.....	4
<b>1.2 Modelling metapopulations.....</b>	<b>6</b>
1.2.1 Models with implicit local dynamics .....	6
1.2.2 Models with explicit local dynamics.....	8
<b>1.3 Nature and scope of this investigation .....</b>	<b>9</b>
<b>2. The effects of density-dependence and local dispersal in individual-based stochastic metapopulations.....</b>	<b>12</b>
<b>2.1 Introduction.....</b>	<b>12</b>
<b>2.2 Model .....</b>	<b>13</b>
2.2.1 Stochastic local dynamics.....	13
2.2.2 Metapopulation structure.....	15
2.2.3 Model application.....	15
<b>2.3 Results.....</b>	<b>18</b>
2.3.1 Density-independent metapopulations .....	18
2.3.2 Density-dependent metapopulations.....	24
<b>2.4 Discussion .....</b>	<b>27</b>
<b>2.5 Summary.....</b>	<b>31</b>

<b>3. Can host-parasitoid metapopulations explain successful biological control? .....</b>	<b>33</b>
<b>3.1 Introduction.....</b>	<b>33</b>
<b>3.2 Models and methodology .....</b>	<b>34</b>
3.2.1 General host-parasitoid models .....	34
3.2.2 Parasitism functional forms .....	36
3.2.3 Host density-dependence .....	37
3.2.4 Parameter values.....	38
3.2.5 Metapopulation structure.....	39
3.2.6 Initial conditions .....	39
<b>3.3 Results from non-spatial models .....</b>	<b>40</b>
3.3.1 Relationship between parasitism and host suppression.....	40
3.3.2 Stability and host suppression .....	42
<b>3.4 Results from metapopulation models.....</b>	<b>44</b>
3.4.1 Spatial heterogeneity and patterning .....	44
3.4.2 Initialisation and transient behaviour .....	46
3.4.3 Host suppression.....	47
3.4.4 Metapopulation mean dynamics.....	50
3.4.5 Emergent subpopulation dynamics.....	52
<b>3.5 Discussion .....</b>	<b>54</b>
<b>3.6 Summary.....</b>	<b>58</b>
<b>4. Field study of a host-parasitoid metapopulation: <i>Sitona discoideus</i> and <i>Microctonus aethiopoidea</i> .....</b>	<b>59</b>
<b>4.1 Introduction.....</b>	<b>59</b>
<b>4.2 Methods .....</b>	<b>60</b>
4.2.1 Field assessment of <i>S. discoideus</i> biological control.....	60
4.2.2 Estimation of $CV^2$ of parasitism.....	61
4.2.3 Estimating the scale of homogeneity.....	61
4.2.4 Test of a non-spatial model .....	62
<b>4.3 Results .....</b>	<b>62</b>
<b>4.4 Discussion .....</b>	<b>68</b>

4.5 Summary.....	70
<b>5. A spatial model for the successful biological control of <i>Sitona discoideus</i> by <i>Microctonus aethiopoides</i> .....</b>	<b>72</b>
5.1 Introduction.....	72
5.2 Methods .....	74
5.2.1 Non-spatial model .....	74
5.2.2 Metapopulation model.....	75
5.2.3 Australian variant .....	80
5.3 Results.....	80
5.3.1 Model results .....	80
5.3.2 Sensitivity to parameter values.....	81
5.3.3 Effect of crop density on dispersal survival .....	86
5.4 Discussion .....	86
5.5 Summary.....	89
<b>6. Disease metapopulation dynamics in continuous time .....</b>	<b>90</b>
6.1 Introduction.....	90
6.2 Models.....	91
6.2.1 SIR model.....	91
6.2.2 SEI model .....	93
6.2.3 Metapopulation formulations .....	94
6.3 Results.....	96
6.3.1 Model behaviour and spatial patterning .....	96
6.3.2 Effect of space on disease persistence.....	98
6.3.3 Effects of assumptions about very low densities.....	100
6.4 Discussion .....	104
6.5 Summary.....	107
<b>7. Conclusions .....</b>	<b>109</b>
7.1 Metapopulation structure promotes persistence.....	109
7.2 Sometimes you don't need to know dynamics in space in order to understand and predict dynamics in time .....	110

7.3 Do self-organised spatial patterns occur in natural metapopulations? .	111
7.4 Metapopulation processes have not been important for the control of <i>Sitona discoideus</i> by <i>Microctonus aethiopoulos</i> .....	112
7.5 Directions for further research.....	113
<b>Acknowledgements .....</b>	<b>109</b>
<b>References.....</b>	<b>116</b>
<b>Appendices .....</b>	<b>134</b>
<b>Appendix 1: Glossary of terms.....</b>	<b>134</b>
<b>Appendix 2: List of symbols used .....</b>	<b>137</b>
A2.1 General symbols used throughout the thesis .....	137
A2.2 Statistical and mathematical abbreviations .....	138
A2.3 Additional symbols used in <i>Sitona discoideus</i> models and analysis .	138
A2.4 Other symbols used .....	139
<b>Appendix 3: Effects of dispersal on local dynamics .....</b>	<b>141</b>
<b>Appendix 4: Supporting material .....</b>	<b>147</b>
A4.1 Derivation of general host-parasitoid models.....	147
A4.2 Derivation of default host-parasitoid model parameter values.....	148
A4.3 Derivation of the proportion of hosts parasitised at equilibrium.....	148
A4.4 Relationships between parasitism and host suppression at equilibrium .....	149
A4.5 Host-parasitoid models with Ricker host density-dependence and random parasitoid attack.....	150
A4.6 $CV^2$ in host-parasitoid metapopulations.....	150
A4.7 Results from fitting models to metapopulation mean dynamics .....	151
A4.8 Results from fitting models to emergent subpopulation dynamics ...	153
A4.9 Derivation of <i>Sitona discoideus</i> model parameters .....	156
A4.10 Derivation of dispersal radius for the <i>Sitona discoideus</i> model .....	157
A4.11 Derivation of disease basic reproductive rate, $R_0$ .....	158
A4.12 Derivation of disease intrinsic rate of increase, $r_d$ .....	158

## List of Figures

<b>Figure 1.1</b> A classification of metapopulation model types .....	6
<b>Figure 2.1</b> Different dispersal neighbourhoods around a source population.....	16
<b>Figure 2.2</b> Demonstration of different lattice boundary conditions .....	16
<b>Figure 2.3</b> Sample trajectories from random-walk metapopulations .....	19
<b>Figure 2.4</b> Snapshots of the metapopulations plotted in figure 2.3(a) .....	20
<b>Figure 2.5</b> Behaviour of density-independent metapopulation in terms of basic model parameters.....	21
<b>Figure 2.6</b> The effect of lattice size on persistence time .....	23
<b>Figure 2.7</b> Snapshots of the metapopulations plotted in figure 2.3(b) .....	26
<b>Figure 2.8</b> The effect of lattice size on the incidence of local density-dependence ..	26
<b>Figure 2.9</b> Mean dynamics of a perturbed density-dependent metapopulation.....	27
<b>Figure 3.1</b> A general insect host life cycle. ....	35
<b>Figure 3.2</b> Relationship between equilibrium proportion parasitised and the proportional reduction in host density for a non-spatial host-parasitoid model ....	41
<b>Figure 3.3</b> Stability and host suppression in non-spatial host-parasitoid models ....	43
<b>Figure 3.4</b> Persistence and host reduction in host-parasitoid metapopulations.....	48
<b>Figure 3.5</b> An example of high host suppression in a metapopulation model .....	49
<b>Figure 3.6</b> Metapopulation trajectories under different spatial patterns.....	51
<b>Figure 3.7</b> Local population trajectories under different spatial patterns.....	53
<b>Figure 4.1</b> Relationship between autumn weevil density and percent parasitism.....	65
<b>Figure 4.2</b> Relationship between longitude and autumn weevil density.....	67
<b>Figure 4.3</b> Goodness-of-fit of regressions relating mean weevil density within some radius to local density in the following autumn .....	67

<b>Figure 4.4</b> Model predictions and actual values for autumn weevil density and percent parasitism at Darfield.....	68
<b>Figure 5.1</b> Annual life cycle of <i>Sitona discoideus</i> and <i>Microctonus aethiopoides</i> ...	73
<b>Figure 5.2</b> Relationship between parasitised weevils in March and percent parasitism in the following May .....	79
<b>Figure 5.3</b> Autumn weevil densities and parasitism levels, as predicted by new and old non-spatial models, and as observed at Darfield.....	82
<b>Figure 5.4</b> Metapopulation model predictions for autumn weevil densities and percent parasitism .....	83
<b>Figure 5.5</b> Predicted Australian weevil densities and parasitism rates .....	84
<b>Figure 5.6</b> Sensitivity of the mean and spatial variance of local weevil densities to parameter values .....	85
<b>Figure 5.7</b> Sensitivity of weevil suppression to parameter values .....	85
<b>Figure 5.8</b> Hypothesised relationship between lucerne abundance and local weevil density.....	87
<b>Figure 6.1</b> Comparison of metapopulation results arising from different assumptions about very low densities and dispersal .....	98
<b>Figure 6.2</b> Spatial patterns arising from disease-host metapopulations .....	99
<b>Figure 6.3</b> Local fox/rabies dynamics in a metapopulation model. ....	101
<b>Figure 6.4</b> Snapshots of an individual-based fox/rabies metapopulation.....	102
<b>Figure 6.5</b> Effect of assumptions about low densities on metapopulation patterns	103
<b>Figure 6.6</b> Disease prevalence in an unstable possum/Tb metapopulation model ..	103
<b>Figure A3.1</b> Population spread with density-dependent increase .....	143
<b>Figure A3.2</b> Dynamics of local sites within a dispersing population.....	144
<b>Figure A3.3</b> Local net immigration in a density-dependent spatial population .....	144
<b>Figure A3.4</b> Local growth rates within a density-dependent spatial population.....	145

## List of Tables

<b>Table 2.1</b> Default parameter values for the random-walk models. ....	17
<b>Table 2.2</b> Results from sensitivity analysis of the density-independent model.....	22
<b>Table 2.3</b> Results from sensitivity analysis of the density-dependent model.....	25
<b>Table 3.1</b> Some common parasitism and density-dependence functional forms.....	37
<b>Table 3.2</b> Host-parasitoid metapopulation model parameters and default values. ....	38
<b>Table 3.3</b> Comparison of spatial patterns in host-parasitoid metapopulations.....	45
<b>Table 4.1</b> Summary of field survey results. ....	63
<b>Table 4.2</b> Dependence of weevil density, parasitism rate, and sex ratio on year and site .....	63
<b>Table 4.3</b> Effect of weevil sex on density and parasitism rate .....	64
<b>Table 4.4</b> Dependence of parasitism rate on weevil density at two spatial scales.....	65
<b>Table 4.5</b> Dependence of weevil density on longitude.....	66
<b>Table 5.1</b> <i>Sitona discoideus</i> metapopulation model parameters, their default values and source.....	79
<b>Table 6.1</b> Default parameter values for disease/host metapopulations .....	94
<b>Table 6.2</b> Behaviour of disease-host metapopulation models .....	96
<b>Table A4.1</b> Results from fitting models to ‘homogeneous’ metapopulations.....	151
<b>Table A4.2</b> Results from fitting models to ‘regionally synchronised’ metapopulations .....	151
<b>Table A4.3</b> Results from fitting models to ‘large spiral’ metapopulations .....	152
<b>Table A4.4</b> Results from fitting models to ‘spatial chaos’ metapopulations. ....	152
<b>Table A4.5</b> Results from fitting models to local dynamics in ‘homogeneous’ metapopulations.....	153

<b>Table A4.6</b> Results from fitting models to local dynamics in ‘spatial chaos’ metapopulations.....	154
<b>Table A4.7</b> Results from fitting models to local dynamics in metapopulations with negative-binomial aggregated parasitism .....	155
<b>Table A4.8</b> Calculation of <i>S. discoideus</i> survival parameters from Darfield data ..	156
<b>Table A4.9</b> Flight trap catches for two Darfield sites.....	157
<b>Table A4.10</b> Day-degree calculation results for autumn parasitoids.....	157



# 1. Introduction

## 1.1 The metapopulation paradigm

### 1.1.1 Population regulation and the birth of the ‘metapopulation’

The metapopulation paradigm represents one of the most recent developments in a long-running ecological debate on population regulation. Ecology is “the scientific study of the interactions that determine the distribution and abundance of organisms” (Krebs 1994 p.3). Organisms typically occur as groups of conspecific individuals, or ‘populations’. Making the reasonable assumption that the distribution and abundance of populations is not random but determined by various regulatory mechanisms, then population regulation forms the central issue of the science of ecology.

Two types of regulatory mechanisms were identified by Howard and Fiske (1911): firstly those such as competition for food, which depend on the size or density of the population, and secondly those due to extrinsic influences such as drought, which are not related to population size. These have since been termed ‘density-dependent’ and ‘density-independent’ mechanisms, respectively (Smith 1935). This dichotomy formed the central issue of a long-running and hotly-contested debate, which at times reached “an almost religious fervour” (MacArthur 1960 p.83). One school of ecology, championed by A. J. Nicholson (1935, 1954), argued in favour of density-dependent effects bringing about a ‘balance of nature’, while others such as Andrewartha and Birch (1954) rejected this for a more pragmatic view emphasising the importance of abiotic factors.

Closer inspection reveals that much of the controversy resulted from the differing backgrounds of the researchers, and from inconsistent or ambiguous use of terms (Bakker 1964). For example, Nicholson used the word ‘competition’ to apply to any density-dependent mechanism, including predation. To Andrewartha and Birch (1954), whose outlook focused on the factors affecting individuals, this suggested the

ridiculous notion that prey compete amongst themselves for the opportunity of being eaten by a predator. Others, such as W. R. Thompson (1924), opposed Nicholson's ideas because their extension to evolutionary theory conflicted with strongly-held religious beliefs (Kingsland 1996). Nicholson's central thesis was that no population can continue to exist in the absence of some feed-back mechanism to limit its variability: populations are governed by density-dependent processes in combination with modifying density-independent processes (Mackerras 1970). This is remarkably consistent with the synthetic view agreed upon by the majority of today's population ecologists (Bonsall *et al.* 1998; Turchin 1999), though some continue to misinterpret the meaning of 'density-dependence' (e.g. Murray 1999).

Putting aside ambiguous terminology and personal philosophy, the only real biological difference between the ideas of Nicholson and his detractors is the relative importance of density-dependent and density-independent mechanisms acting on a particular population (MacArthur 1960). Nicholson happened to study populations in which abiotic factors had little effect, while Andrewartha and Birch (1954) were concerned with populations for which environmental patchiness and climate were important. The populations of the latter experienced large fluctuations in abundance, with localised extinctions being balanced by recolonisation during more favourable times. Similar dynamics led den Boer (1968) to propose that persistence of a population in an uncertain world could be achieved through 'spreading of risk', whereby the likelihood of overall extinction is minimised when a population is structured as a collection of independently fluctuating local groups linked by dispersal.

Levins (1969) introduced the term 'metapopulation' to describe systems in which interacting local groups exist in discrete habitat patches, and proposed a simple model to describe the proportion of patches occupied in relation to local colonisation and extinction rates. Based on the work of Levins (1969), 'classical' metapopulation models (e.g. Reddingius & den Boer 1970; Roff 1974) feature stochastic local dynamics leading to local extinctions and later recolonisation by metapopulation-wide dispersal. In these models, dispersal provides a form of population regulation which was largely overlooked by earlier workers.

### 1.1.2 Classical metapopulations and conservation biology

The early classical metapopulation models led to some novel hypotheses about the persistence of species in fragmented habitats. In particular, they suggested that unoccupied habitat may play an important part in long-term persistence. These results should have been of particular interest for conservation ecologists, yet went largely unnoticed. Conservation ecology of the 1970s was dominated by MacArthur and Wilson's (1967) theories of 'island biogeography', which describe how species richness (the number of different species present) of a habitat patch could be expected to depend on its size, shape, and proximity to other patches of similar habitat. By the 1980s, however, the general applicability of island biogeography was being questioned (e.g. Gilbert 1980). There was a growing realisation that predictions from the theory were overly simplistic (e.g. Soulé and Simberloff 1986) and that island biogeographic processes in practice are often dominated by species of little ecological interest (Williamson 1989). The obvious way to address the shortcomings of island biogeography was to consider the dynamics of key species, that is those whose activities are important in determining community structure, across their patchy habitats. Thus, a 'paradigm shift' took place in the late 1980s as metapopulation theory was finally embraced by conservation biologists (Hanski & Simberloff 1997).

The influence of island biogeography and the precarious existence of rare species led conservation biologists to adopt the classical view of metapopulations, where local extinctions are common and caused largely by extrinsic factors. This contrasts with a broader view of the metapopulation, which was arrived at, largely independently, by ecologists studying pest management systems (Harrison & Taylor 1997).

### 1.1.3 Metapopulations in pest management

Population ecologists had long pondered the problem that the simplest host-parasitoid and predation models (Thompson 1924; Lotka 1925; Volterra 1926; Nicholson & Bailey 1935) predicted unstable or, more rarely, oscillatory interactions. However, theory (Bailey *et al.* 1962) and experiment (Gause 1934) showed that

persistence can be achieved in these systems if prey are provided with some refuge where they are safe from predation. Laboratory studies by Huffaker (1958) showed that spatial heterogeneity and dispersal can alone provide suitable refuges, and that these change in time and space as predator and prey play ‘hide and seek’. Early multi-species metapopulation models showed similar results (e.g. Allen 1975; Hilborn 1975), but differed from the classical models in that local extinctions did not necessarily occur, despite the instability of subpopulation dynamics.

Many of the early metapopulation models assumed ‘global dispersal’, with equal migration between all subpopulations (e.g. Hilborn 1975; Hassell & May 1988; Godfray & Pacala 1992; Ives 1992). Persistence in these models relies on asynchrony between subpopulations, which, with global dispersal, cannot be maintained without some local randomness (Crowley 1981). With ‘local dispersal’ confining migrants to nearby patches, however, persistence and population asynchrony do not necessarily require stochasticity. Also, metapopulation models based on unstable interactions and local dispersal gave rise to self-organising spatial patterns in local density (Allen 1975; Hassell *et al.* 1991a). This led to an explosion of theory exploring the physical properties of these patterns (e.g. Solé *et al.* 1992b; Boerlijst *et al.* 1993; Hassell *et al.* 1994; Rohani & Miramontes 1995; White *et al.* 1996; Savill *et al.* 1997). While field ecologists remained wary of this work, much of which paid little attention to the real world, some pragmatists defended the theory by pointing to similar pattern-generating processes in physics and molecular biology (Rohani *et al.* 1997). Evidence for spatial patterning in natural metapopulations, however, is confined to a handful of largely circumstantial cases (Godfray & Hassell 1997; Maron & Harrison 1997).

#### **1.1.4 Metapopulations, persistence, and stability**

The contemporary definition of a metapopulation embraces both the classical concept of conservation biologists as well as the broader interpretation arising from multi-species modelling. In a recent review, Hanski and Simberloff (1997, p.11) defined a metapopulation as a “set of local populations within some larger area, where typically migration from one local population to at least some other patches is possible”. Their focus was on conservation of species confined to a system of habitat patches, where in some cases dispersal may no longer occur due, for example, to

human modification of the inter-patch environment. Their definition, therefore, was deliberately broad enough to include modified, non-equilibrium systems, where the species was on the verge of extinction. A slightly simpler version, and the one adopted in this thesis, defines a metapopulation as a set of potential local populations between which dispersal is possible. A local population, or ‘subpopulation’, is defined as a group of individuals which inhabit a particular habitat patch and interact with each other. Metapopulations are defined in terms of ‘potential’ populations because empty habitat patches may play an important part in the dynamics of some systems. The critical features of a metapopulation are therefore patchy habitat, within which local interactions occur, and the possibility for dispersal from one patch to another.

The metapopulation concept originated in both conservation and pest management as an explanation for species persistence. It is particularly important to distinguish clearly between ‘stability’ and ‘persistence’, since the literature has sometimes confused the two. ‘Persistence’ describes the continued presence of a species or set of interacting species through time. Here, persistence is used to refer to the presence at all times of a species in one or more patches of a metapopulation. ‘Stability’, on the other hand, is a mathematical term used narrowly to describe the tendency for population values to return to some temporal equilibrium level when disturbed (e.g. Edelstein-Keshet 1988). Here, ‘stability’ is used exclusively in reference to non-spatial systems, such as a local population with no dispersal. This is done in order to avoid the confusion that has arisen in the literature about the stability of metapopulations.

One of the clearest results from metapopulation theory is that dispersal promotes population persistence in time. In addition, it has been shown (e.g. Allen *et al.* 1993; Stone 1993; Ruxton 1994) that metapopulation structure promotes constancy, by reducing the amplitude of fluctuations caused by stochastic or chaotic local dynamics. Careless reference to this as “the stabilising effects” of dispersal (Allen *et al.* 1993, p.232) and the widespread intuition that “dispersal stabilises populations” (Vance 1984, p.231) led to considerable confusion over the effect of dispersal on stability in its true sense: the qualitative tendency to return to a particular equilibrium state following a small disturbance. In addition, the theory was muddled by

contradictory results arising from the biologically unreasonable models of Vance (1984), Solé *et al.* (1992a), and Bascompte and Solé (1994), which failed to separate the processes of survival and dispersal, allowing dead animals to disperse and contribute to other populations (Hassell *et al.* 1995). The effect of dispersal on metapopulation stability in its correct sense was eventually shown by Rohani *et al.* (1996; 1999): dispersal actually has no effect on stability, except in host-parasitoid metapopulations with extremely disparate dispersal rates, when it may be destabilising.

## 1.2 Modelling metapopulations

### 1.2.1 Models with implicit local dynamics

Many different approaches have been used for modelling metapopulations (figure 1.1). The simplest models, often referred to as ‘patch models’, consider both the temporal and spatial characteristics of subpopulations implicitly. In these models, local habitat patches may exist in a small number of discrete states (normally just

		<b>Subpopulation Dynamics</b>	
		Implicit	Explicit
<b>Space</b>	Implicit	<b>Patch Models</b> e.g. Levins (1969) Amarasekare (1998)	<b>Global Dispersal Models</b> e.g. Crowley (1981) Hanski <i>et al.</i> (1996, model 1)
	Explicit	<b>Cellular Automata</b> (for local populations) e.g. Mollison and Kuulasmaa (1985) Comins <i>et al.</i> (1992, model 2)  <b>Incidence Function Models</b> e.g. Hanski (1994b) Moilanen <i>et al.</i> (1998) Lindenmayer <i>et al.</i> (1999)	<b>Coupled Map Lattice Metapopulation Models</b> e.g. Allen (1975) Comins <i>et al.</i> (1992, model 1) Hassell <i>et al.</i> (1995) Comins and Hassell (1996)  <b>Landscape Models</b> e.g. Hanski and Thomas (1994)

**Figure 1.1** A classification of metapopulation model types, based on their treatment of local dynamics and spatial structure.

empty or occupied), and simple rules govern the transitions between these states. Patch models assume that all habitat patches are identical and that all are equally available to dispersing animals.

The simplest patch model assumes that occupied patches go extinct at a constant rate  $E$ , while empty patches are recolonised at a rate  $C$ . The proportion of available patches that are occupied,  $J$ , changes with time,  $t$ , as

$$\frac{dJ}{dt} = C(1 - J) - EJ \quad (1.1)$$

Levins (1969) made the additional assumption that the colonisation rate depends on the number of occupied patches, since these provide the pool of dispersing animals. This gives the ‘Levins model’, with  $C'$  now expressed per occupied patch:

$$\frac{dJ}{dt} = C'J(1 - J) - EJ \quad (1.2)$$

Hanski (1994b) drew on concepts from island biogeography (MacArthur & Wilson 1967) to suggest that colonisation and extinction rates may vary from patch to patch depending on their spatial characteristics such as size, shape, and isolation. Adding explicit spatial information such as this, denoting the values for a specific patch by the subscript  $x$ , and solving equation 1.1 at equilibrium, gives the ‘incidence function model’:

$$J_x = \frac{C_x}{C_x + E_x} \quad (1.3)$$

where  $J_x$  is the stationary (equilibrium) probability of patch  $x$  being occupied, and  $C_x$  and  $E_x$  may be functions of spatial variables and life-history traits of the species (Hanski 1994b). In the Levins model (equation 1.2),  $J$  is dynamic, changing with time to eventually reach a non-zero equilibrium value of  $1 - E/C$ . The incidence function model (equation 1.3), however, only applies at the equilibrium between local extinction and colonisation. The extinction-colonisation balance with which such classical metapopulations persist has been criticised as improbable and is not supported by evidence from many natural systems (Harrison 1994). Nevertheless,

models of this type have been successfully applied to several species inhabiting patchy habitats (e.g. Hanski 1994b, 1998; Moilanen *et al.* 1998; Lindenmayer *et al.* 1999).

A simple two-state ‘cellular automaton’ may be viewed as a special case of the incidence function model, where patches are distributed evenly on a (normally square) grid, and local colonisation and extinction rates depend on the mean occupancy of nearby patches. These models tend to focus on spatial patterning, however, rather than metapopulation persistence and turn-over. Perhaps the most well-known cellular automaton is the ‘game of life’ (Gardner 1970), though more complex models may include more than two different local states. In ecology, cellular automata have most commonly been applied to individual-based systems, where each grid location holds an individual organism (e.g. Mollison & Kuulasmaa 1985; Barlow & Kean 1996). They have occasionally been used to model metapopulations, where each grid location represents a subpopulation (e.g. Comins *et al.* 1992), but mainly as a standard for comparison with more detailed models which include explicit local population dynamics.

### **1.2.2 Models with explicit local dynamics**

The simplest metapopulation models with explicit local dynamics assume global dispersal, that is, dispersing organisms have an equal chance of settling in any patch (e.g. Reddingius & den Boer 1970; Hilborn 1975; Reeve 1988; Godfray & Pacala 1992; Allen *et al.* 1993; Hanski *et al.* 1996). Local stochasticity is an important part of these models, since otherwise the dynamics of subpopulations eventually become synchronised and the stabilising effect is lost (Crowley 1981). The most detailed metapopulation models include explicit spatial layout (which is only meaningful when dispersal range is limited) as well as local dynamics. ‘Landscape models’ involve very little abstraction, so that all of the major details of the system under investigation are included, such as the arrangement and size of the habitat patches. These models may be useful for specific case studies, such as the butterflies of Hanski and Thomas (1994), but have little to offer by way of general insight.

A much more common approach is to use ‘coupled map lattice’ models, in which habitat patches are assumed to occur regularly on a (usually two-dimensional) grid (Kaneko 1989). These can act as a suitable approximation for more detailed spatial models, but are general enough to be used to examine theory. Indeed, much recent theory has been developed with the use of lattice models (e.g. Hassell *et al.* 1991a, 1994, 1995; Solé *et al.* 1992b; Boerlijst *et al.* 1993; Rohani & Miramontes 1995; Comins & Hassell 1996; White *et al.* 1996; Wood & Thomas 1996; Ruxton *et al.* 1997; Savill *et al.* 1997; Rohani & Ruxton 1999; Wilson *et al.* 1999). A coupled map lattice approach has also been chosen for the metapopulation models presented in subsequent chapters.

It is important to note that not all spatial models are metapopulation models. By definition, a metapopulation features patchy habitat within which local interactions occur, and dispersal between patches. Models that treat space continuously (reviewed by Holmes *et al.* 1994) may be derived from metapopulation-like first principles (appendix 3), but in scaling time and space to very small units, they lose the defining characteristic of patchy habitat. Similarly, models that include the effect of aggregation implicitly (e.g. Hassell & May 1973, 1974; May 1978; Chesson & Murdoch 1986; Murdoch & Stewart-Oaten 1989; Rohani *et al.* 1994) do not represent metapopulations because interactions between individuals are not necessarily confined to patches, and dispersal is not a separate process. On the other hand, some non-spatial models may be applicable to metapopulations. Simple disease models, in particular, are closely related to metapopulation patch models, where hosts act as habitat patches and disease is either present or absent (Grenfell & Harwood 1997).

### **1.3 Nature and scope of this investigation**

Metapopulation models have been applied with some success in conservation biology (e.g. Hanski & Thomas 1994; Lei & Hanski 1998; Moilanen *et al.* 1998). However, much recent metapopulation theory has focused solely on the mathematical properties of metapopulation models (e.g. Solé *et al.* 1992b; Ruxton & Doebeli 1996; Rohani & Ruxton 1999), and much of the theory derived for multi-species systems

remains untested in the field. The primary aim of this thesis, therefore, is to marry metapopulation theory with ecological reality. This is done by analysis of a range of metapopulation models in which the primary concern is realism, together with a detailed field study of a host-parasitoid metapopulation.

Chapter 2 investigates the possible role of metapopulation dynamics in regulating highly stochastic populations. Single-species individual-based models are used to expand the work of Hanski *et al.* (1996), exploring in some detail the effects of metapopulation size on the persistence and incidence of density-dependence in stochastic metapopulations.

Chapter 3 deals with some general issues arising in deterministic host-parasitoid metapopulation models. The overall aim of the chapter is to investigate the ways in which metapopulation structure may affect the success of biological control. General formulations for host-parasitoid models are presented, and their dynamics explored both in metapopulations and in isolation. The relationship between local and global behaviour in these metapopulations, and the importance of initial conditions, are emphasised. The conditions under which self-organising spatial patterns arise are critically examined, and the implications of the results for successful biological control are discussed.

Chapters 4 and 5 examine a real host-parasitoid system, consisting of the pest weevil *Sitona discoideus* and its biocontrol agent *Microctonus aethiopoidea*. Chapter 4 describes a three-year field study in which autumn weevil densities and parasitism levels were measured with the aim of estimating the importance of metapopulation processes in the system and testing the predictions of an earlier non-spatial model. In particular, evidence is sought for the spatial patterning suggested by many of the models in chapter 3. This is followed in chapter 5 by a detailed modelling analysis of the system, using the new data plus older records, to address the question of whether metapopulation interactions are important for understanding and predicting the population dynamics of this pest.

Few metapopulation models have used continuous-time dynamics, and those that have focus on a particular strategic problem. Chapter 6 takes a broader look at metapopulations in continuous time, comparing their behaviour with that of discrete-

time models, highlighting some of the important assumptions in such models, and exploring the criteria for disease persistence. Finally, chapter 7 presents an overall synthesis of results and suggests directions for further research needed to relate metapopulation theory to practice.

## 2. The effects of density-dependence and local dispersal in individual-based stochastic metapopulations

### 2.1 Introduction

Natural populations have long been recognised as experiencing large fluctuations in size (e.g. Andrewartha & Birch 1954; Hanski 1990). It is usually assumed that the consequences of extreme population sizes are mitigated by density-dependent feedback mechanisms, but such self-regulation is not always apparent (Strong 1986; den Boer & Reddingius 1989). Indeed, the temporal fluctuations of some populations may be indistinguishable from random walks over a twenty year period or more (den Boer 1991). The question of how such populations persist has led to the development of a rich heritage of ecological theory.

Den Boer (1968) recognised that population persistence may be enhanced by the ‘spreading of risk’ over independently fluctuating local groups linked by dispersal. This spatial persistence has been widely demonstrated in theoretical models (e.g. Roff 1974; Hassell *et al.* 1991a; Adler 1993; Ruxton 1994), but less so in real populations (den Boer 1981). A parallel line of thought led Levins (1969) to develop the ‘metapopulation’ concept, strongly reminiscent of ‘island biogeography’ (MacArthur & Wilson 1967), whereby an assemblage of extinction-prone populations may persist through continual recolonisation of locally extinct areas.

Metapopulation theory has flourished in recent years (Hanski & Gilpin 1997). Most attention has focused on three areas: firstly, the mathematical stability of populations (Vance 1984; Gyllenberg *et al.* 1993; Rohani *et al.* 1996); secondly, the distinctive spatial patterns that may be generated (Hassell *et al.* 1991a; Rohani *et al.* 1997); and thirdly, the possibility for ecological applications of chaos theory (Ruxton 1993; Bascompte & Solé 1994). Indeed, the implication of the original ‘spreading of

risk' and metapopulation theories, that spatial interactions may be sufficient to regulate populations in the absence of density-dependence, has been largely overlooked. A recent exception is Hanski *et al.* (1996), who investigated how much density-dependence was necessary to allow long-term persistence of a stochastic metapopulation. Their analysis was based on an extension of Levins' (1969) original metapopulation model by including random walk local dynamics (Foley 1994).

This chapter investigates further the characteristics required for the persistence of stochastic metapopulations, based on Hanski *et al.* (1996). However, a quite different metapopulation formulation is adopted: a coupled map lattice with local dispersal, as was also used in a range of other metapopulation studies (Hassell *et al.* 1991a, 1995; Comins *et al.* 1992). This allows investigation of further characteristics required for the persistence of stochastic metapopulations, and in particular addresses the effects of local dispersal, density-dependence, and metapopulation size. As well as examining the question of how much density-dependence is necessary for persistence, this chapter also considers the corollary: to what extent is persistence possible in the absence of density-dependence?

## 2.2 Model

A simple model was constructed by replicating random-walk local models (Foley 1994) across the many grid locations of a coupled map lattice (Kaneko 1989). A second model included a simple density-dependence mechanism acting on local populations. Dispersal within the metapopulation was assumed to occur only between neighbouring subpopulations.

### 2.2.1 Stochastic local dynamics

Changes in local population size,  $N_t$ , from one non-overlapping generation,  $t$ , to the next were modelled as

$$N_{t+1} = N_t e^{r_t} \tag{2.1}$$

where  $r_t$  is the realised per capita reproductive rate. Spatio-temporal stochasticity was incorporated by making  $r_t$  a normally distributed (Gaussian) random variable with mean  $r_m$  and variance  $v_r$ . As in Hanski *et al.* (1996), these growth rates,  $r_t$ , were assumed to be uncorrelated in space and time, giving a simple random walk model for local population dynamics. Allee effects (Allee *et al.* 1949, p. 393), catastrophes, and environmental autocorrelation were assumed to be negligible; these have been analysed elsewhere in relation to the model (Foley 1994, 1997).

The model is individual-based, so that all population processes involve discrete numbers of individuals. A local population, therefore, was considered to be extinct when its size,  $N_t$ , became zero. At the other extreme there are two variants on the basic model which differ in their treatment of arbitrarily large subpopulation densities. In the ‘density-independent’ model no upper limit was imposed on local population sizes, although simulations were recognised as being unrealistic when the overall metapopulation mean became very large. In contrast, the ‘density-dependent’ model imposed an upper limit,  $K$ , on all local population sizes.

Hanski *et al.* (1996) modelled density-dependence as a simple ‘reflecting ceiling’, in which any population size  $N_t$  exceeding the carrying capacity  $K$  was instantaneously reduced to the value  $K^2/N_t$  (which is equivalent to inverting the fraction  $N_t/K$ ). This approach has been shown to give similar behaviour to both the Verhulst (Foley 1994) and Ricker (Foley 1997) logistic models, in which density-dependence is more pervasive. This chapter adopts the milder approach used by Roff (1974), whereby  $K$  behaved as a ‘truncating ceiling’, so that any subpopulation exceeding  $K$  was reduced to  $K$ . This corresponds to Nicholson’s (1954) concept of ‘contest’ intraspecific competition, and is both simpler than the reflecting ceiling (comparable to Nicholson’s ‘scramble’ competition) and conceptually more similar to the classic logistic models. There is, however, little difference between truncating and reflecting ceilings when realised rates of increase are small.

### 2.2.2 Metapopulation structure

The local dynamics described above were assembled using a coupled map lattice (Kaneko 1989) to form a metapopulation. Each generation, these dynamics occurred within each of the  $H$  local populations, arranged on a square grid of dimension  $\sqrt{H}$ . Dispersal was modelled as an integer number of animals, corresponding to a Binomial proportion  $\mu$  of each local population, being reassigned randomly among the nearest  $c$  neighbouring populations (figure 2.1). Default values of  $H = 225$  ( $= 15 \times 15$ ) and  $c = 8$  were used. Lattice boundaries were either ‘periodic’, with dispersers off an edge reappearing at the opposite edge, ‘reflecting’, with dispersers being repelled from the edges, or ‘absorbing’, with dispersers off the edges being lost from the system (figure 2.2). By default, periodic boundaries were assumed, so that the metapopulation was conceptually a subset of a larger model universe.

Global extinction occurred when all subpopulations became extinct. Following den Boer (1991), initial subpopulation sizes were  $N_0 = \sqrt{K}$ .

### 2.2.3 Model application

For each of the density-independent simulations, an exponential model was fitted using least-squares to the time-series of the mean subpopulation size. Each simulation was, therefore, characterised by the exponential rate at which the metapopulation density changed, denoted  $r_p$ . Negative  $r_p$  indicated population sizes declining on average to global extinction, while positive  $r_p$  indicated the metapopulation mean size increasing. The number of generations after which a metapopulation became either extinct or unrealistically large was recorded as the persistence time,  $t_p$ . Metapopulations for which  $r_p = 0$  neither increased nor declined over time, so that on average  $N_{t+1} = N_t = N_0$  and  $t_p \rightarrow \infty$ . Following Hanski *et al.* (1996), the term ‘persistent’ is used to refer to metapopulations which do not become extinct, nor attain unrealistically high local population sizes, for at least 1000 generations:  $t_p \geq 1000$ . A tally was kept of the proportion of simulations that persisted for 1000 or more generations, denoted  $p(t_{1000})$ , as well as the proportion of

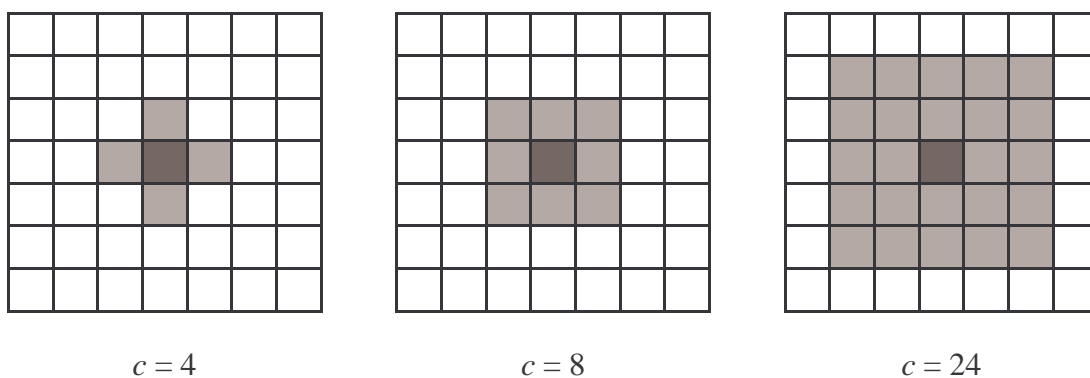


**Figure 2.1** Different dispersal neighbourhoods (grey) around a source population (black).

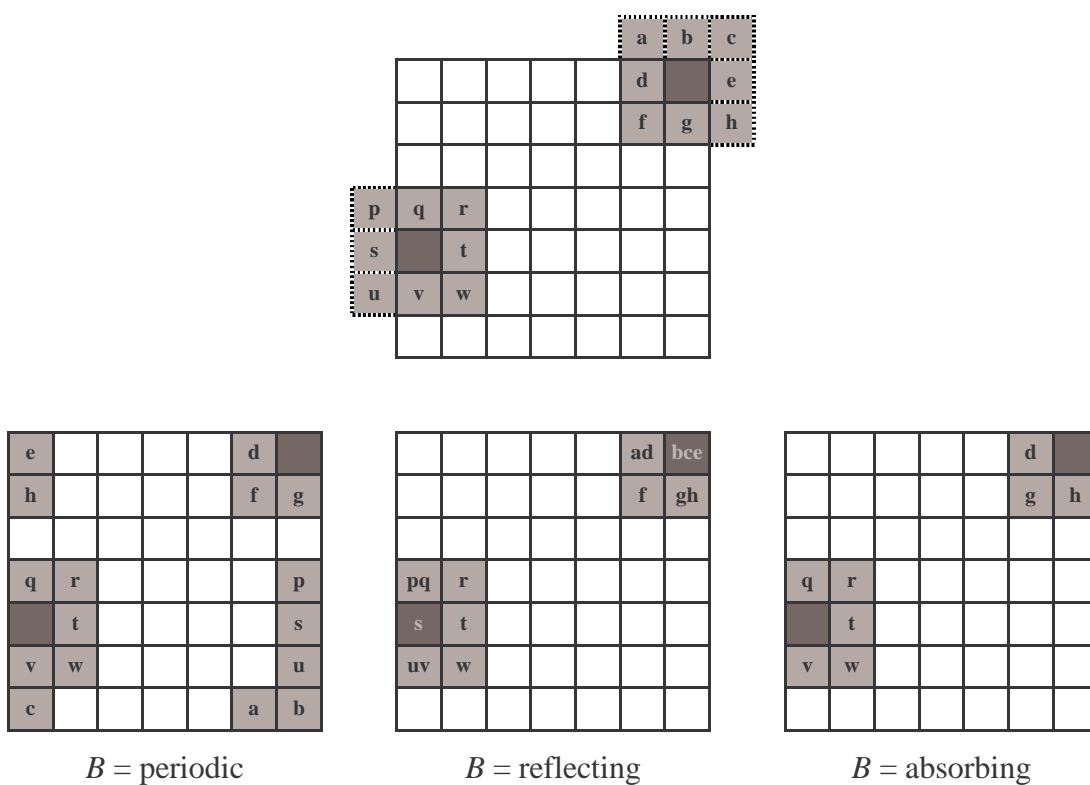


**Figure 2.2** Demonstration of different lattice boundary conditions,  $B$ , for a  $7 \times 7$  lattice with dispersal range  $c = 8$ . Results are shown for two source populations (dark squares). Top figure is before applying boundary rules, bottom figures show the results after applying the rules.

metapopulations that eventually went extinct,  $p(0)$ , as opposed to becoming unrealistically large. Mean subpopulation size,  $N_p$ , was also tallied for the duration of each simulation.

For density-dependent simulations, unrealistically large population sizes were not possible, so persistence time,  $t_p$ , simply reflected the time at which the metapopulation became extinct. The presence of density-dependent feedback meant that persistence time for some metapopulations was effectively infinite, though the stochastic nature of local dynamics meant that there was always the possibility for metapopulation extinction. An appropriate time to halt such simulations was found to be the time after which all subpopulations had experienced density-dependence at least once. Therefore,  $p(0)$  was defined to be the proportion of metapopulations going extinct before all subpopulations had experienced density-dependence.

Table 2.1 summarises the default parameter values used in the simulations. Sensitivity analyses were used to investigate how changes in these parameter values affect metapopulation behaviour.

**Table 2.1** Default parameter values used in the models.

Parameter	Meaning	Default value	Range investigated
$r_m$	mean exponential growth rate	-0.12	-0.20 to 0.00
$v_r$	variance of growth rate	0.25	0.00 to 1.00
$\mu$	dispersal rate per time step	0.1, 0.2	0.0 to 1.0
$K$	maximum local population size	100	-
$c$	number of subpopulations within dispersal range	8	0, 4, 8, 24, $H$
$\sqrt{H}$	lattice edge = square root of the number of subpopulations in the metapopulation	15	1, 5, 15, 25, 40, 50
$B$	boundary conditions (as in Comins <i>et al.</i> 1992)	periodic	reflecting, periodic, absorbing

## 2.3 Results

### 2.3.1 Density-independent metapopulations

Without density-dependence, all simulations eventually went extinct or grew to unrealistically high densities (figures 2.3(a) and 2.4), although in some cases this was not for several hundreds of generations. Because of the underlying random-walk dynamics, metapopulation trajectories tended to be characterised by very sudden increases or declines, and the long-term result was difficult to predict. For example, trajectories that came close to extinction later increased until the metapopulation mean became unrealistically large. An exponential curve was not a particularly good quantitative fit to most metapopulation trajectories, but was found to provide a useful index of the model's qualitative behaviour in relation to the parameter values.

Metapopulation behaviour, in terms of average trend, depended primarily on the parameters  $r_m$ ,  $v_r$ , and  $\mu$  (figure 2.5). Above  $\mu = 0.2$ , dispersal rate had little effect on mean metapopulation trend, though spatial heterogeneity in subpopulation densities was evident even at the highest rates of dispersal. The effects of the local reproductive rate mean,  $r_m$ , and variance,  $v_r$ , were relatively simple. However, as noted by Kuno (1981), local reproductive rates may be negative on average and yet produce positive growth in the metapopulation as a whole. Since the current study focuses on the boundary between metapopulation persistence and extinction, it was necessary to have by default a negative mean reproductive rate (table 2.1).

The results of a more detailed model sensitivity analysis (table 2.2) suggest that the behaviour of the model was most sensitive to the distribution of rates of increase, determined by parameters  $r_m$  and  $v_r$ . Lattice size also had a major effect, with persistence time and probability of persisting 1000 generations increasing with lattice size, but saturating as lattices exceeded  $40 \times 40$  subpopulations (figure 2.6(a)). Dispersal rate  $\mu$  and dispersal range  $c$  had similar effects on model behaviour (table 2.2);  $\mu = 0$  is equivalent to  $c = 0$ , and both parameters had the largest influence on model dynamics at the lower end of their tested ranges. The boundary conditions had little effect on metapopulation dynamics, except that absorbing boundaries imposed

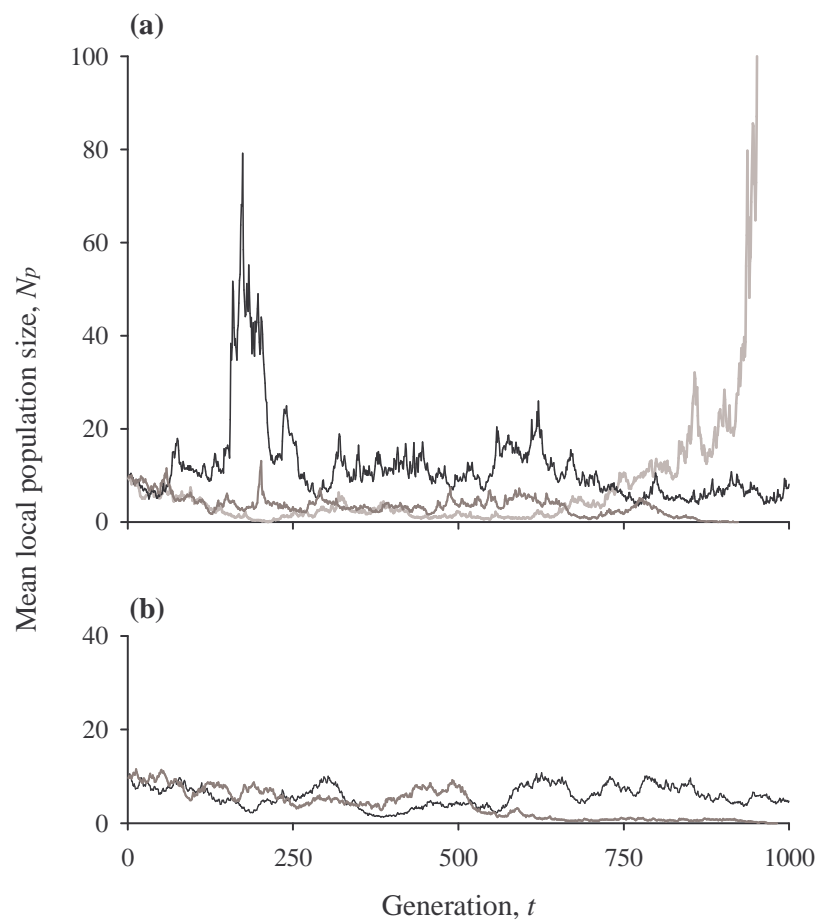


**Figure 2.3** Sample metapopulation trajectories from the models, with default parameter values. The simulations in dark grey became extinct, while those in black persisted, and that in light grey experienced unrealistically high local population densities. (a) density-independent model; (b) density-dependent model. Discrete generation values are joined with lines to aid interpretation.

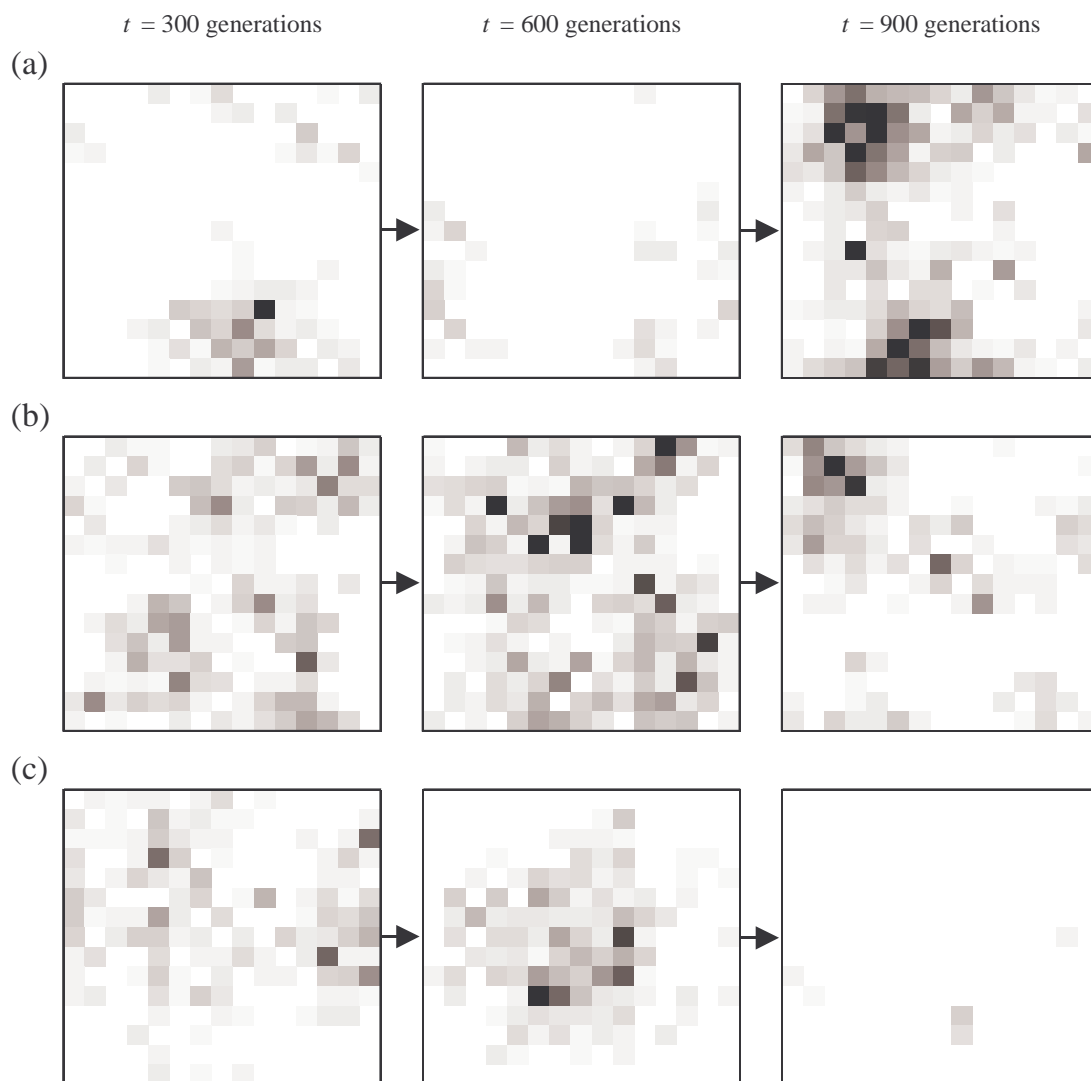


**Figure 2.4** Snapshots of the metapopulations plotted in figure 2.3(a). Empty subpopulations appear white, and colour darkens with increasing local density. (a) metapopulation mean becomes unrealistically large; (b) metapopulation mean remains within realistic bounds; (c) metapopulation goes extinct.

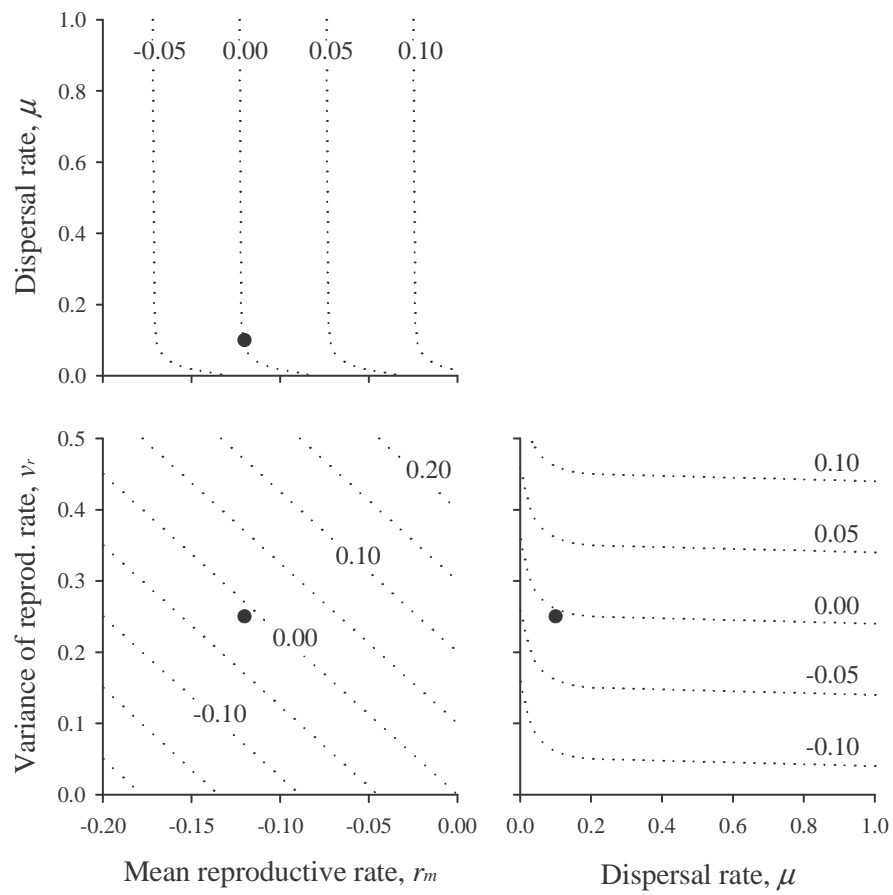


**Figure 2.5** The behaviour of the density-independent model in terms of parameters  $r_m$ ,  $v_r$ , and  $\mu$ . Contours refer to values of  $r_p$ , the effective metapopulation reproductive rate obtained by fitting an exponential curve to each metapopulation trajectory. Dots indicate default parameter values.

**Table 2.2** Results from sensitivity analysis of the density-independent model. Each result represents the mean of 100 simulations. Model parameters as defined in table 2.1; italics indicate default parameter values.  $r_p$  denotes mean exponential rate of metapopulation change;  $N_p$  is mean subpopulation size up to time  $t = 1000$  generations (or extinction if that occurred sooner);  $p(0)$  denotes the proportion of simulations ending in metapopulation extinction;  $t_p$  is mean persistence time in generations;  $p(t_{1000})$  is the proportion of simulations that persisted for 1000 generations.

Parameter	Value	$r_p \times 10^3$	$N_p$	$p(0)$ (%)	$t_p$	$p(t_{1000})$ (%)
$r_m$	-0.15	-38.3	3	100	150	0
	-0.13	-13.8	4	96	354	0
	<i>-0.12</i>	<i>-1.0</i>	<i>14</i>	<i>47</i>	<i>623</i>	<i>18</i>
	-0.11	11.5	30	0	220	0
	-0.09	31.8	36	0	77	0
$v_r$	0.10	-73.4	2	100	89	0
	0.20	-30.3	2	100	191	0
	<i>0.25</i>	<i>-1.0</i>	<i>14</i>	<i>47</i>	<i>623</i>	<i>18</i>
	0.30	22.3	33	0	104	0
	0.40	70.3	35	0	34	0
$\mu$	0.00	-46.0	6	92	115	0
	0.05	-12.9	6	87	351	0
	<i>0.10</i>	<i>-1.0</i>	<i>14</i>	<i>47</i>	<i>623</i>	<i>18</i>
	0.20	3.0	26	4	848	28
	0.30	3.8	29	1	671	13
	0.50	4.0	32	0	607	6
	1.00	4.3	33	0	572	6
c	0	-46.6	6	93	114	0
	4	-4.1	11	72	576	9
	8	<i>-1.0</i>	<i>14</i>	<i>47</i>	<i>623</i>	<i>18</i>
	24	1.2	18	31	898	28
	225	1.3	21	17	785	27
$\sqrt{H}$	1	-190.6	11	89	15	0
	5	-26.3	8	87	166	0
	<i>15</i>	<i>-1.0</i>	<i>14</i>	<i>47</i>	<i>623</i>	<i>18</i>
	25	0.9	20	26	1126	45
	40	1.4	32	4	1631	72
	50	1.4	36	0	1724	76
B	reflecting	-4.6	10	70	642	17
	<i>periodic</i>	<i>-1.0</i>	<i>14</i>	<i>47</i>	<i>623</i>	<i>18</i>
	absorbing	-8.6	6	88	489	6

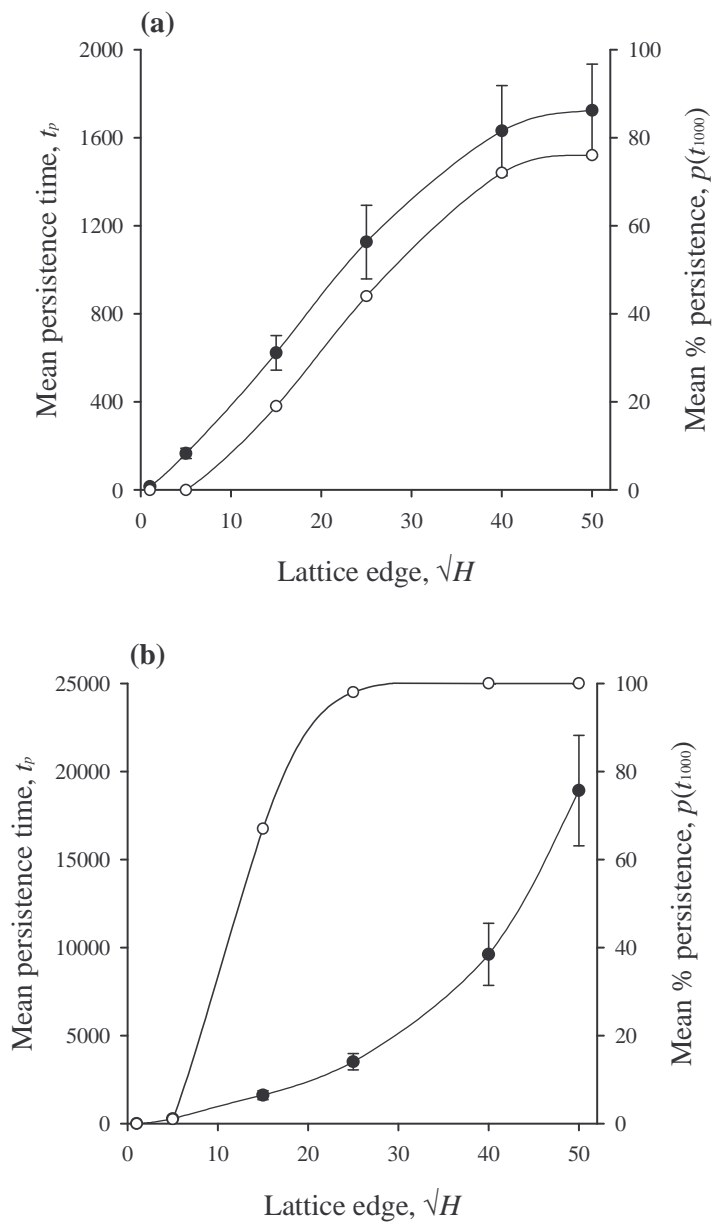


**Figure 2.6** The effect of lattice size on persistence time in generations (closed dots) and the percentage of populations persisting for 1000 generations or more (open dots) in (a) density-independent and (b) density-dependent models with default parameter values. 95% confidence intervals on persistence times were calculated from 100 simulations. Spline curves are shown to emphasise trends.

an additional mortality on the metapopulation, which was reflected in the results. The dome-shaped responses (with maximum persistence times achieved at intermediate values) to several different parameters arise from the assumption of a maximum mean population size for realistic persistence, as discussed above.

### 2.3.2 Density-dependent metapopulations

Metapopulation trajectories were less erratic in the density-dependent model (figures 2.3(b) and 2.7), with lower observed temporal and spatial variance. Sensitivity analysis of the density-dependent model (table 2.3) yielded similar results to the density-independent model, but allowed for much longer persistence times, particularly on large lattices (figure 2.6(b)). In this case, persistence times were a monotonically increasing function of lattice width, while the probability of persisting for at least 1000 generations reached 100% with a 30×30 lattice. In addition, long persistence times on large lattices were often associated with very low incidence of density-dependence,  $p(K_{hit})$ , in the order of 0.03% per generation (figure 2.8). In such metapopulations, local densities were typically very low (around 2%) compared with their potential,  $K$ .

Parameter combinations which gave net increase ( $r_p > 0$ ) in the density-independent model, interacted with density-dependence to result in an equilibrium mean density ( $N_{eq}$  in table 2.3), which was considerably lower than the local carrying capacity ( $K = 100$ ).

After a perturbation involving a global reduction in densities, the metapopulation mean tended towards this equilibrium (figure 2.9), though for some parameter combinations (those that gave  $r_p$  close to zero in the density-independent model) the rate of return was slow. Simulations with the highest density-independent net growth rates,  $r_p$ , resulted, with density-dependence, in the highest equilibrium mean densities (tables 2.2 and 2.3) and the most rapid approach to these equilibria after perturbation.

**Table 2.3** Results as for table 2.2, but from the density-dependent model with carrying capacity  $K = 100$ .  $p(K_{hit})$  denotes the mean incidence of density-dependence per subpopulation per generation, and  $N_{eq}$  is the equilibrium mean subpopulation size for persistent metapopulations.

Parameter	Value	$p(K_{hit}) \times 10^3$	$N_{eq}$	$p(0)$ (%)	$t_p$	$p(t_{1000})$ (%)
$r_m$	-0.15	0.2	0	100	163	0
	-0.13	0.3	0	100	405	0
	-0.12	0.8	0	100	1619	67
	-0.11	5.8	13	0	>10000	100
	-0.09	24.9	26	0	>10000	100
$v_r$	0.10	0.0	0	100	83	0
	0.20	0.1	0	100	214	0
	0.25	0.8	0	100	1619	67
	0.30	14.0	18	0	>10000	100
	0.40	44.3	27	0	>10000	100
$\mu$	0.00	2.7	0	100	95	0
	0.05	1.6	0	100	221	0
	0.10	1.0	0	100	431	1
	0.20	0.8	0	100	1619	67
	0.30	1.5	9	29	3680	99
	0.50	3.2	17	1	5635	99
$c$	0	2.6	0	100	102	0
	4	0.8	0	100	864	30
	8	0.8	0	100	1619	67
	24	0.9	6	88	3494	84
	225	1.0	6	70	3442	90
$\sqrt{H}$	1	2.6	0	100	15	0
	5	1.8	0	100	282	1
	15	0.8	0	100	1619	67
	25	0.5	0	100	3780	98
	40	0.4	0	100	9609	100
	50	0.3	2	95	18915	100
$B$	reflecting	0.8	0	100	1064	47
	periodic	0.8	0	100	1619	67
	absorbing	0.4	0	100	441	1

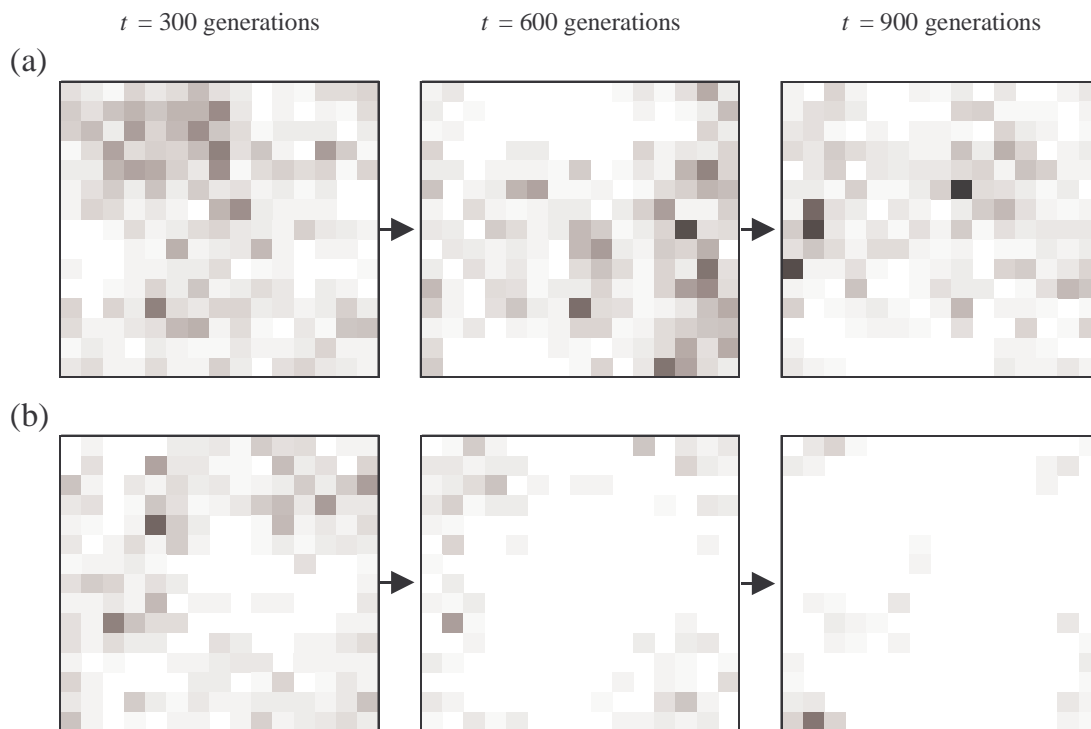


**Figure 2.7** Snapshots of the metapopulations plotted in figure 2.3(b). Empty subpopulations appear white, and colour darkens with increasing local density. (a) metapopulation persists for 1000 generations; (b) metapopulation goes extinct.

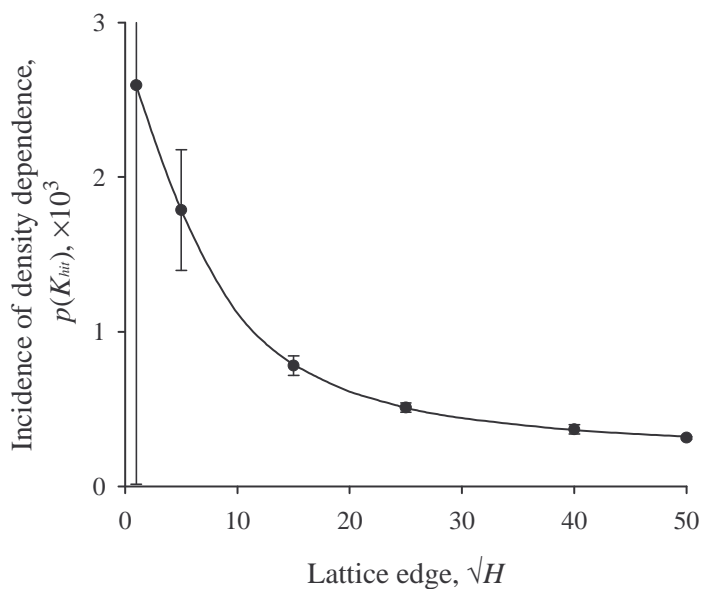


**Figure 2.8** The effect of lattice size on the incidence of local density-dependence per subpopulation per generation, assuming default parameter values. The 95% confidence intervals indicated were calculated from 100 simulations. The upper confidence limit for lattice size 1 was  $5.6 \times 10^{-3}$ .

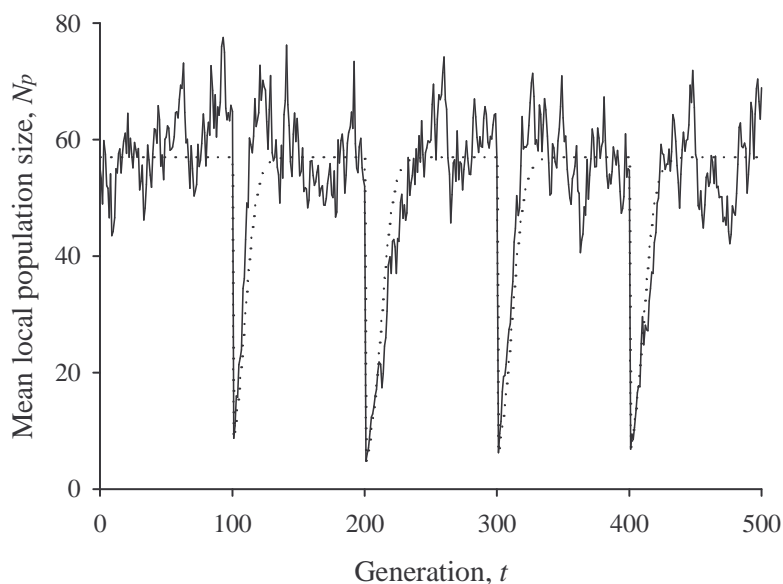


**Figure 2.9** Behaviour of the metapopulation mean for one example simulation on a  $5 \times 5$  lattice, with density-dependence and default parameters except that  $r_m = 0.0$ . Perturbations were applied every 100 generations, by reducing all subpopulation densities by 90%. The solid line shows the metapopulation mean, while the dotted line is for Ricker logistic growth,  $N_{t+1} = N_t \exp[r_p(1 - N_t/N_{eq})]$ , fitted to alternate years data using non-linear least squares in Genstat 5 (Genstat 5 Committee 1993): equilibrium mean density  $N_{eq} = 57$ ; rate of increase for metapopulation mean  $r_p = 0.201$ ;  $R^2 = 96.2\%$ ;  $p < 0.001$ . The mean incidence of density-dependence in this simulation was  $p(K_{hit}) = 0.144$ . Discrete generation values are joined with lines to aid interpretation.

## 2.4 Discussion

Hanski *et al.* (1996) considered the amount of density-dependence necessary for population persistence using analytical and simulation models based on Levins' (1969) original presence/absence metapopulation model, incorporating random walk dynamics (Foley 1994) for local population sizes. The current models differ by using coupled map lattices, individual-based local dispersal, and a less extreme form of local density-dependence. Despite these differences, when applied to the same questions both approaches yielded similar qualitative results, suggesting that the conclusions are robust.

The parameters that had the greatest effect on metapopulation net growth rate were the mean and variance of the local rate of increase. Persistent metapopulations often had negative mean local reproductive rates (figure 2.5). Kuno (1981) proved mathematically that spatial heterogeneity in a well-mixed population enhances the overall growth rate and decreases variability in population size. The results obtained here demonstrate that this is true for even the smallest dispersal rate (figure 2.5) or dispersal distance (tables 2.2 and 2.3). The enhancement of overall growth rate by spatial heterogeneity may allow the persistence of a complex of otherwise non-persistent local populations (e.g. Hassell *et al.* 1991a; Adler 1993; Ruxton 1994; Hanski *et al.* 1996).

Factors which enhance metapopulation mean growth rate in the density-independent metapopulations would be expected to increase persistence time and the incidence of density-dependence in the density-dependent model. Increasing the local variance,  $v_r$ , enhanced metapopulation increase (figure 2.5), but also promoted heterogeneity, since local growth rates were assumed to be uncorrelated in time and space. Increasing the dispersal rate above  $\mu = 0.2$  had little effect on metapopulation growth rate (figure 2.5) as did dispersal distances,  $c$ , of greater than 24 neighbours (tables 2.2 and 2.3). Even with the greatest amounts of mixing (high  $\mu$  and  $c$ ), local stochasticity ensured that not all heterogeneity in local population densities was lost.

The results discussed above agree remarkably well with those of Hanski *et al.* (1996), suggesting that model structure has no biologically significant consequences for the conclusions. Unlike Hanski *et al.* (1996), however, this chapter deals in some detail with the effects of metapopulation size on persistence and the incidence of density-dependence. Their main model assumed that all subpopulations were equally accessible to dispersers (the 'island' model of Maynard Smith 1974), and so to be biologically reasonable they considered only metapopulations comprised of relatively few local populations (50). In their variant which used local dispersal, and therefore made it reasonable to consider much larger population complexes, they limited their analysis to metapopulations of 20 local populations. Whether this change of scale in itself significantly affected their results was not reported. Here, however, coupled map lattice models have been used, with individual-based local dispersal (the

‘stepping-stone’ model of Maynard Smith 1974), which realistically allow much more extensive complexes of subpopulations.

Large lattices allowed several local patch patterns to coexist (Hassell *et al.* 1991a, 1993), and persistence in such cases was of the order of evolutionary time (figure 2.6), sometimes with low mean density and very little incidence of density-dependence. For example, with the default parameter values and a 40×40 lattice, mean persistence time was 9609 generations, mean subpopulation size was 2% of the local carrying capacity, and the mean incidence of density-dependence,  $p(K_{hit})$ , was only 0.04% per subpopulation per generation (table 2.3). In large metapopulations (containing more than 30×30 subpopulations) the incidence of local density-dependence approached a rate of just one in every 4000 generations (figure 2.8). With  $p(K_{hit}) = 5\%$ , Hanski *et al.* (1996) could detect density-dependence using standard methods in only 40% of metapopulation time series longer than 20 generations. It is unlikely that density-dependence could be detected by similar techniques from the metapopulations presented here, where  $p(K_{hit})$  was often much smaller.

The incidence of density-dependence experienced in the models was often much lower than the 10-20% per subpopulation per generation typically observed in the models of Hanski *et al.* (1996), despite the fact that the ‘truncating ceiling’ density-dependence used here should result in more occurrences than their ‘reflecting ceiling’. One factor contributing to this was lattice size; there were generally fewer subpopulations in the metapopulations of Hanski *et al.* ( $H = 20$  or  $50$ ) than in those examined here ( $H = 1$  to  $2500$ ). The other explanation is that the current study has been particularly interested in exploring the boundary between persistence and extinction, and therefore used parameter sets which gave net metapopulation growth rates of  $r_p \cong 0$ . By contrast, Hanski *et al.* (1996) often used parameters which gave positive metapopulation growth ( $r_p > 0$ ) and therefore higher incidence of density-dependence.

Even with little density-dependence, mean densities for the metapopulations showed a tendency to equilibrate, and this equilibrium,  $N_{eq}$ , was often very low in comparison to the carrying capacity,  $K$ . For example, on a 50×50 lattice, local

population sizes were on average only 2% of their potential maximum, and this level was sustained for thousands of generations (table 2.3). This apparent sub-optimal use of resources arises from the assumption of incomplete mixing (local, rather than global, dispersal), and suggests a possible mechanism for ‘why the world is green’ (Harrison 1997). These results may also have implications for the study of rare but persistent species.

Overall, the results clearly demonstrate that metapopulation size may have an important effect on global persistence. It makes intuitive sense that longer persistence times were found on larger lattices: with an infinite lattice, the chance of all occupied subpopulations going extinct at the same time is infinitely small. This relationship has now been demonstrated explicitly, for both density-independent and density-dependent metapopulations (figure 2.6). Specifically, with the default parameters, mean persistence time saturates to a maximum of around 1800 generations for density-independent metapopulations, at sizes exceeding about  $40 \times 40$  subpopulations. In density-dependent metapopulations, however, persistence time is far greater, and increases monotonically with lattice width while the local incidence of density-dependence decreases to a minimum of approximately 0.03% per generation (figure 2.8).

But what size are real metapopulations? Citations of real metapopulation sizes range from around 60 local populations (see examples cited in Hanski 1994a) to more than a thousand (Hanski *et al.* 1995). While many of the real metapopulations that have been studied contain under 100 local populations ( $\sqrt{H} < 10$ ), some may contain several thousand. For example, the spatial dynamics of the western tussock moth, *Orgyia vetusta*, have been studied in detail (Harrison 1997; Maron & Harrison 1997; Wilson *et al.* 1999). This species exists in local populations on individual host plants (Harrison 1997), of which thousands may exist within a tussock moth metapopulation. Wilson *et al.* (1999) used a lattice of  $10^4$  local populations when modelling this system ( $\sqrt{H} = 100$ ). Likewise, agricultural landscapes may provide thousands of potential population sites (fields) for plants and animals. Indeed, the models may be particularly applicable to the dynamics of annual agricultural weeds. Many species, however, exist in metapopulations of intermediate scale, like the

arboreal marsupials studied by Lindenmayer *et al.* (1999) which have metapopulation sizes of approximately  $\sqrt{H} = 15$  patches, the model default.

Though metapopulation mean dynamics tended to resemble those of the standard logistic population growth model, the emergent equilibrium and rate of increase bore little resemblance to the values acting at the local population level. For example, the simulation shown in Fig. 2.9 had a metapopulation equilibrium at  $N_{eq} = 57$  and rate of increase  $r_p = 0.2$ , though the corresponding parameters at the subpopulation level were  $K = 100$  and  $r_m = 0.0$ . This highlights the danger of sampling populations at an inappropriate scale, in this case at too broad a scale to understand the mechanisms behind the dynamics. It would appear that in this case it is necessary to know the dynamics of subpopulations in space in order to understand the dynamics of the metapopulation in time.

## 2.5 Summary

Simulation models are described for metapopulations of individual-based random walk populations with local dispersal on a coupled map lattice. The models were used to assess the factors determining persistence time, in particular the incidence of density-dependence required for long-term persistence of a temporally and spatially stochastic metapopulation, the extent of persistence possible in the absence of density-dependence, and the factors that affect this.

Metapopulation persistence depended on the overall rate of increase of the metapopulation mean. This was maximised by (in order of importance) high mean and variance in the local rate of increase, high dispersal rates (20% or more of individuals dispersing each generation), large lattice size, and large dispersal range (to at least 24 neighbouring subpopulations).

With density-dependence, the emergent dynamics of the metapopulation mean following global perturbation (reduction in density) resembled those of the logistic growth model. However, the overall metapopulation rate of increase and equilibrium level bore no resemblance to those of the subpopulations: rate of increase was higher (negative mean local rates of increase may give positive overall growth), and

equilibrium mean metapopulation density was well below the local carrying capacity. This highlights the need to sample populations at an appropriate scale when seeking to understand regulatory mechanisms.

Metapopulations with the strongest tendency to grow gave the highest equilibrium mean density, the highest incidence of density-dependence, and the longest persistence time. However, long-term persistence with low average density and very low incidence of density-dependence was possible on a sufficiently large lattice. For example, with  $40 \times 40$  subpopulations, mean metapopulation persistence time was around  $10^4$  generations, with mean subpopulation size of 2% of the carrying capacity, and local density-dependence acting just once every 2500 generations on average. Metapopulation processes may explain our inability to detect density-dependence in many real populations, and may also play an important part in the persistence of rare species.

### 3. Can host-parasitoid metapopulations explain successful biological control?

#### 3.1 Introduction

The previous chapter showed how a metapopulation structure may allow long-term persistence of otherwise unstable populations. There, extinctions were caused by stochastic variations in the local population growth rate. This chapter deals with a deterministic system, in which population instability may be caused by the interaction between host and parasitoid. Host-parasitoid systems may be exploited for pest control, and so are one of the most economically important biological interactions.

Parasitoids introduced for classical biological control may often cause a permanent reduction of 90% or more in field populations of their hosts (Beddington *et al.* 1978). This has been interpreted to mean that a successful biocontrol agent drives its host to a low stable equilibrium. However, conventional simple models, lacking either implicit or explicit spatial heterogeneity of risk, cannot reproduce stable host reductions of greater than 60% (Beddington *et al.* 1978).

As a mechanism for stability in host-parasitoid models, implicit spatial heterogeneity was an early suggestion (Varley 1947; Bailey *et al.* 1962; Hassell & Varley 1969). Beddington *et al.* (1978) showed that it also provided the most likely mechanism for high host suppression. Later, explicitly spatial metapopulation models (Levins 1969; Hanski & Gilpin 1991; Hanski & Simberloff 1997) showed that dispersal between subpopulations may allow long-term persistence of an otherwise non-persistent interaction, though the stability *per se* of the equilibria was unaffected (Reeve 1988, 1990; Rohani *et al.* 1996; Rohani & Ruxton 1999). Even as few as two subpopulations linked by dispersal may allow persistence of unstable host-parasitoid models (Adler 1993). This result relies on asynchrony in subpopulation dynamics (Crowley 1981), so that local population extremes may be buffered by dispersal to

and from surrounding localities. It also demonstrates that stability is not a necessary condition for a persistent host-parasitoid interaction, so long as the system is divided into discrete, semi-independent subpopulations (Murdoch *et al.* 1985).

Long-term persistence of a locally unstable host-parasitoid metapopulation was demonstrated by Allen (1975) and Hassell *et al.* (1991a), the latter emphasising the remarkable range of dynamic behaviour emerging from the simplest host-parasitoid metapopulation models with local dispersal. Their demonstration of self-organising spatial patterns in such systems led to considerable subsequent research and debate (e.g. Comins *et al.* 1992; Hassell *et al.* 1993, 1994; Rohani & Miramontes 1995; Comins & Hassell 1996; Ruxton & Rohani 1996; Rohani *et al.* 1997; Savill *et al.* 1997; Sherratt *et al.* 1997; Wilson & Hassell 1997).

This chapter considers how realistic these spatial patterns are, and whether such behaviour can occur in more realistic models which include local host density-dependence. In terms of biological control, this chapter investigates whether persistence is possible with high overall host suppression in a metapopulation context, and what form the overall model for such a metapopulation takes. More generally, this work asks whether non-spatial models may be sufficient to capture the dynamics of a spatial world, and if so, how? Is it necessary to understand the behaviour of a population in space in order to understand and predict its behaviour in time?

## **3.2 Models and methodology**

Few host-parasitoid models have dealt in a general way with the effects of explicit host density-dependence. The following sections describe general local and metapopulation models, and look in particular at the effects of host density-dependence, handling time, and aggregated attack.

### **3.2.1 General host-parasitoid models**

The models assume a typical insect life cycle for the host (figure 3.1), in which density-dependent mortality or parasitism may occur on the larval, pupal, or adult



**Figure 3.1** A general insect host life cycle.

stages. It is assumed that host larvae are the stage of interest, and peak densities of this stage in generation  $t$  are denoted  $N_t$ . Similarly, the density of adult parasitoids is denoted  $P_t$ . Since the host egg stage is assumed to experience neither density-dependence nor parasitism, host reproduction is always the last process to occur in each generation. The host reproductive rate is given by  $\lambda$ , the ratio of the densities of successive generations of larvae in the absence of density-dependent mortality and parasitism. The proportions of hosts surviving parasitism and density-dependence are given by the functions  $f(N_t, P_t)$  and  $g(N_t)$  respectively. Each parasitised host is assumed to give rise to exactly one adult parasitoid in the next generation.

The order in which density-dependent mortality and parasitism occur in the host life cycle gives rise to three different models, as detailed in appendix 4.1. In model 1, parasitism acts before density-dependence, giving

$$\begin{aligned} N_{t+1} &= \lambda N_t f(N_t, P_t) g(N_t f(N_t, P_t)) \\ P_{t+1} &= N_t [1 - f(N_t, P_t)] \end{aligned} \quad (3.1)$$

In model 2, density-dependence precedes parasitism:

$$\begin{aligned} N_{t+1} &= \lambda N_t g(N_t) f(N_t g(N_t), P_t) \\ P_{t+1} &= N_t g(N_t) [1 - f(N_t g(N_t), P_t)] \end{aligned} \quad (3.2)$$

And in model 3, density-dependence acts on the parasitised host stage, so that both parasitised and unparasitised hosts contribute to the density-dependent effect:

$$\begin{aligned} N_{t+1} &= \lambda N_t g(N_t) f(N_t, P_t) \\ P_{t+1} &= N_t g(N_t) [1 - f(N_t, P_t)] \end{aligned} \quad (3.3)$$

In these equations, the parasitism function,  $f(N,P)$ , describes the proportion of  $N$  host larvae surviving parasitism by  $P$  parasitoids. Similarly, host density-dependence is described by the function  $g(N)$ , which gives the fraction of  $N$  hosts surviving density-dependent mortality. The biological differences between the models are illustrated by May *et al.* (1981), whose figures 2a, 2b and 3 correspond respectively to equations 3.2, 3.3, and 3.1 above. Unlike those of May *et al.* (1981), models 1 to 3 above allow for parasitism functions which depend on the densities of both host and parasitoid populations, such as those suggested by Thompson (1924), Holling (1959), or Hassell (1980). If, however, the parasitism function is independent of host density, as in the models of Nicholson and Bailey (1935) or May (1978), then models 2 and 3 are identical, and the equations collapse to those of May *et al.* (1981).

### 3.2.2 Parasitism functional forms

The simplest host-parasitoid model (Nicholson & Bailey 1935) assumes that parasitoid attack is random, and is therefore modelled by the zero-term of the Poisson distribution:  $f(N,P) = e^{-aP}$ , where  $a$  is the characteristic area of discovery, or ‘searching efficiency’ of the parasitoid. Another common model assumes aggregated attack (May 1978) modelled by the zero term of the negative binomial distribution:  $f(N,P) = (1 + aP/k)^{-k}$ , where  $k$  defines the degree of aggregation, and attack becomes random as  $k$  gets very large. Hassell (1980) showed that  $k$  may itself depend on host density, suggesting  $f(N,P) = (1 + aP/wN)^{-wN}$  where the coefficient  $w$  modifies the density-dependence effect. Another model arises when searching parasitoids interfere with each other:  $f(N,P) = \exp(-aP^{1-m})$  (Hassell & Varley 1969). This is usually referred to as ‘pseudo-interference’ since the same effect can arise through spatial aggregation in the absence of actual interference (Free *et al.* 1977).

All of these parasitism functions assume that parasitoids have infinite fecundity, but are limited by their ability to find suitable hosts. An alternative assumption is that parasitism is limited by parasitoid fecundity (Thompson 1924). This effect is captured by Holling’s (1959) Type II functional response, where handling time effectively limits the number of hosts able to be attacked by an adult parasitoid and may therefore be interpreted as proportional to the inverse of parasitoid fecundity (Barlow & Wratten 1996). Handling time may be modelled by replacing  $a$  in the

preceding functions with  $a/(1 + ahN)$ , where  $h$  is the proportion of the total available searching time which is used in handling (parasitising) each prey encountered. The predator-prey literature, reviewed by Barlow and Wratten (1996), describes a range of other functional responses which may be biologically appropriate. The parasitism functions discussed above are summarised in table 3.1.

### 3.2.3 Host density-dependence

Many simple host-parasitoid models make the assumption that parasitism is the major proximate cause of host regulation, and therefore that host density-dependence is unimportant. In the general models described above, this corresponds to  $g(N) = d$ , and  $d = 1$  if  $\lambda$  includes all density-independent mortality. In this case, all three general models become the same:

$$\begin{aligned} N_{t+1} &= \lambda N_t f(N_t, P_t) \\ P_{t+1} &= N_t [1 - f(N_t, P_t)] \end{aligned} \tag{3.4}$$

Explicit host density-dependence may be modelled by a range of functional forms, a selection of which are listed by May and Oster (1976). These typically assume a host ‘carrying capacity’, denoted  $K$ , above which densities tend to decline as a result of over-crowding. Here, the widely-used Ricker function (Ricker 1954) is adopted:  $g(N) = e^{-rN/K}$ , where  $e^r = \lambda$  (table 3.1).

**Table 3.1** Some common parasitism and density-dependence functional forms.

Name	Model	Reference
random parasitoid attack	$f(N,P) = \exp(-aP)$	Nicholson and Bailey (1935)
aggregated attack	$f(N,P) = (1 + aP/k)^{-k}$	May (1978)
density-dependent aggregation	$f(N,P) = (1 + aP/wN)^{-wN}$	Hassell (1980)
pseudo-interference	$f(N,P) = \exp(-aP^{1-m})$	Hassell and Varley (1969)
random attack + handling time	$f(N,P) = \exp[-aP/(1+ahN)]$	Holling (1959)
no host density-dependence	$g(N) = 1$	
Ricker density-dependence	$g(N) = \exp(-rN/K)$	Ricker (1954)

### 3.2.4 Parameter values

Default parameter values for the models (table 3.2) were chosen so as to be biologically reasonable, and also to scale the equilibrium host and parasitoid densities for the simplest host-parasitoid model ( $f(N,P) = e^{-aP}$ ,  $g(N) = 1$ , Nicholson & Bailey 1935) to  $N_{eq} = 1.0$  and  $P_{eq} = 0.5$  (appendix 4.2). This provided a convenient benchmark with which to compare the magnitude of the host carrying capacity  $K$  and its effects. A wide range of values was explored for the parameters  $r$  and  $K$ . In many host-parasitoid models searching efficiency,  $a$ , has the same affect on model dynamics as host carrying capacity,  $K$  (May *et al.* 1981; Hochberg & Lawton 1990). The results, therefore, could equivalently be expressed in terms of the product  $aK$ , which is a measure of parasitoid efficiency (Beddington *et al.* 1978) and for some models may also represent the ‘basic reproductive rate’ of the parasitoid (May & Hassell 1988; Hochberg & Lawton 1990).

**Table 3.2** Model parameters and their default values.

Parameter	Meaning	Default value
<i>local model parameters:</i>		
$\lambda$	host fecundity = $\exp(r)$	2.0
$r$	host reproductive rate = $\ln(\lambda)$	0.693
$K$	host carrying capacity	2.0
$a$	parasitoid searching efficiency	1.386
<i>metapopulation parameters:</i>		
$\mu_N$	host dispersal rate	0.5
$\mu_P$	parasitoid dispersal rate	0.5
$H$	lattice size	30×30
$B$	boundary condition	reflecting

### 3.2.5 Metapopulation structure

Individual subpopulations with dynamics as described above were assembled into a coupled map lattice metapopulation (Kaneko 1989) of  $30 \times 30$  habitat patches ( $H = 900$ ). Following Comins *et al.* (1992), reflecting lattice boundaries were adopted (figure 2.2). Dispersal was assumed to be density-independent, with constant proportions  $\mu_N$  of adult hosts and  $\mu_P$  of parasitoids being distributed evenly among the nearest eight neighbouring populations at each generation ( $c = 8$ ; figure 2.1). It was assumed that hosts disperse as adults. Since both dispersal and reproduction were density-independent and occurred together in the life cycle, their ordering was unimportant. Therefore, dispersal was implemented at the end of each time step, after the local dynamics.

Following Comins *et al.* (1992), a lower threshold was imposed on local host and parasitoid densities in the models, avoiding any possible effects of unrealistically low densities. Local densities lower than  $10^{-3}$  (corresponding to 1/1000 of the Nicholson-Bailey host equilibrium) were set to zero; this is equivalent to an ‘Allee effect’ (Allee *et al.* 1949, p.393). An alternative, the use of individual-based spatial host-parasitoid models, was shown by Wilson and Hassell (1997) to increase local fluctuations and the likelihood of extinction, but with little effect on spatial dynamics.

### 3.2.6 Initial conditions

Comins *et al.* (1992) used two different configurations to initialise their host-parasitoid metapopulations. The first, termed ‘co-introduction’, involves both host and parasitoid being introduced together at one point in an otherwise empty lattice. When persistence was not possible from this configuration, Comins *et al.* (1992) used a ‘parameter shift’ initial condition, whereby the model parameters were adjusted to those desired from an established, persistent metapopulation simulation. In this chapter, a third, ‘biocontrol’ initial condition is predominantly used, with hosts initialised globally to their parasitoid-free equilibrium,  $K$ , and parasitoids introduced at a single location. In general, site (3,1) at the edge of the lattice was used for introduction, though a range of other introduction sites were also investigated.

### 3.3 Results from non-spatial models

Comins *et al.* (1992) showed that heterogeneity in a coupled map lattice metapopulation depends on the stability of local dynamics. When local dynamics are stable, heterogeneity decays and the metapopulation behaves similarly to a single local population. Therefore, it was useful firstly to examine the dynamics of the local host-parasitoid models without the complication of spatial structure.

#### 3.3.1 Relationship between parasitism and host suppression

One of the simplest and most frequently measured indicators of parasitoid activity in the field is the proportion of sampled hosts that are parasitised. While this does not give a direct indication of the success of biological control, it can be related to host suppression using the general models of equations 3.1 to 3.3. Denoting the proportion of hosts parasitised in generation  $t$  as  $Q_t$ , and recalling the model assumption that each parasitised host gives rise to exactly one searching adult parasitoid in the following generation, then  $Q_t = P_{t+1}/N_t$ . It may then be shown (appendix 4.3) that the proportion of hosts parasitised at equilibrium,  $Q_{eq}$ , is related to the equilibrium host and parasitoid densities,  $N_{eq}$  and  $P_{eq}$ , as

$$Q_{eq} = 1 - \frac{1}{\lambda g(N_{eq} - P_{eq})} \quad (3.6)$$

for model 1, and

$$Q_{eq} = 1 - \frac{1}{\lambda g(N_{eq})} \quad (3.7)$$

for models 2 and 3. These are general solutions for the models at equilibrium. Specific equilibrium solutions depend on the form of the density-dependence function,  $g(N)$ . For example, with Ricker hosts density-dependence (table 3.1), and defining  $(1 - q)$  to be the level of host suppression at equilibrium, where  $q = N_{eq}/K$ , then models 2 and 3 (equation 3.7) suggest

$$1 - q = -\ln\left(1 - Q_{eq}\right) \left(\frac{1}{r}\right) \quad (3.8)$$

(appendix 4.4). Here, the logarithm term captures the parasitism effect, which is then discounted by the ability of the host to compensate for this according to its rate of increase. If the host grows slowly, then a low realised proportion parasitised may be sufficient to give substantial host suppression (Figure 3.2). On the other hand, fast-growing hosts may require very high levels of parasitism in the field in order to achieve biological control.

Model 1 is slightly more complicated, requiring both the host density-dependence and parasitism functions,  $g(N)$  and  $f(N,P)$ , to be defined in order to obtain an explicit equilibrium solution. As an example, with random parasitoid search and Ricker density-dependence (table 3.1), the equilibrium solution (appendix 4.4) is

$$1 - q = -\ln(1 - Q_{eq}) \left( \frac{1}{r} - \frac{1}{aK} \right) \quad (3.9)$$

In this case, the ability for the host to compensate for parasitism is reduced by the parasitoid's own basic reproductive rate,  $aK$ , and biological control will be more difficult to achieve.

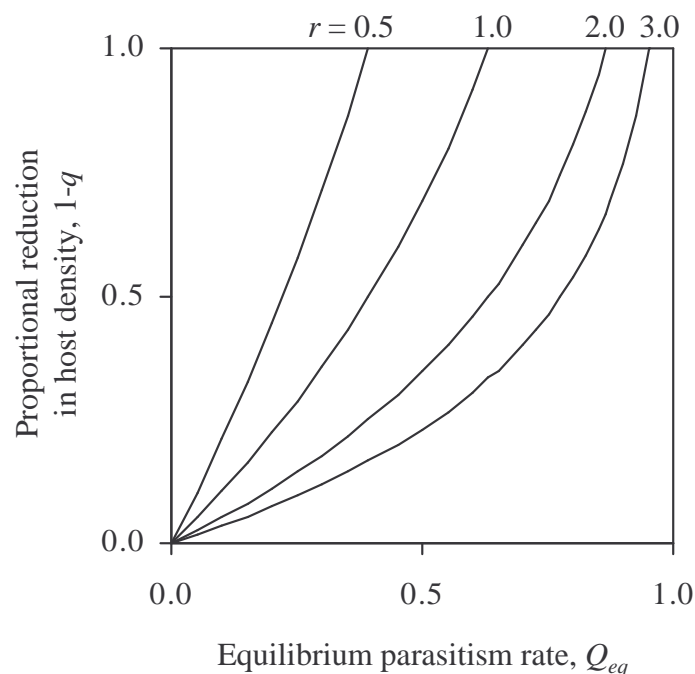


**Figure 3.2** Relationship between the proportion of hosts parasitised at equilibrium,  $Q_{eq}$ , and proportional reduction in host density,  $1-q$ , for non-spatial host-parasitoid models with Ricker host density-dependence occurring before emergence of parasitoids.

### 3.3.2 Stability and host suppression

May *et al.* (1981) present stability diagrams for models 1 to 3 with Ricker host density-dependence and aggregated parasitoid attack. Similar results were obtained here by numerical simulation, and following Hochberg and Lawton (1990) they are presented in parameter space (figure 3.3) rather than as functions of  $q$ , giving a better indication of which results are likely under realistic circumstances. In all of the cases investigated, searching efficiency,  $a$ , had the same affect on model stability as carrying capacity,  $K$ . At high host reproductive rates the Ricker map by itself exhibits period-doubling (for  $r > 2$ ) and deterministic chaos (for  $r > 2.7$ ) (May & Oster 1976). Results for  $r > 2$  should therefore be treated with caution.

With Ricker density-dependence and random parasitoid attack (appendix 4.5), model 1 was stable only for low values of the host carrying capacity, while models 2 and 3 exhibited stability in a wider area of parameter space (figure 3.3). Maximum host suppression was just over 50% for model 1, where host density-dependence could immediately compensate for any parasitism-induced mortality. In fact, when  $r$  was high, adding a parasitoid sometimes increased host equilibrium density, as noted by May *et al.* (1981). Higher levels of host suppression were possible in models 2 and 3, where host density-dependence did not have the chance to compensate for parasitism.

Handling time had only minor effects on the area of stable parameter space shown in figure 3.3(a) and (b). Models 2 and 3 differed with handling time, which had the effect of shifting stable parameter space slightly toward lower  $r$  values. Model 3 with handling time  $h = 0.1$  was stable over a noticeably narrower band of  $r$  values (figure 3.3(e)), but model 1 showed stable dynamics for a wider range of  $a$  and  $K$  values (figure 3.3(c)). This concurs with the results of Barlow and Wratten (1996), who demonstrated that handling time may be either stabilising or destabilising depending on the values of other parameters.

Aggregated parasitoid attack, with  $k = 1.2$ , greatly enhanced the area of  $r$ - $K$  parameter space in which stability was observed, and also allowed greater levels of host suppression to be achieved (figure 3.3(f) and (g)).

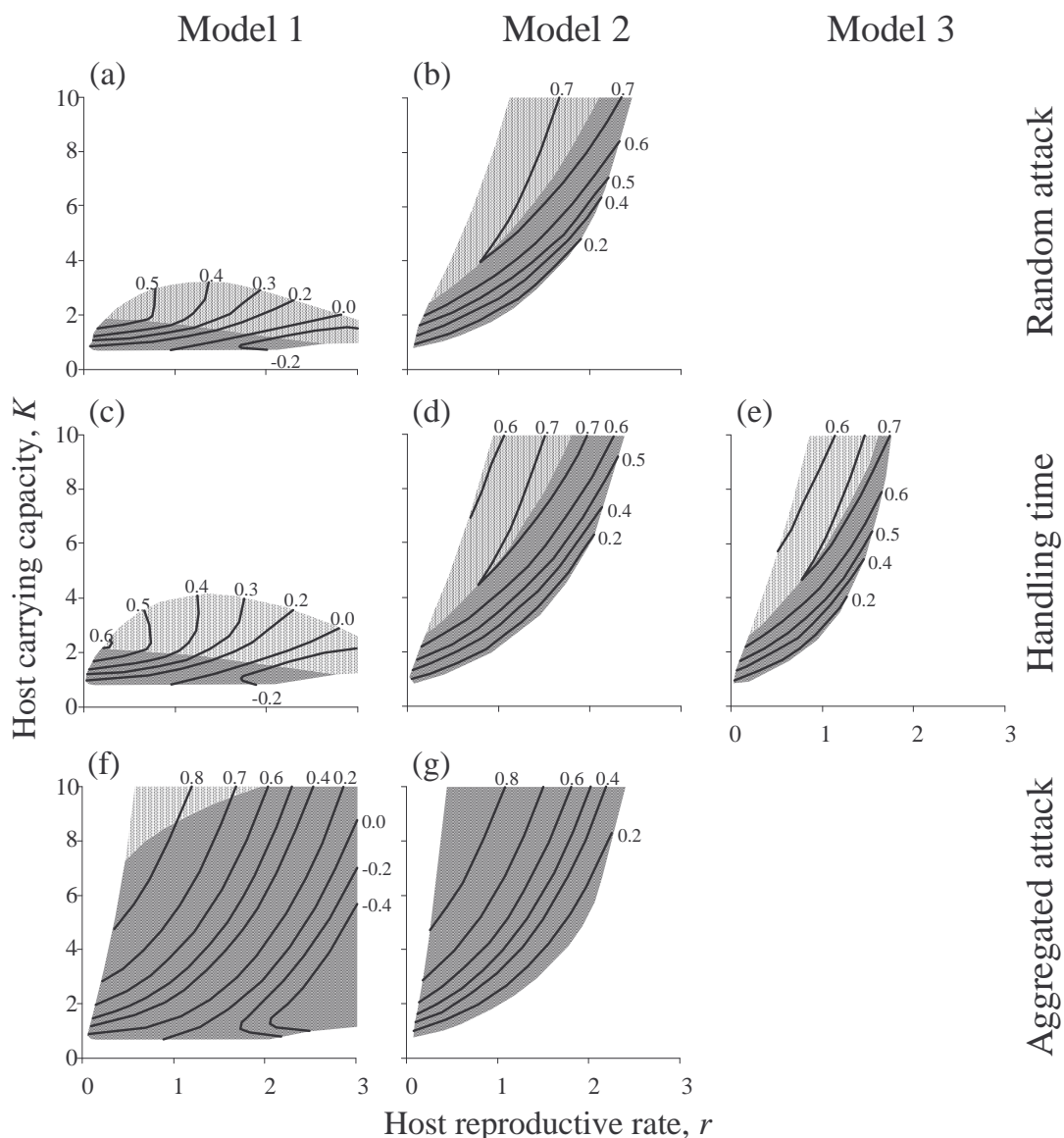


**Figure 3.3** Stability boundaries (dark shaded = stable, light = stable limit cycles, white = unstable) and mean proportional reduction in host density,  $1-q$ , (contours) in non-spatial models, for different combinations of host rate of increase,  $r$ , and carrying capacity,  $K$ .

Figures (a) and (b) show results for random parasitoid attack and Ricker host density-dependence: (a) density-dependence acting after parasitism (model 1); (b) density-dependence acting before parasitism or on parasitised hosts (models 2 and 3).

Figures (c) to (e) include handling time ( $h = 0.1$ ): (c) density-dependence acting after parasitism (model 1); (d) density-dependence acting before parasitism (model 2); (e) density-dependence acting on parasitised hosts (model 3).

Figures (f) and (g) are without handling time, but include aggregated parasitoid attack ( $k = 1.2$ ): (f) density-dependence acting after parasitism (model 1); (g) density-dependence acting before parasitism or on parasitised hosts (models 2 and 3). See table 3.2 for other parameter values.

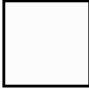




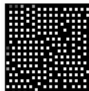
## 3.4 Results from metapopulation models

### 3.4.1 Spatial heterogeneity and patterning

The spatial patterns emerging from the metapopulation model were intimately linked to the stability properties of the local population model (table 3.3), and were consistent for all local parasitism and density-dependence functions tested. The most interesting spatial dynamics always emerged when local populations were unstable. Initial ‘target’ patterns of radiating waves, as found by Allen (1975) gave way on interaction with the symmetry-breaking boundary conditions, to give ‘spirals’, ‘spatial chaos’, and ‘crystal lattice’ patterns (Hassell *et al.* 1991a). Rohani and Miramontes (1995) identified another characteristic pattern, in which large spirals coexisted with small, for a model with more complex parasitoid dispersal rules. All of these patterns were composed of curved wave fronts, each spiralling around a central focus point with more stable than usual emergent dynamics (Comins *et al.* 1992). This was found to provide a convenient method of detecting foci, by tallying the maximum density experienced in each cell over a few time steps. Czárán and Bartha (1992) postulated that the spatial patterns observed in models of this type differ only in the number and size of spirals present in the lattice. By counting spiral foci (table 3.3) the current study has shown that this appears to be true, and the number of spiral foci present provides a convenient way of quantifying these spatial patterns. For all metapopulations with persistent spatial heterogeneity, the coefficient of variation squared of parasitoids per host ( $CV^2$ : appendix 4.6; Hassell & May 1988; Comins *et al.* 1992) was around 1 (table 3.3).

When local dynamics were oscillatory (with stable limit cycles) a small amount of spatial heterogeneity was maintained in the metapopulation, giving rise to a ‘regionally synchronised’ pattern of gentle density gradients. In this case, the homogenising influence of dispersal was not powerful enough to overcome the tendency for local populations to oscillate, but did synchronise the oscillations of neighbouring subpopulations. With stable local dynamics, metapopulation densities

**Table 3.3** Comparison of different spatial patterns emerging from a host-parasitoid coupled map lattice. Local dynamics feature random parasitoid attack and Ricker host density-dependence occurring after parasitism (model 1; appendix 4.5). Parameter values as for table 3.2 except as listed.

Non-default parameters	Local dynamics	Metapopulation pattern <sup>†</sup>	Visual pattern	CV <sup>2</sup> of parasitism	Spiral density
$K = 1.5$	converging oscillations (stable)	homogeneous		0.00	0
$K = 2.5$	stable limit cycles	regionally synchronised		0.99	0
$K = 10$ $\mu_N = 0.9$	diverging oscillations (unstable)	large spiral		1.66	1
$K = 10$ $\mu_N = 0.3$	diverging oscillations (unstable)	small spirals		1.57	9
$K = 10$ $\mu_N = 0.1$	diverging oscillations (unstable)	spatial chaos		0.82	13
$K = 20$ $\mu_N = 0.01$ $\mu_P = 0.99$	exponentially unstable	crystal lattice		1.07	≈650

<sup>†</sup>using the notation of Hassell *et al.* (1991)

rapidly homogenised, and the overall dynamics became the same as those for the local populations. However, the metapopulation structure was still important in governing the transient behaviour after local perturbations.

Comins *et al.* (1992) showed that moderate levels of stochastic local perturbation had little effect on the persistence and patterning of their metapopulations, while Ruxton and Rohani (1996) showed that stochasticity in their similar model did not affect the ability of competing parasitoids to coexist, though it did make spatial patterns less recognisable. Similarly, the same spatial patterns were present, but less clearly defined, in a variant of the basic metapopulation model in which host carrying capacity was allowed to vary randomly (from a uniform distribution between 0 and  $2K$ ) in space but not time. As in Comins *et al.* (1992), the choice of boundary

conditions had little effect on the patterns generated, but did have some effect on the temporal dynamics of the metapopulation. In particular, absorbing boundaries imposed an additional mortality, which resulted in more metapopulation extinctions than for other boundary types.

The site of introduction for the biocontrol and co-introduction initial conditions had little effect on the model dynamics. However, pattern formation depended on the interaction between initial travelling waves and lattice boundaries, so patterns formed most rapidly when the introduction site was close to a boundary, such as the default site at position (3,1).

Long-term host-parasitoid persistence depended on the ability of the metapopulation to contain the type of spatial pattern that emerged (Hassell *et al.* 1993), implying a threshold metapopulation size necessary for the persistence of an unstable biological control interaction. Large spirals required large lattices, while small spirals (e.g. crystal lattice pattern) could persist in tiny lattices. The size of a pattern, conveniently measured by the inverse of the number of spiral foci in the lattice, was determined by the width of its radiating wave-front, which in turn depended on the dispersal probabilities of host and parasitoid as well as the ‘return time’ of the host (time taken for host population to recover after a wave of parasitism). Different patterns arose from different dispersal rates (table 3.3; Hassell *et al.* 1991a), and longer-range dispersal could destabilise a metapopulation by increasing the size of patterns beyond what could be contained in the lattice (Rohani & Miramontes 1995). The default lattice size,  $H = 30 \times 30$ , was sufficient to give spatial dynamics similar to much larger lattices (e.g.  $H = 256 \times 256$  in Solé *et al.* 1992b).

### 3.4.2 Initialisation and transient behaviour

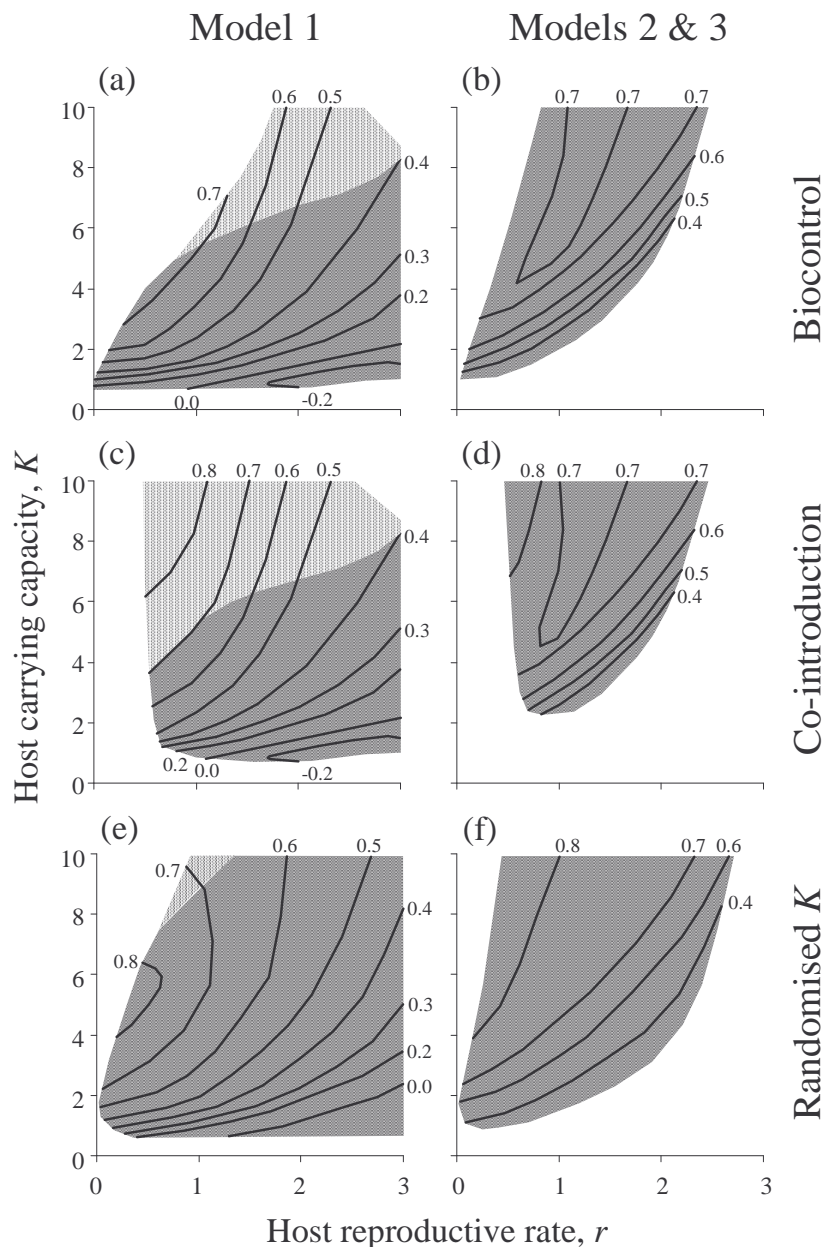
Biological control programs most often fail because of unsuccessful parasitoid establishment (Waage 1990). Successful biocontrol introduction in the models required that the parasitoid establish itself without causing large amplitude oscillations in host densities. If the initial wave of parasitism left sub-threshold host densities in its wake then parasitoids became extinct once the wave reached the

metapopulation boundaries. This occurred when the host's carrying capacity, and hence the initial density on contact with the parasitoids, was high (figure 3.3(a) and (b)). For a co-introduction, however, initial persistence depended primarily on the ability of the host to establish and provide a resource for the parasitoid. This required adequate host reproductive rate and carrying capacity (figure 3.3(c) and (d)).

Similar principles applied when considering perturbations to the metapopulation: any perturbation that induced large-amplitude oscillations could lead to metapopulation extinction. Perturbations that affected the whole metapopulation simultaneously were the most likely to cause extinction of host or parasitoid. The 'spirals' metapopulation of table 3.3 was unable to persist after an 86% global reduction in host density, yet survived complete removal of hosts from 99% of the subpopulations. Of the metapopulations with unstable local dynamics illustrated in table 3.2, the 'spatial chaos' pattern could withstand the greatest global reduction in host densities (97%), while the 'crystal lattice' pattern was the least robust, being unable to persist after a 79% global reduction in hosts.

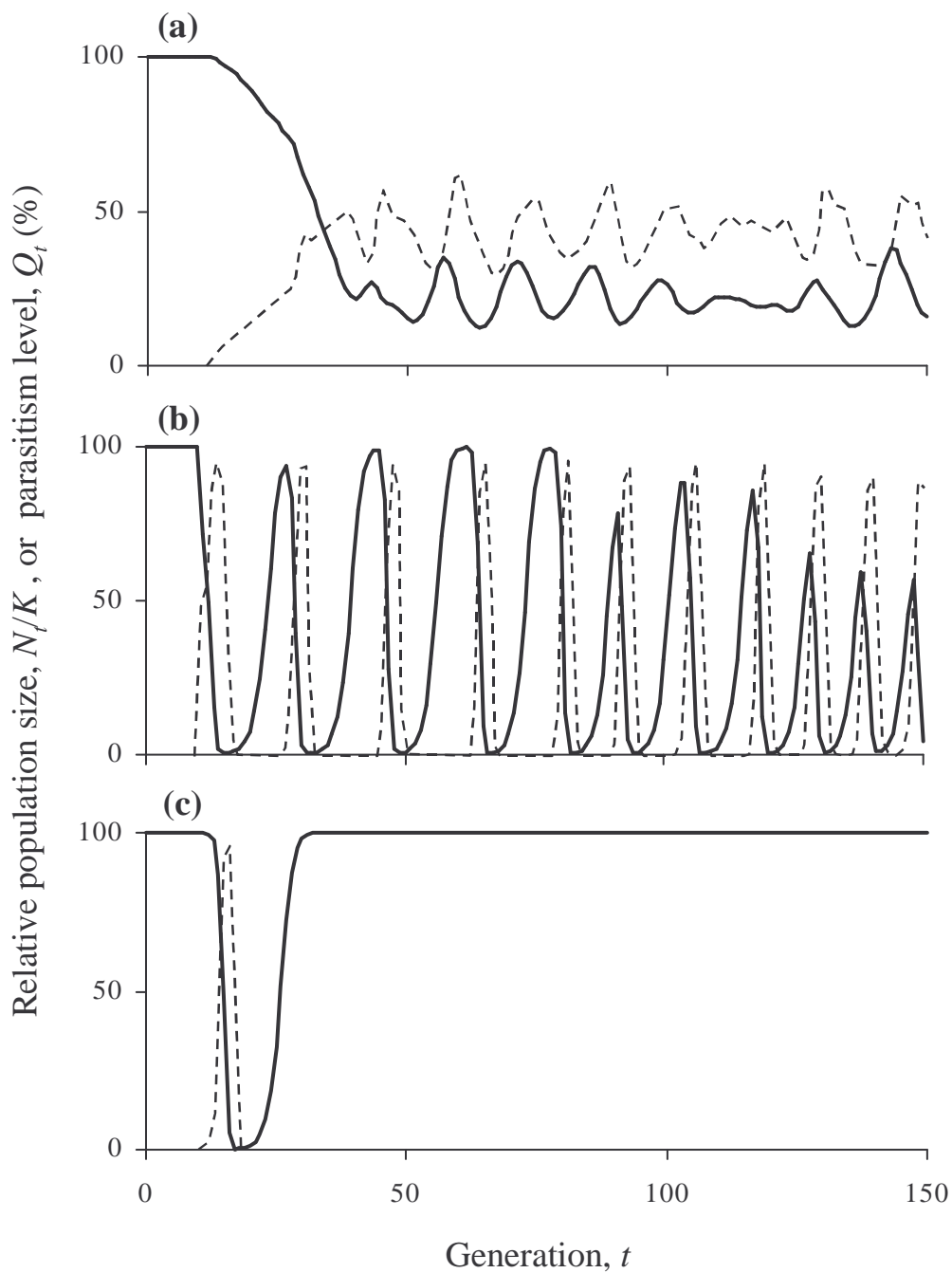
### 3.4.3 Host suppression

Figure 3.4 shows levels of host suppression achieved in the metapopulations. The area of parameter space in which metapopulations persisted was larger than for the non-spatial equivalents (figure 3.3) because local dispersal relaxed the requirement for stable local dynamics. The extra area of persistent parameter space allowed for greater host suppression on average than local dynamics alone could predict. For density-dependent metapopulation models with random parasitoid attack, the greatest mean host suppression,  $1-q$ , possible from a biocontrol initialisation was approximately 84%, compared with around 60% for the non-spatial equivalent (Beddington *et al.* 1978). This result was robust to variation in the spatial model parameters, such as dispersal rates and lattice size. Figure 3.5 compares the metapopulation, local, and non-spatial dynamics for a simulation in which mean host suppression was 78%. With spatial variation in host carrying capacity, high mean host suppression was possible over a wider range of parameter space (figure 3.4(e) and (f)), but 84% remained the maximum mean suppression level possible.



**Figure 3.4** Metapopulation persistence (dark shaded = persistent; light = persistence may be dependent on which lattice cell introduction occurs in; white = non-persistent) and mean proportional reductions in host density,  $1-q$ , (contours) for different combinations of host rate of increase,  $r$ , and carrying capacity,  $K$ . The model assumes random parasitoid attack, Ricker host density-dependence, and other parameter values as in table 3.2.

Figures (a) and (b) show results from a ‘biocontrol’ introduction, with the parasitoid introduced at location (3,1) of a  $30 \times 30$  lattice with hosts at their carrying capacity; (c) and (d) have ‘co-introduction’, with host and parasitoid introduced together at location (3,1) of an empty lattice; (e) and (f) are as for (a) and (b) but with local carrying capacity randomised (uniformly distributed between 0 and  $2K_p$ ) in space but not time. Figures (a), (c), and (e) have density-dependence acting after parasitism (model 1); (b), (d), and (f) have density-dependence acting before parasitism or on parasitised hosts (models 2 and 3);



**Figure 3.5** An example of high average host suppression from a biological control initialisation (at generation 10), assuming Ricker host density-dependence before random parasitism, and all parameters at their default values except that  $K = 8.0$  and  $\mu_p = 0.8$ . Solid line = host density relative to the carrying capacity, dashed line = percent parasitism.

Figure (a) metapopulation means (mean host suppression = 78%); figure (b) local population values at point of introduction; figure (c) corresponding local dynamics without spatial structure. Discrete generation values are joined with lines to aid interpretation.

Co-introduction or parameter shift initial conditions, however, allowed higher host suppression levels to be achieved, since these avoided the problem of large-amplitude initial oscillations which prevented persistence of the same interaction with a biocontrol starting point. Any level of host suppression was possible with a parameter-shift initialisation, because once the host was being regulated by the parasitoid rather than by its own density-dependence,  $K$  could be increased to any value. With  $K \rightarrow \infty$  the models become equivalent to the density-independent metapopulation model of Comins *et al.* (1992), in which parameter-shift initialisation was often required.

#### 3.4.4 Metapopulation mean dynamics

Overall metapopulation dynamics were investigated by fitting parasitism and host density-dependence functions to the metapopulation mean host and parasitoid densities. The scenarios listed in table 3.3 were used as starting conditions, and host and parasitoid densities were reduced by 80% globally after every 100 generations. Mean host and parasitoid densities were tallied over the whole metapopulation for 300 generations, and every second generation was excluded in order to increase the statistical independence of data points. Parasitism, then host density-dependence functions, as listed in table 3.1, were fitted to the data using non-linear least-squares in Genstat 5 (Genstat 5 Committee 1993).

Fitting simple models to the metapopulation dynamics was always most successful when local dynamics were stable (figure 3.6(a)). In these situations, with the absence of spatial heterogeneity, the global dynamics simply represented the local dynamics and it was possible to get a perfect fit ( $R^2 = 100\%$ ) and correct estimates for the model parameters with the appropriate model (appendix 4.7). Good fits ( $R^2 > 98\%$ ) and accurate parameter estimates were also possible with regionally synchronised metapopulations. Where the local dynamics were unstable, however, simple models had limited success at capturing metapopulation mean dynamics. For example, the mean densities in a metapopulation exhibiting spatial chaos (table 3.2, figure 3.6(d)) were best represented by random parasitism (appendix 4.7,  $R^2 = 76\%$ )

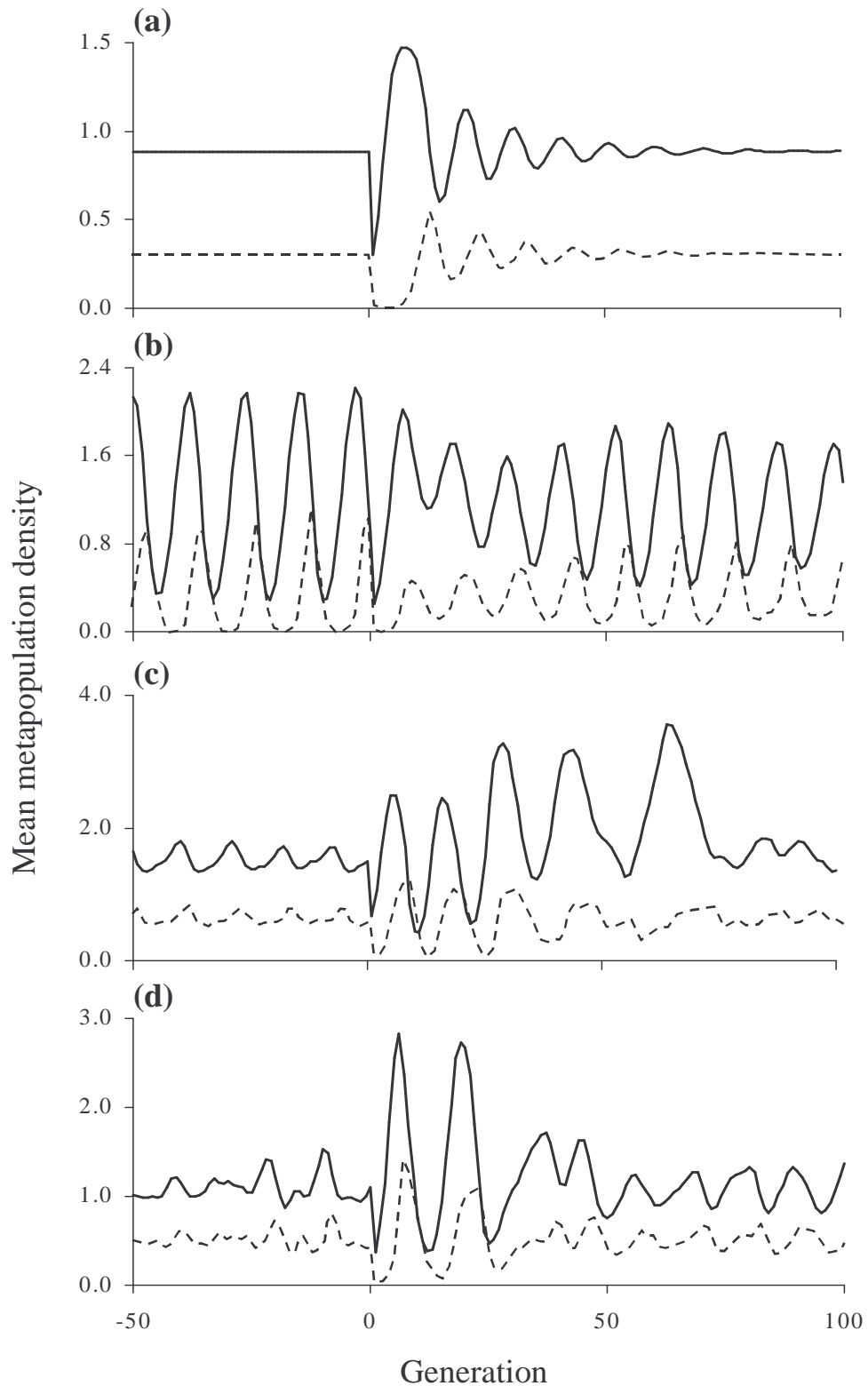


**Figure 3.6** Mean metapopulation trajectories (solid line = hosts, dashed line = parasitoids) for four of the patterns listed in table 3.2. Both host and parasitoid are reduced globally by 80% at generation 0. Figure (a) homogeneous,  $K = 1.5$ ; (b) regionally synchronised,  $K = 2.5$ ; (c) large spiral,  $K = 10$ ,  $\mu_N = 0.9$ ; (d) spatial chaos,  $K = 10$ ,  $\mu_N = 0.1$ . Discrete generation values are joined with lines to aid interpretation.

and host density-independence ( $R^2 = 92\%$ ), which together form the unstable and non-persistent Nicholson-Bailey model (Nicholson & Bailey 1935) despite the persistent dynamics of the metapopulation to which the model was fitted. Similar results were obtained for a metapopulation exhibiting large spirals (table 3.2, figure 3.5(c), table 3.6,  $R^2 = 73\%$  for parasitoid equation, 96% for host). The estimates for model parameters obtained by this method were typically very different from their true local population values. For example, estimates for the parasitoid searching efficiency,  $a$ , were around half the true value (appendix 4.7).

Neither of the simple models which purport to mimic spatial parasitism effects (aggregated attack, pseudo-interference) gave better fits to mean metapopulation dynamics than the simplest random attack model. This was even the case when local dynamics included these effects explicitly, except when the local dynamics were stable.

### 3.4.5 Emergent subpopulation dynamics

Simple models were also fitted to the dynamics emerging from a subpopulation in the assemblage. In addition to the models fitted above, the effects of dispersal were modelled by adding a constant at the end of each equation, representing the net immigration of either host ( $N_{imm}$ ) or parasitoid ( $P_{imm}$ ) each generation. Thus model 1 (equations 3.1) became:

$$\begin{aligned} N_{t+1} &= \lambda N_t f(N_t, P_t) g(N_t f(N_t, P_t)) + N_{imm} \\ P_{t+1} &= N_t [1 - f(N_t, P_t)] + P_{imm} \end{aligned} \tag{3.10}$$

Perturbations were applied by reducing both host and parasitoid densities to zero in the subpopulation being tallied. Recovery from local perturbations (figure 3.7) was much more rapid than for mean population density after global perturbation (figure 3.6) because of immigration from surrounding populations. When dispersal rates were high, as in the large spiral pattern for example, local perturbation had no noticeable effect at all (figure 3.7(c)).

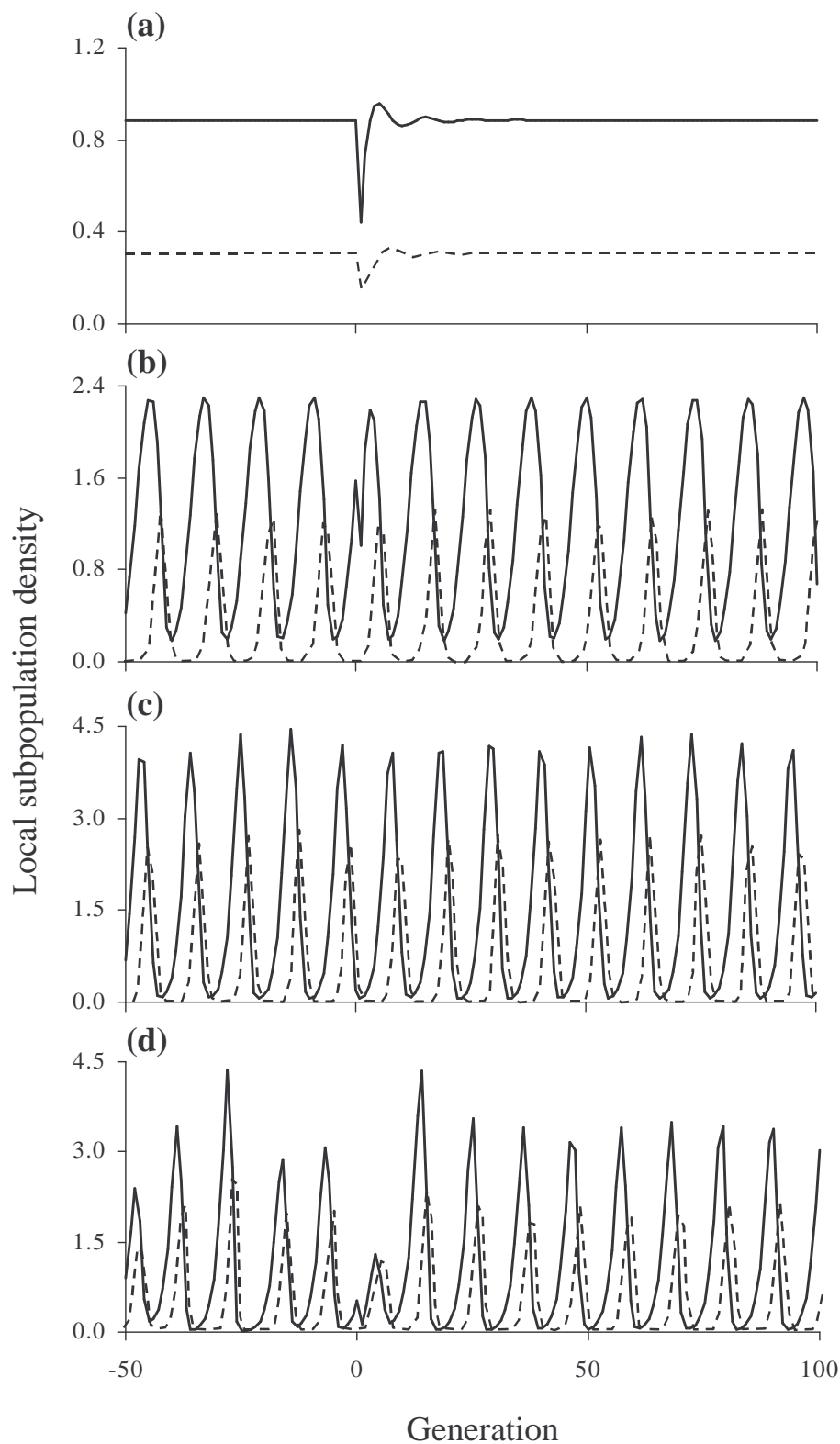


**Figure 3.7** Local subpopulation trajectories (solid line = hosts, dashed line = parasitoids) for four of the patterns listed in table 3.3. Both host and parasitoid are reduced to 0 at the end of generation 0 in the subpopulation being tallied, then allowed to recover. Figure (a) homogeneous,  $K = 1.5$ ; (b) regionally synchronised,  $K = 2.5$ ; (c) large spiral,  $K = 10$ ,  $\mu_N = 0.9$ ; (d) spatial chaos,  $K = 10$ ,  $\mu_N = 0.1$ . Discrete generation values are joined with lines to aid interpretation.

Again the best model fits were afforded when local dynamics were stable or stable limit cycles (appendix 4.8), although perfect fits were not possible, presumably due to the effects of net immigration. In general, however, model fits were very good for all scenarios, with  $R^2$  values for both host and parasitoid equations lying in the range 91 to 99% (appendix 4.8). Random parasitoid attack always gave a good fit to local dynamics even when the true function was otherwise, in which case random attack gave very nearly as good a fit as the true model. Inclusion of the immigration terms  $N_{imm}$  and  $P_{imm}$  never gave a significant improvement in the model fit.

Most parameter estimates were reasonably close to the true values when the correct local model was fitted. However, in some models where parasitism maintained low host densities, the host carrying capacity,  $K$ , could only be estimated by its influence on host recovery after perturbation. In this case, positive net immigration resulted in consistent overestimation of the intrinsic rate of host increase,  $r$ , even when net immigration terms were included. This in turn caused the fitted models to underestimate  $K$ .

### 3.5 Discussion

Beddington *et al.* (1978) showed that the simple host-parasitoid models in common use are unable to account for a stable reduction in host density of more than 60%, compared to reductions of greater than 90% routinely observed in the field. They concluded that field populations must exhibit either aggregated parasitoid attack or complex host density-dependence in order to account for the suppression observed. May *et al.* (1981) analysed more biologically-valid models which, with random attack, nevertheless came to a similar conclusion. However, a broader range of stable host suppression levels was possible depending on the order of occurrence of host density-dependence and parasitism, as well as the level of parasitoid aggregation. Barlow and Wratten (1996) presented similar results for a model with handling time. Similar to results of Hochberg and Lawton (1990), the analyses presented here suggest that the low stable equilibrium sought by these authors may be possible in only a very small range of realistic parameter space, specifically high host carrying capacity or parasitoid search efficiency, low host rate of increase (which

tends not to be the case in many pest insects), and reasonable aggregation of parasitoid attack between hosts.

Hawkins and Cornell (1994) noted a correlation between parasitism rate in the field and the realised success of biological control; this chapter has confirmed and quantified this relationship for a family of host-parasitoid models. The results suggest that, depending on the host rate of increase, substantial host reduction does not necessarily require high rates of parasitism (figure 3.2).

Murdoch (1990) highlighted the fact that all simple host-parasitoid models involve a trade-off between stability and host suppression, and concluded that a stable interaction was an unrealistic expectation in successful biocontrol. Murdoch *et al.* (1985) suggested that better overall host suppression might be achieved by an unstable interaction in which persistence arises from dispersal between adjacent subpopulations, allowing local extinction to be balanced by recolonisation as in Levins' (1969) classical definition for a metapopulation. Murdoch *et al.* (1985) cited examples of local extinctions in host-parasitoid systems, and strong evidence for the role of parasitoids in causing such local extinctions has recently been presented (Lei & Hanski 1997). Allen (1975) and Hassell *et al.* (1991a) demonstrated that stable local dynamics are not necessary for long-term persistence of a host-parasitoid assemblage, but also that local extinctions need not be a feature of such persistence.

This chapter furthers these analyses by addressing the level of host suppression, typically the most important factor of successful biological control. Prior to this, only Solé *et al.* (1992b) and Rohani & Ruxton (1999) included explicit host density-dependence in host-parasitoid metapopulation models. The focus of the former was spatial patterning, and they implemented host density-dependence in a biologically unrealistic way (see discussion of the model of Beddington *et al.* (1978) in May *et al.* (1981)). Rohani & Ruxton (1999) focussed on the persistence of local populations when host and parasitoid dispersal rates are highly asynchronous. Both of these studies were of a theoretical nature, and neither addressed the relevance of their findings to biological control.

This study has shown that host-parasitoid metapopulations can yield high host suppression and parasitoid persistence. In fact, the models suggest that any degree of

host suppression is possible, depending on the relative magnitudes of  $K$  and  $N_{eq}$ . The key to this result is that dispersal within the metapopulation allows persistence of local populations which would otherwise be unstable. The results also suggest that those situations which give the greatest degree of host suppression are those in which it is most difficult to achieve successful introduction of a parasitoid into an existing host population. This is because the host density, being far from  $N_{eq}$ , induces violent oscillations which do not allow the interaction to persist. With random parasitoid attack this study found a maximum of 84% mean host suppression could be achieved from a biological control introduction; the same result emerged when host carrying capacity was randomised in space. The models did not, however, include dispersal barriers, nor reduced parasitoid performance in the first generation after release, though these may be observed in the field and might affect initial establishment and persistence of parasitoids. If the problem of initial establishment can be overcome, then the models suggested that any degree of host suppression is possible in a metapopulation.

The spatial structure of host-parasitoid metapopulations offers physical refuges from parasitism, allowing persistence even when local dynamics are unstable. In simple non-spatial models refuges are most often represented using May's (1978) model for aggregated parasitoid attack. There, aggregation may arise from any source: physical, physiological, or behavioural, though it implies that the distribution of parasitoids is independent of that of their hosts (Chesson & Murdoch 1986). The pseudo-interference model for parasitoid attack (Hassell & Varley 1969) mimics the effect of parasitoids aggregating their attacks to patches of high host density, offering an effective refuge to hosts on low density areas. These models failed to capture the overall dynamics of the coupled map lattice host-parasitoid metapopulations studied here, probably because they assume complete redistribution of hosts and parasitoids each generation. Random parasitoid attack provided the best fit to metapopulation dynamics, and was also effective at capturing local dynamics, even when the true underlying attack process was otherwise. This suggests that it may be difficult to deduce the nature of parasitoid attack in the field by fitting models to population dynamics at too large a scale.

Hochberg and Lawton (1990) called for more attention to be paid to density-dependence in host rates of increase. The current analysis has suggested that net immigration may affect estimates of host rate of increase,  $r$ , and carrying capacity,  $K$ , even when allowed for in fitting a model to population data. The apparent trade-off between  $r$  and  $K$  when parasitism contributes to host mortality means that independent estimates of  $K$  may be needed in order to make accurate estimates of  $r$  from field data.

Most of the metapopulation behaviour observed depends on the stability of local population interactions in the absence of dispersal. If local dynamics are stable, then in the absence of stochasticity and heterogeneity the metapopulation behaves identically at any scale. Spatial effects, specifically net immigration, may be important in governing the response to local perturbation or any other process resulting in heterogeneity. More unpredictable dynamics, including spatial patterning, emerge when local dynamics are not stable. Though recent field studies (e.g. Maron & Harrison 1997; Ranta *et al.* 1997) have begun to address this issue, the challenge remains for ecologists to examine real systems for locally unstable interactions and the non-random spatial heterogeneity predicted by these models. The following chapter documents one such attempt.

The models presented here have demonstrated that host-parasitoid metapopulations may give very high host suppression, but persistence of the interaction depends critically on the starting conditions. For a realistic biological control starting point, a maximum mean suppression of 84% is possible. Higher host suppression over a larger range of parameter values occurs in the metapopulations than in non-spatial host-parasitoid models, but the greater than 90% suppression observed in the field could not be achieved by simulated biological control in a metapopulation with random parasitoid search.

### 3.6 Summary

Host-parasitoid models with host density-dependence were used to investigate the features that maximise biological control success. Relationships were derived in non-spatial models between parasitism level and host suppression at equilibrium. Spatially-explicit metapopulation models could produce higher host suppression, and over a larger range of parameters, than non-spatial models. However, persistence of the metapopulation interaction depended critically on the starting conditions: for a realistic biological control starting point, a maximum mean suppression of 84% was compatible with persistence, although much greater host suppression could be achieved from less realistic initial conditions. This result was unchanged by spatial stochasticity. Overall metapopulation dynamics, as well as those of individual subpopulations, were best modelled by random parasitoid attack, even when the true attack behaviour was otherwise. Fitting such models suggested that an independent estimate of host carrying capacity may be required when estimating host rate of increase from subpopulation data within a host-parasitoid metapopulation.

## 4. Field study of a host-parasitoid metapopulation: *Sitona discoideus* and *Microctonus aethiopoides*

### 4.1 Introduction

The previous chapter showed how local dispersal may produce spatial patterning and persistence in theoretical host-parasitoid metapopulations. Similar results abound in the literature (Rohani *et al.* 1997), yet few attempts have been made to address whether such dynamics occur in nature. This chapter describes an investigation of this type.

The Mediterranean weevil *Sitona discoideus* Gyllenhal (Coleoptera: Curculionidae) was first found in New Zealand in 1974 and quickly became a serious pest in lucerne (*Medicago sativa* L.). Most damage is done in spring by the root-feeding larvae, which may peak at densities of up to 2800 m<sup>-2</sup> in late November (Hopkins 1981, 1989; Goldson *et al.* 1984). Teneral adults cause further damage in late December, feeding on foliage for around two weeks while their flight muscles develop. They then disperse to nearby aestivation sites, such as hedgerows, where they remain over the summer. Post-aestivatory weevils disperse widely in early autumn (Goldson & French 1983), and adult densities in the crop peak in May when all surviving weevils have returned from aestivation. Adults lay eggs in the crop throughout winter, but particularly in early spring (Goldson *et al.* 1984).

In 1982, the parasitoid *Microctonus aethiopoides* Loan (Hymenoptera: Braconidae) was introduced as a biological control for the weevil (Stufkens *et al.* 1987). Unlike its univoltine host, *M. aethiopoides* has 4-6 generations per year in New Zealand, attacking teneral weevils in summer, post-aestivatory immigrants in autumn, and the last remaining adult weevils in spring (Goldson *et al.* 1990).

Parasitism sterilises weevils, so autumn-parasitised weevils do not contribute to the damaging larvae the following spring (Goldson *et al.* 1990).

An early model (Barlow & Goldson 1993) suggested that *M. aethiopoidea* was likely to be successful at reducing *S. discoideus* densities to where they are no longer economically damaging. This chapter presents a field study which measured the results of the biological control more than a decade after its induction, and tests the predictions of the Barlow and Goldson (1993) model. The data also allows the scale of spatial heterogeneity and density-dependent parasitism to be investigated.

## 4.2 Methods

### 4.2.1 Field assessment of *S. discoideus* biological control

Lucerne paddocks of different ages were selected without conscious bias within a 90 km band of central Canterbury farmland in the South Island of New Zealand. The study area ranged from Tai Tapu (43°40'S, 172°34'E) in the east, through the Darfield area, to Lake Coleridge (43°21'S, 171°32'E) in the west. A modified high-power vacuum cleaner was used to collect the litter and surface soil from each of fifteen 0.2 m<sup>2</sup> randomly chosen quadrats at each site in late autumn. The bagged samples were then removed to the laboratory, where weevils were extracted from the litter on a heated metal plate. Weevils were mounted in wax, flooded with alcohol, and dissected under a microscope, recording the gender and parasitism status of each.

At each collection the main physical details of the crop were recorded by visual scoring: herbage size, crop weediness, abundance of litter, dampness at time of sampling, and evidence of recent pesticide use. In addition, crop age, date collected, number of days between sampling and sorting, latitude, longitude, and density of other weevil species present were recorded for each site sampled. A total of 13 sites were sampled in 1996, 25 in 1997, and 23 in 1998. All data were analysed using Genstat 5 (Genstat 5 Committee 1993).

### 4.2.2 Estimation of $CV^2$ of parasitism

The squared coefficient of variation ( $CV^2$ ) of searching parasitoid adults in the vicinity of each host provides an indication of the importance of heterogeneity in parasitism for population regulation. Specifically, if  $CV^2$  exceeds unity, then this implies that there is sufficient heterogeneity of risk of parasitism to induce stability in the interacting populations (Hassell & May 1988; Hassell *et al.* 1991b; Taylor 1993). Pacala and Hassell (1991) presented a method for estimating  $CV^2$  from data relating percent parasitism to host density, the crux of which involves estimating the density of adult searching parasitoids based on a generalised host-parasitoid model. The host-parasitoid system studied here, however, involves multiple generations of parasitoids as well as host density-dependence and dispersal each year, so does not conform to the assumptions of their model.

In the current system, however, it was possible to estimate  $CV^2$  for the autumn parasitoid generation. Though the density of searching adult parasitoids in autumn,  $P_{aut}$ , was not measured, it is known from thermal summation that these are present as parasitised hosts in March (Goldson *et al.* 1990; see also chapter 5). Furthermore, chapter 5 gives the relationship between the density of parasitised weevils in March,  $W_{Mar}$ , and subsequent percent parasitism in autumn,  $Q_{aut} = 1 - \exp(-0.46 W_{Mar}^{0.27})$ . Rearranging this equation, it was possible to infer the density of searching parasitoids in autumn from the percent parasitism measured at that time:

$$P_{aut} \cong W_{Mar} = \left[ \frac{\ln(1 - Q_{aut})}{0.46} \right]^{1/0.27} \quad (4.1)$$

Now this could be used along with the autumn weevil density,  $N_{aut}$ , to estimate the  $CV^2$  across all sites, as detailed in appendix 4.6. Unlike that of Pacala & Hassell (1991), this method for estimating  $CV^2$  did not allow relative comparison of density-dependent and density-independent components of stability.

### 4.2.3 Estimating the scale of homogeneity

The scale of homogeneity in weevil dynamics was estimated by examining how local weevil densities were related to densities in nearby sites in the previous

generation. The weevil density in autumn at each site was regressed against a weighted average of the densities of unparasitised weevils at all sites in the previous autumn,  $C_w$ . Specifically,  $C_w = \sum(w_x C_x) / \sum w_x$ , where  $C_x$  is the autumn unparasitised weevil density in site  $x$  in the previous year, and  $w_x$  is the weighting for that site. Two different weighting systems were tried. Defining  $d_x$  as the distance to site  $x$ , and  $d_l$  as a constant radius being tested, ‘rectangular’ weighting was given by  $w_x = 1$  if  $d_x \leq d_l$  or  $w_x = 0$  otherwise (so that sites within radius  $d_l$  were weighted evenly, while more distant sites were ignored), and ‘Gaussian’ weighting by  $w_x = \exp[-(d_x/d_l)^2/2]$  (so that all sites were weighted, according to their proximity  $d_x$ , using the normal distribution with mean 0 and standard deviation  $d_l$ ).

#### 4.2.4 Test of a non-spatial model

Barlow & Goldson (1993) produced a model for *S. discoideus* dynamics in the Darfield area:

$$N_{next} = \frac{102 s_{spr} N_{aut} (1 - Q_{aut})}{27.8 + N_{aut} (1 - Q_{aut})} \exp[-0.11(N_{aut} Q_{aut})^{0.37}] \quad (4.2)$$

$$Q_{next} = 1 - \exp[-0.3(N_{aut} Q_{aut})^{0.37}]$$

where  $N_{aut}$  and  $Q_{aut}$  denote peak adult weevil density and proportion parasitised, respectively, in autumn of the current year,  $N_{next}$  and  $Q_{next}$  are the corresponding values in the following autumn, and survival factor  $s_{spr}$  determines the effect of spring droughts on subsequent weevil densities:  $s_{spr} = 0.67$  for drought years (September + October rainfall <80 mm), otherwise  $s_{spr} = 1$ . Rainfall data for Darfield were taken from New Zealand Meteorological Service records, and the model’s predictions were compared to the field results.

### 4.3 Results

Table 4.1 summarises the mean results from the 3 year study. The 1996 data were excluded from many of the analyses because they were collected much later in the year and relatively few sites were sampled that year.

Generalised linear modelling with terms added sequentially (table 4.2) suggested that both autumn adult weevil density and autumn parasitism rates varied significantly between sites and years, with a significant interaction. Weevil sex ratios,

**Table 4.1** Summary of survey results.

Year	1996	1997	1998	
Time of sampling	August	May-July	June-July	
No sites sampled	13	25	23	
Mean <i>S. discoideus</i> m <sup>-2</sup> : all sites	6.5	12.3	10.7	
	Darfield area	10.7	15.7	10.4
Mean % parasitism: all sites	18.6	26.5	29.4	
	Darfield area	18.7	38.2	32.5
CV <sup>2</sup> of parasitism	5.9	3.6	2.5	

**Table 4.2** Dependence of weevil density (total number per quadrat), parasitism rate (number parasitised per quadrat), and sex ratio (number female per quadrat) on year and site. Results are from generalised linear modelling with the usual link function and terms added sequentially as shown. (n.s. not significant at 5%; \* significant at 5%; \*\* significant at 1%,\*\*\* significant at 0.1%).

	Weevil density	Percent parasitised	Sex ratio
Assumed distribution	Poisson	binomial	binomial
Residual degrees of freedom	673	482	477
Residual mean deviance	1.48	1.15	1.13
Deviance ratio for:			
year effect	7.76 **	4.30 *	3.76 n.s.
+ site effect	24.25 ***	3.84 ***	1.53 *
+ year × site interaction	8.77 ***	3.87 ***	1.17 n.s.

however, did not differ, apart from a marginally significant site effect ( $p = 0.046$ ). Mean sex ratio (table 4.3) was 59.4% female, which was significantly different from 50%, and a significantly higher proportion of the males (39%) were parasitised than females (21%). This contrasts with the results of Fusco and Hower (1973) for the same parasitoid species, who found that there was no preference for *Hypera postica* hosts of one particular sex. Though there was slight evidence for density-dependent parasitism between sites (table 4.4, figure 4.1,  $d.f. = 59$ ,  $R^2 = 0.06$ ,  $p = 0.03$ ), this relationship depended critically on six points near the origin. There was no density-dependence in parasitism at the scale of individual samples. Calculated  $CV^2$  values were 5.9 for 1996, 3.6 for 1997, 2.5 for 1998, and 4.0 over all.

**Table 4.3** Effect of weevil sex on density (total weevils per quadrat) and parasitism rate (number parasitised per quadrat). Results from generalised linear modelling of 1997-98 data. In each case, the usual link function was assumed, and terms were added sequentially as shown. (n.s. not significant at 5%; \* significant at 5%; \*\*\* significant at 0.1%).

	Weevil density	Percent parasitised
Assumed distribution	Poisson	binomial
Residual degrees of freedom	1368	742
Residual mean deviance	1.12	1.09
Deviance ratio for:		
year effect	2.58 n.s.	8.66 ***
+ site effect	23.48 ***	3.82 ***
+ year $\times$ site interaction	8.03 ***	4.05 ***
+ sex effect	56.33 ***	64.79 ***
+ year $\times$ sex interaction	3.49 n.s.	0.74 n.s.
+ site $\times$ sex interaction	1.54 *	0.94 n.s.
Prediction for:		
females	6.5 m <sup>-2</sup>	21%
males	4.5 m <sup>-2</sup>	39%

**Table 4.4** Dependence of parasitism rate on weevil density at two different spatial scales. Results from analysis of variance of percent parasitism at site and quadrat scales. All 1996-98 percent parasitism data were subjected to angular transformation before analysis. (n.s. not significant at 5%; \* significant at 5%; \*\*\* significant at 0.1%).

	Site	Quadrat
Residual degrees of freedom	56	481
Residual mean square	0.047	0.229
Variance ratio for:		
year effect	2.32 n.s.	2.75 n.s.
+ site effect		3.13 ***
+ year $\times$ site interaction		2.72 ***
+ weevil density	5.39 *	2.11 n.s.

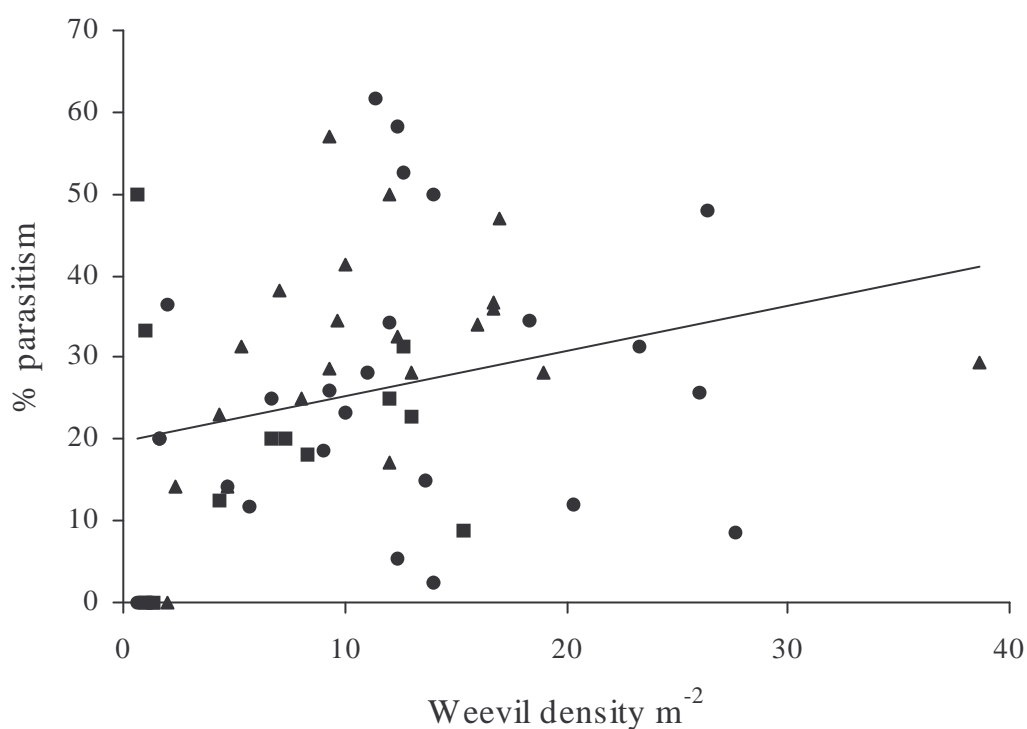


**Figure 4.1** The relationship between autumn weevil density and percent parasitism in central Canterbury lucerne paddocks: squares indicate 1996 data, circles 1997, and triangles 1998.

After taking year and site effects into account, a stepwise backwards multiple regression suggested that the results were not significantly affected by crop age, herbage size, crop weediness, abundance of litter, dampness at time of sampling, recent herbicide use, date collected, number of days between sampling and sorting, latitude, or density of other weevil species, suggesting that the sampling method was robust. There was, however, a very highly significant relationship (table 4.5,  $d.f. = 59$ ,  $R^2 = 0.55$ ,  $p < 0.001$ ) between autumn weevil densities and longitude (east-west position), which may reflect soil type (figure 4.2).

The best estimate for the scale of homogeneity of weevil dynamics was the radius  $d_l$  which gave the best fit for the regression of weighted local densities against weevil densities on the following season (figure 4.3). With rectangular weighting, the best fit occurred with  $d_l = 12$  km ( $N_x = 1.0 + 1.33C_x$ ,  $d.f. = 30$ ,  $R^2 = 0.45$ ,  $p < 0.001$ ). The best fit with Gaussian weighting occurred with standard deviation distance  $d_l = 8$  km ( $N_x = 1.4 + 1.27C_x$ ,  $d.f. = 30$ ,  $R^2 = 0.39$ ,  $p < 0.001$ ). From this, it seems reasonable to estimate the scale of homogeneity at  $12 \pm 4$  km. With neither weighting system was it significantly better to consider each site separately from its weighted neighbours in a multiple regression.

**Table 4.5** Summary of results for dependence of weevil density on longitude. Each years data was first regressed separately and the slopes of the fitted lines were compared using t-tests. There was no significant difference between each years fitted slope, so the data were pooled and analysis of covariance (ANCOVA) was used to find a common slope and test for differences in the elevation of each years fitted line. ( $n$  is number of data points,  $s.e.$  denotes standard error of estimates, and significance tests used the 5% level).

Year	$n$	Regression analysis of individual years			ANCOVA using common slope	
		slope	$s.e.$	group	elevation	group
1996	13	-0.0270	0.0063	a	8.0	a
1997	25	-0.0243	0.0054	a	11.7	b
1998	23	-0.0303	0.0060	a	10.5	a,b
Common value		-0.0269	0.0035		10.5	

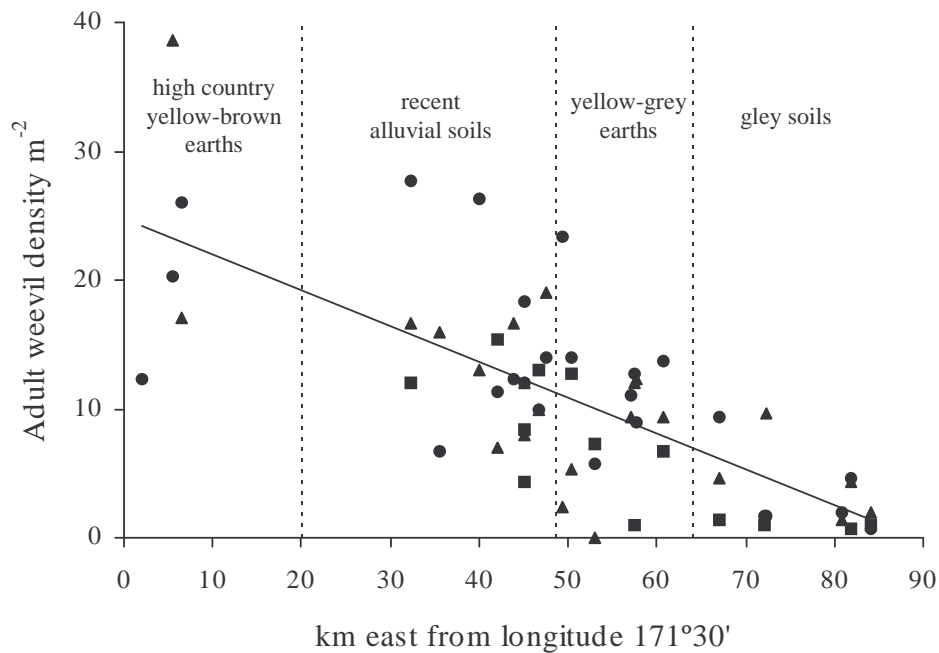


**Figure 4.2** The relationship between longitude and autumn adult weevil density for central Canterbury sites: squares indicate 1996 data, circles 1997, and triangles 1998. General soil type is indicated between the dotted lines.

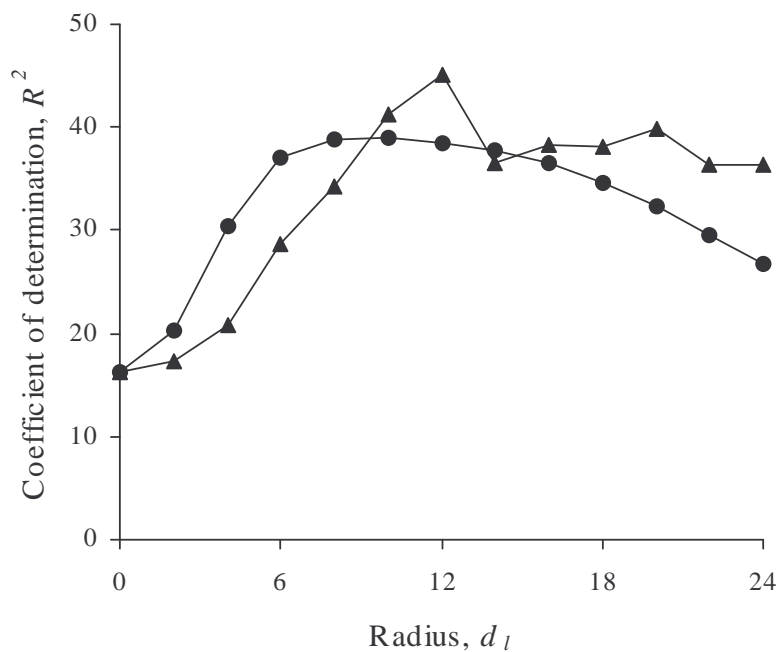


**Figure 4.3** Goodness-of-fit of regressions relating mean density within radius  $d_l$  km to site density the following autumn. Triangles denote results from equal contribution by all sites within radius  $d_l$  (rectangular weighting); circles denote results from Gaussian weighting with standard deviation distance  $d_l$ . Points are joined by lines to aid interpretation.

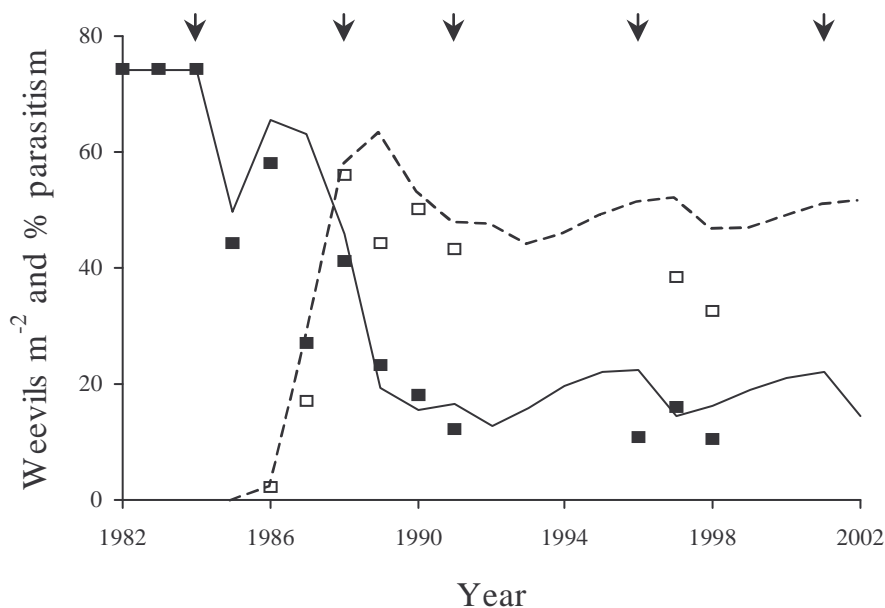


**Figure 4.4** Model predictions of autumn weevil densities (solid line) and parasitism levels (dashed lines) over time, together with observed values from Darfield (filled squares weevil density; open squares % parasitism). Arrows indicate the timing of actual spring droughts up to 1998, and hypothetical droughts afterwards. Discrete model results are joined with lines to aid interpretation.

The model predicted that in the long-term *M. aethiopoidea* should maintain weevil densities at 10 to 20  $\text{m}^{-2}$  in autumn, and this was consistent with actual densities (figure 4.4), including the 1996 to 1998 results. However, the model did tend to over-estimate parasitism levels, predicting that parasitism levels of around 50% observed from 1988 to 1991 would be sustained in the long term. The more recent data, however, suggest 30 to 40% parasitism in autumn.

#### 4.4 Discussion

By sampling weevil populations immediately after dispersal, the results reflect its effects. Therefore, like Goldson and French (1983), this study found no relationship between crop age and post-aestivation weevil density, despite a strong relationship prior to dispersal (Goldson & French 1983; Barlow & Goldson 1993). The observed significant differences in weevil density between sites could largely be accounted for by longitude, with densities increasing from east to west (figure 4.2). This is possibly

a reflection of soil type, with the shallower, less nitrogen-retentive soils of the west favouring greater larval densities (Goldson & Muscroft-Taylor 1988). In addition, rainfall tends to be higher in the west (New Zealand Meteorological Service 1981). Another possibility is that the volume of lucerne grown varies from east to west; unfortunately there are insufficient data available to quantify this. Habitat abundance may influence pest density by affecting the success of dispersal (see chapter 5). Either way, the east-west trend in post-aestivation weevil densities suggests that the weevil populations are not well mixed at this scale, and this conclusion is supported by the results for the scale of homogeneity of weevil populations. Local weevil dynamics appear have a degree of homogeneity within a radius of about 12 km, which implies a similar effective annual dispersal distance. Hopkins (1981) measured dispersal of *M. aethiopoides* at 10 to 15 km annually after being released to control *S. discoideus* in Australia; if the primary method of parasitoid dispersal is as early-instar larvae in dispersing weevils (Ferguson *et al.* 1994), then his result is comparable to that of  $12 \pm 4$  km suggested by the current study.

Examples of direct density-dependence in parasitoid attack (figure 4.1) are less common in the literature than either density-independence or inverse density-dependence (Morrison & Strong 1980; Stiling 1987; Walde & Murdoch 1988). Only about half of published examples show density-dependent parasitism. Of these, half demonstrate inverse density-dependence, while the remainder, showing direct density-dependence, tend to have been measured at relatively large spatial scales, such as the paddock scale used in the present study. Walde & Murdoch (1988) suggested that the aggregation observed at large spatial scales may be a product of semi-independent dynamics at a smaller scale within the sample area, though Hopper *et al.* (1991) disputed this for their highly-mobile parasitoid *Microplitis croceipes*. As with the braconid parasitoid studied by Hopper *et al.* (1991), the current study found some evidence for direct density-dependent parasitism at a large spatial scale, but none at the scale of sample units. A stronger density-dependence appears to exist in the life cycle, acting on spring larval populations (Goldson *et al.* 1988), but this is largely obscured by subsequent dispersal. In terms of weevil egg densities (and therefore the potential population of damaging spring larvae), density-dependent parasitism in autumn may be more important.

The estimates for  $CV^2$  of parasitism of *S. discoideus* by *M. aethiopoidea* range from 2.5 to 5.9. This is within the range of values reported for other systems, though considerably higher than the estimates obtained for two other braconid parasitoids (0.6 for *Apanteles tedellae* on *Epinotia tedella*, and 1.5 for *Agathis pumila* on *Coleophora laricella*; Hassell & Pacala 1990). The fact that the values are greater than unity suggests that heterogeneity in parasitism alone should be sufficient to stabilise the population dynamics. The parasitoid generation that this applies to, however, is just one of 4-6 each season (Goldson *et al.* 1990), so caution should be exercised when extrapolating this result to the complete system. Moreover, stability is also conferred by host density-dependence (Goldson *et al.* 1988), dispersal within a metapopulation structure (see chapter 5), and density-dependent parasitoid attack (Barlow & Goldson 1993).

The long-term prediction of the model, of 10 to 20 weevils  $m^{-2}$  in autumn, seems to have been consistent with the 1996 to 1998 data. Successful biological control has been maintained, with approximately 75% suppression of weevil densities below their pre-control level. The slightly lower weevil densities observed in 1996 and 1998 may be related to the later timing of these surveys, in winter rather than late autumn. Observed parasitism rates of around 35% were slightly lower than those predicted by the model, but this did not seem to affect the level of control. In conclusion, follow-up sampling has confirmed that *M. aethiopoidea* is a valuable and successful biological control agent for *S. discoideus* in New Zealand.

## 4.5 Summary

Autumn densities of the pest weevil *Sitona discoideus* and its braconid parasitoid *Microctonus aethiopoidea* were monitored for 3 years on the Canterbury Plains, South Island, New Zealand, from 1996 to 1998. *M. aethiopoidea* was introduced in 1982 and first appeared in the study area in 1986. The initial phase of parasitoid build-up and reduction in weevil numbers was then monitored until 1991. By this time parasitism had reached around 50% and weevil density had been reduced by 75%. A published model for the system suggested that this level of suppression would be sustained.

In agreement with the model, the survey from 1996 to 1998 confirmed that successful biological control had been maintained, with 75% suppression of weevil density but slightly lower rates of parasitism of around 35%. Weevil densities showed a significant trend across the area surveyed, increasing from east to west probably as a reflection of soil types. Weevil sex ratio was significantly biased towards females, yet the proportion of males that were parasitised was twice that of females. Percent parasitism in autumn related positively to weevil density over time and space, and spatial heterogeneity in parasitoid attack contributed to the apparent stability of the population dynamics. The scale of homogeneity, and by implication effective annual dispersal, is estimated at  $12 \pm 4$  km radius for the weevil.

## 5. A spatial model for the successful biological control of *Sitona discoideus* by *Microctonus aethiopoides*

### 5.1 Introduction

It is widely recognised that spatial interactions may play an important part in population dynamics. Despite the abundance of theoretical evidence, reviewed by Hanski and Gilpin (1991), Taylor (1993), and Barlow and Wratten (1996), there have been few attempts to investigate the importance of spatial dynamics in real biological control systems. In particular, we need to know whether we must understand the dynamics of a population in space in order to understand and predict its behaviour in time. This chapter represents an attempt to address the importance of spatial processes in the *Sitona discoideus*/*Microctonus aethiopoides* biocontrol system investigated in the previous chapter.

The parasitoid *Microctonus aethiopoides* was introduced as a biological control for the pest weevil *Sitona discoideus* (Stufkens *et al.* 1987). Unlike its univoltine host, *M. aethiopoides* has 4-6 generations each year in New Zealand (Goldson *et al.* 1990; figure 5.1). The first, in spring, occurs when overwintering pupae eclose and the adult parasitoids attack the last of the adult weevils remaining in the crop from the previous autumn. A second generation parasitises the teneral weevils as they appear in early summer. The development of third generation parasitoids is arrested at the first instar as their hosts undergo aestivation, resuming once the weevils return to the crop in autumn. In New Zealand, however, approximately 3% of parasitised pre-aestivatory weevils exhibit atypical behaviour, whereby parasitoid development in teneral weevils continues beyond the first instar, inhibiting the flight ability of their hosts (Goldson *et al.* 1990). These weevils, therefore, remain in the crop, where

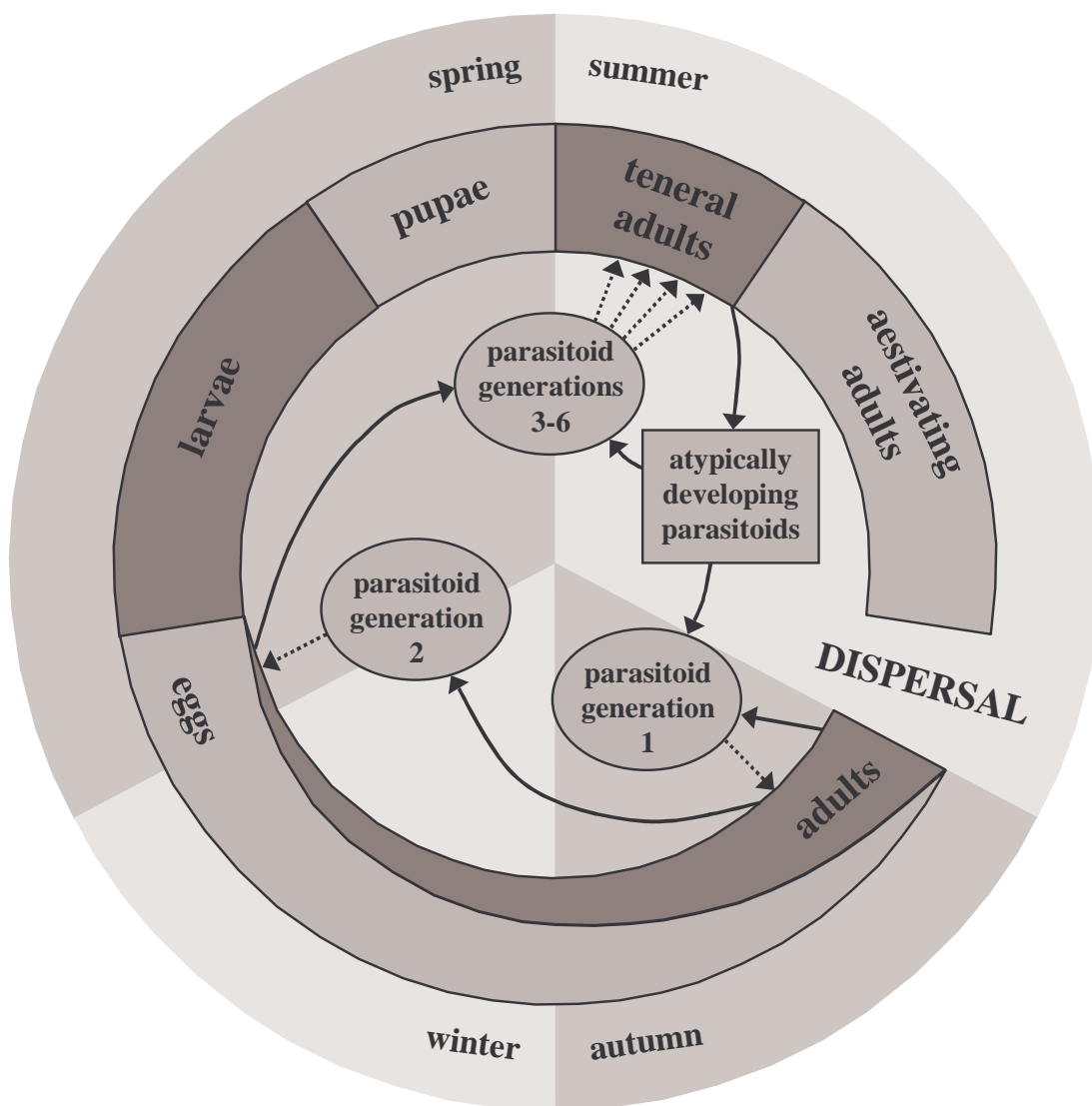


**Figure 5.1** Annual life cycles of the weevil *Sitona discoideus* and its braconid parasitoid *Microctonus aethiopoies* in New Zealand.

the summer temperatures allow further generations of parasitoids to be supported on late-emerging weevils, plus another generation laid by waiting parasitoids in post-aestivatory weevils as they return to the crop in autumn (Goldson *et al.* 1990). This atypical behaviour and the additional summer parasitoid generations would seem to account for the greater reductions in weevil densities observed in New Zealand than in Australia (Barlow & Goldson 1993).

An early, non-spatial model (Barlow & Goldson 1993) suggested that *M. aethiopoides* would successfully control *S. discoideus*, and this was confirmed by the field study reported in the previous chapter. Here, the largely empirical model of Barlow & Goldson (1993) is elaborated to include further biological detail. The expanded model is formulated as a metapopulation, with explicit dispersal between local subpopulations, as suggested by the field data (chapter 4). The focus of this exercise is to ask if including spatial processes allows better understanding of the system, and in particular whether spatial processes are important for successful biological control in this case. The model also allows the influence of host plant abundance on pest densities and biological control to be investigated.

## 5.2 Methods

### 5.2.1 Non-spatial model

Barlow & Goldson (1993) constructed a model for *S. discoideus* dynamics, with host density-dependence and heterogeneous parasitism. Their model (hereafter referred to as the “B&G” model) is

$$N_{next} = \frac{v s_{spr} N_{aut} (1 - Q_{aut}) (1 - Q_{aest})}{w + N_{aut} (1 - Q_{aut})} \quad (5.1)$$

where  $N_{aut}$  is peak adult weevil density in autumn of the current year,  $N_{next}$  is weevil density in autumn of the following year,  $Q_{aut}$  is the proportion of autumn weevils that are parasitised, and  $Q_{aest}$  is the proportion of summer aestivating weevils that are parasitised. Parameters  $v$  and  $w$  determine the shape of the density-dependence function relating unparasitised autumn adult densities to the densities of teneral

weevils emerging the following summer, and  $s_s$  determines the effect of spring droughts on weevil larval survival as compared to  $s_s = 1$  for non-drought years. The density-dependence and drought functions were fitted empirically, using data from the Darfield district prior to parasitoid introduction, which suggested  $v = 102 \text{ m}^{-2}$ ,  $w = 27.8 \text{ m}^{-2}$ , and  $s_{spr} = 0.67$  for drought years (when September + October rainfall  $< 80 \text{ mm}$ ). Parasitism rates in aestivation and in autumn were also fitted empirically, and conformed to the pseudo-interference function (Hassell and Varley 1969; Free *et al.* 1977; table 3.1):

$$Q_{next} = 1 - \exp\left[-a(W_{aut})^{1-m_{Dec}}\right] \quad (5.2)$$

$$Q_{aest} = 1 - \exp\left[-a_{Dec}(W_{aut})^{1-m_{Dec}}\right] \quad (5.3)$$

where  $W_{aut} = N_{aut} \times Q_{aut}$ , the density of parasitised weevils in autumn. Darfield data suggested  $a = 0.30$ ,  $a_{Dec} = 0.11$ , and  $m_{Dec} = 0.63$ . Peak density of weevil larvae in spring,  $N_{spr}$ , was modelled by

$$N_{spr} = \frac{s_{spr} K N_{aut} (1 - Q_{aut})}{w + N_{aut} (1 - Q_{aut})} \quad (5.4)$$

where  $K$  is the carrying capacity of a particular lucerne stand of age  $A$ , and is given by

$$K = K_{max} \exp(-z A) \quad (5.5)$$

with  $K_{max} = 7011$  and  $z = 0.358 \text{ yr}^{-1}$  for Darfield (Barlow & Goldson 1993).

## 5.2.2 Metapopulation model

Here, the largely empirical B&G model is expanded to a more mechanistic representation, including dispersal in space. Equations 5.1 and 5.2 in the B&G model subsume the effects of dispersal. To model these explicitly it was necessary to separate aestivation (with dispersal) and subsequent parasitoid attack, from the earlier stages of the annual cycle (figure 5.1).

Population dynamics from autumn to aestivation were modelled using equations 5.3, 5.4, and 5.5 from the B&G model above. It is assumed that the density of teneral adult weevils emerging in early summer relates to the spring larval peak by a survival factor,  $s_{larv}$ . Data from three Darfield sites over three years suggest  $s_{larv} = 0.90$  (appendix 4.9). Goldson *et al.* (1990) showed that a small proportion,  $p_{atyp} = 0.03$ , of the parasitised tenerals show atypical behaviour whereby they do not disperse to aestivation sites but remain in the lucerne over summer. From this can be inferred the total number of aestivating weevils,  $N_{aest}$ , and the density of those atypical parasitised weevils remaining in the crop,  $W_{crop}$ :

$$N_{aest} = \frac{s_{larv} N_{spr}}{(p_{atyp} / (1 - p_{atyp})) Q_{aest} + 1} \quad (5.6)$$

$$W_{crop} = (p_{atyp} / (1 - p_{atyp})) W_{aest} \quad (5.7)$$

where  $W_{aest} = N_{aest} \times Q_{aest}$ .

To model dispersal, local populations, each representing a lucerne stand, were arrayed on the grid of a  $30 \times 30$  coupled map lattice ( $H = 900$ ; Kaneko 1989). The boundaries of the lattice were assumed to be ‘periodic’ (figure 2.2) so that dispersers off one edge of the lattice reappear at the opposite edge. Initial crop age was randomised in space. As a reasonable simplification of real lucerne management, local stands aged 3 years or more were assumed to have a 50% chance of being renewed each year. Post-aestivation weevils, multiplied by a survival factor,  $s_{disp}$ , were distributed evenly over the  $(2d_l + 1)^2$  lattice locations centred on their source, where  $d_l$  determines to how far on the metapopulation lattice weevils may disperse:

$$N_{imm,x,y} = \frac{s_{disp}}{(2d_l + 1)^2} \sum_{i=x-d_l}^{x+d_l} \sum_{j=y-d_l}^{y+d_l} N_{aest,i,j} \quad (5.8)$$

where  $N_{imm}$  is the local density of immigrating weevils, and subscripts  $x$  and  $y$  denote the lattice co-ordinates of the subpopulation. This differs from the dispersal process used in other chapters, because here all aestivating weevils must disperse, and some may disperse back to the site from which they left to aestivate.

By default,  $d_l = 3$  was used, corresponding to a realistic dispersal range for *S. discoideus* (chapter 4) given realistic abundance and size of lucerne stands in Canterbury (appendix 4.10).  $W_{imm}$ , the local density of immigrating parasitised weevils was modelled in the same way. On average, only 3.2% of those weevils leaving for aestivation are replaced by return flights (appendix 4.9), suggesting  $s_{disp} = 0.032$ . The others must succumb to dispersal mortality or fail to locate a suitable lucerne stand. All parasitoid dispersal was assumed to occur through dispersal of parasitised weevils (Ferguson *et al.* 1994).

Post-aestivation dispersal occurs throughout March and April, with parasitised weevils returning earlier on average than healthy ones (Goldson *et al.* 1984; appendix 4.9). Goldson *et al.* (1990) measured the day-degree requirements of *M. aethiopoidea* egg and larval stages at 144.4 °D (of which half was required for instars II to V) above a threshold of 9.8 °C. Similarly, the requirement for pupal development was 125.4 °D above 8.2 °C (Goldson *et al.* 1990). Thermal summation using these formulae together with Darfield temperatures, suggested that parasitoid development all but ceases from May through the winter (appendix 4.9). In order to complete their development before then, second instar parasitoids would need to be back in the crop by mid-March, since pupal development would take all of May, and the previous larval development would take two weeks of March (appendix 4.9). Any parasitoid larvae returning in post-aestivatory weevils later than this are likely to overwinter as pupae, maturing only in the warmer temperatures of the following spring (Barlow & Goldson 1993). All immigrating parasitised weevils are killed by May, so they do not contribute to either total hosts or parasitised hosts in late autumn. This effect is included in equation 5.1 of the B&G model as a weevil mortality, while dispersal and autumn attack behaviour are subsumed by the empirical fit of equation 5.2. Total weevils in the crop in May represent the total unparasitised immigrants, while parasitism levels in May reflect the attack by parasitoids that were present as larvae in March. The latter includes those parasitised weevils present in the crop as a result of atypical parasitoid development, plus that proportion of immigrating weevils that arrive during March. This may be modelled by

$$N_{next} = N_{imm} - W_{imm} \quad (5.9)$$

$$Q_{next} = 1 - \exp\left[-a_{Mar} \left(s_{crop} W_{crop} + p_{early} W_{imm}\right)^{1-m_{Mar}}\right] \quad (5.10)$$

where  $s_{crop}$  is the ratio of increase of parasitised weevils in the crop over summer,  $p_{early}$  is the proportion of immigrating parasitised weevils that return in March, and  $a_{Mar}$  and  $m_{Mar}$  govern the shape of the autumn attack function (Hassell & Varley 1969). Measurements from Darfield sites suggest  $s_{crop} = 0.34$  and  $p_{early} = 0.58$  (appendix 4.9). Equation 5.10 was fitted by non-linear least-squares regression, using Genstat 5 (Genstat 5 Committee 1993), to Darfield data (figure 5.2), suggesting  $a_{Mar} = 0.47 \pm 0.07$  *s.e.* and  $m_{Mar} = 0.73 \pm 0.09$  *s.e.* (*d.f.* = 12;  $R^2 = 80\%$ ;  $p < 0.001$ ).

Combining equations 5.3 to 5.10, the full metapopulation model is specified by

$$N_{aest} = \frac{s_{spr} s_{larv} K_{max} \exp[-zA] (N_{aut} - W_{aut})}{(w + N_{aut} - W_{aut}) \left[ \frac{p_{atyp}}{(1 - p_{atyp})} \left(1 - \exp[-a_{Dec} (W_{aut})^{1-m_{Dec}}]\right) + 1 \right]}$$

$$W_{aest} = N_{aest} \left(1 - \exp[-a_{Dec} (W_{aut})^{1-m_{Dec}}]\right) \quad (5.11)$$

$$N_{next} = \frac{s_{disp}}{(2d_l + 1)^2} \sum_{i=x-d_l}^{x+d_l} \sum_{j=y-d_l}^{y+d_l} (N_{aest,i,j} - W_{aest,i,j})$$

$$W_{next} = N_{next} \left(1 - \exp\left[-a_{Mar} \left(\frac{s_{crop} p_{atyp}}{(1 - p_{atyp})} W_{aest} + \frac{p_{early} s_{disp}}{(2d_l + 1)^2} \sum_{i=x-d_l}^{x+d_l} \sum_{j=y-d_l}^{y+d_l} W_{aest,i,j}\right)^{1-m_{Dec}}\right]\right)$$

where the model parameters and their default values are summarised in table 5.1.

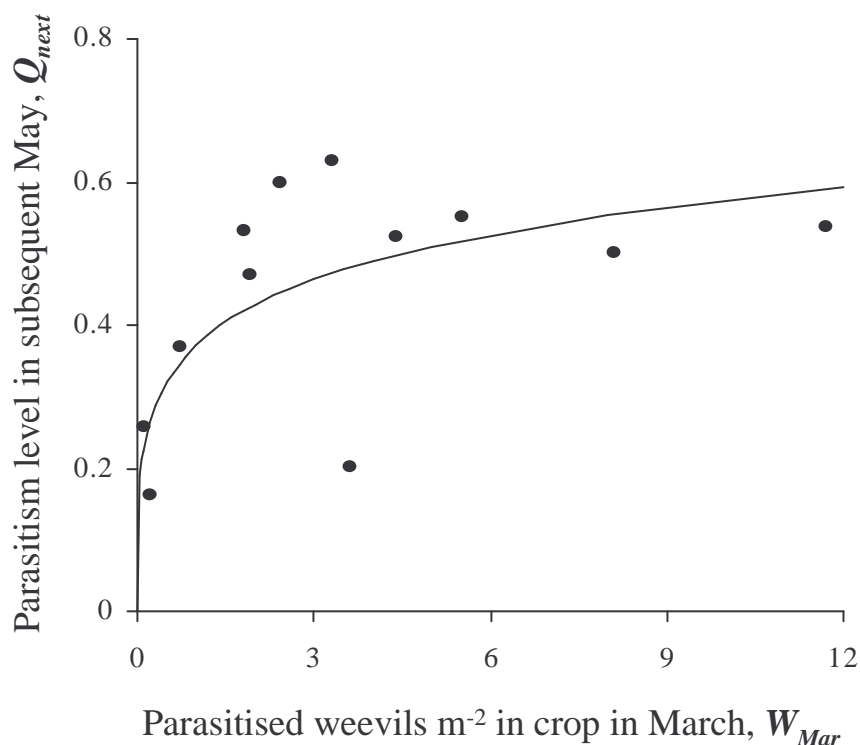


**Figure 5.2** The relationship between density of parasitised weevils in the crop in March and the proportion of weevils parasitised in the following May, for 5 sites (S. Goldson, unpublished data). Fitted line given by  $Q_{next} = 1 - \exp[-0.47(W_{Mar})^{1-0.73}]$  ( $R^2 = 80\%$ ;  $p < 0.001$ ).

**Table 5.1** Metapopulation model parameters, their default values and source.

Parameter	Meaning	Default	Source
$w$	weevil larvae density-dependence parameter	27.8	B&G <sup>†</sup>
$z$	rate at which crop carrying capacity declines with age	0.358	B&G <sup>†</sup>
$K_{max}$	maximum carrying capacity of crop for weevil larvae	7011	B&G <sup>†</sup>
$s_{larv}$	survival rate of weevil larvae to teneral adults	0.90	appendix 4.9
$s_{disp}$	rate of weevil survival through aestivation and dispersal	0.032	appendix 4.9
$a_{Dec}$	summer parasitoid search parameter	0.11	B&G <sup>†</sup>
$m_{Dec}$	summer parasitoid interference parameter	0.63	B&G <sup>†</sup>
$p_{atyp}$	proportion of parasitised weevils undergoing atypical development	0.03	G <i>et al.</i> <sup>‡</sup>
$s_{crop}$	ratio of increase of parasitised weevils in the crop over summer	0.34	appendix 4.9
$p_{early}$	proportion of immigrating parasitised weevils arriving in March	0.58	appendix 4.9
$a_{Mar}$	autumn parasitoid search parameter	0.47	figure 5.2
$m_{Mar}$	autumn parasitoid interference parameter	0.73	figure 5.2

<sup>†</sup>Barlow and Goldson (1993)

<sup>‡</sup>Goldson *et al.* (1990)

### 5.2.3 Australian variant

There are two major differences between the *S. discoideus* host-parasitoid systems in New Zealand and Australia. Late summer and autumn temperatures are generally higher in Australia, and there appears to be no atypical parasitoid development in Australian weevils. Warmer autumn temperatures mean that in Australia the bulk of weevil egg-laying occurs before autumn parasitism (Hopkins 1989). To account for this in the model, equation 5.4 is replaced with

$$N_{spr} = \frac{s_{spr} K N_{aut}}{w + N_{aut}} \quad (5.12)$$

so that spring weevil larvae are unaffected by parasitism the previous autumn. In addition, warmer temperatures probably mean that in Australia the immigrating parasitised weevils all have sufficient thermal time to develop fully before winter ( $p_{early} = 1.0$ ). Barlow and Goldson (1993) showed that the low levels of parasitism observed in aestivating weevils in Australia, of around 6.5% (Cullen & Hopkins 1982), can be attributed to the lack of atypical parasitoid development there ( $p_{atyp} = 0.00$ ). Setting  $a_{Dec} = 0.02$  in the model appropriately scales the summer attack function to capture this effect. Incorporating equation 5.12 and  $p_{atyp} = 0$ , the first of equations 5.11 becomes for Australia

$$N_{aest} = \frac{s_{spr} s_{larv} K_{max} \exp[-zA] N_{aut}}{(w + N_{aut})} \quad (5.13)$$

## 5.3 Results

### 5.3.1 Model results

Results from the metapopulation model were compared to those from the B&G model as well as with real data. The B&G model was intended to represent the behaviour of the host-parasitoid system over a whole district centred on Darfield and including multiple lucerne paddocks (i.e. a metapopulation). It predicted that in the long-term *M. aethioides* should maintain weevil densities at 10 to 20 m<sup>-2</sup> in

autumn, and this was consistent with actual densities (figure 5.3(a)), including the 1996 to 1998 results collected 5-7 years after the data to which the model was originally fitted. However, the model does tend to over-estimate parasitism levels, predicting long-term autumn parasitism levels of around 50%, as was observed in 1988 to 1991. The more recent data, however, suggest 30 to 40% parasitism in autumn.

The new model, run for a single isolated location, gave very similar results to the B&G model (figure 5.3(b)). The main difference is that the new model allows more rapid increase in initial parasitism than the B&G model. In contrast, the initial mean build-up over the whole metapopulation was slower than in the B&G model (figure 5.4(a)) since it includes the time lag required for the parasitoid to spread throughout the model lattice. Despite local perturbations, in the form of crop ageing and renewal, the spatial model was stable on average; global perturbations, notably spring droughts, only temporarily displaced the mean weevil density. Local subpopulations were well buffered by dispersal, and showed little effect of local lucerne age fluctuations (figure 5.4(b)). The Australian variant of the model predicted around 51% parasitism but only 11% suppression of adult weevils in autumn (figure 5.5).

### 5.3.2 Sensitivity to parameter values

Results from the model sensitivity analysis are summarised in figures 5.6 and 5.7. There was an almost linear relationship between metapopulation mean local density in the presence of the biocontrol agent, and spatial variance in local subpopulation densities (figure 5.6). Changes in parameter values affected the mean and variance in the same way, and all results lay along the solid line in figure 5.6, except when the rate at which crop carrying capacity declines with age,  $z$ , or dispersal range,  $d_i$ , were altered. Changes in the value of  $z$  affected the metapopulation mean but had little affect on its variance (dashed line in figure 5.6), whereas dispersal range affected only the variance (dotted line). Survival rate during dispersal,  $s_{disp}$ , had the greatest influence on absolute weevil density (figure 5.6), but was far less important than the parasitism parameters  $a_{Dec}$ ,  $a_{Mar}$ ,  $m_{Dec}$ , and  $m_{Mar}$  in governing the level of suppression by the parasitoid (figure 5.7). The summer survival parameters  $s_{disp}$  and  $s_{larv}$ , and

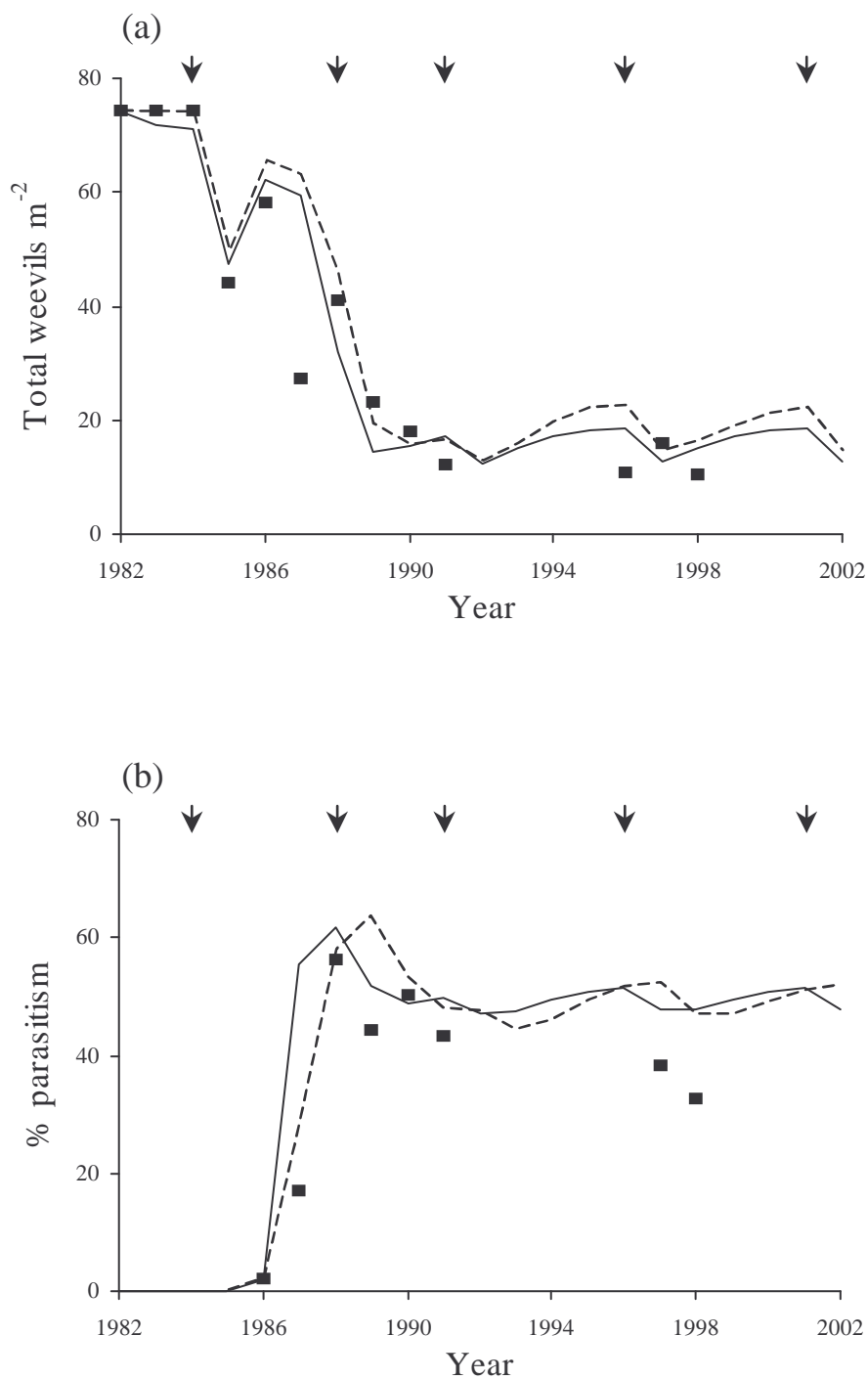


**Figure 5.3** Model predictions of autumn weevil densities (a) and parasitism levels (b) over time, together with observed values from Darfield (filled squares). Arrows indicate the timing of spring droughts. Solid lines: new model run for a single isolated population with constant stand age 2; dashed lines: B&G model (adapted from Barlow & Goldson 1993, additional data from chapter 3).

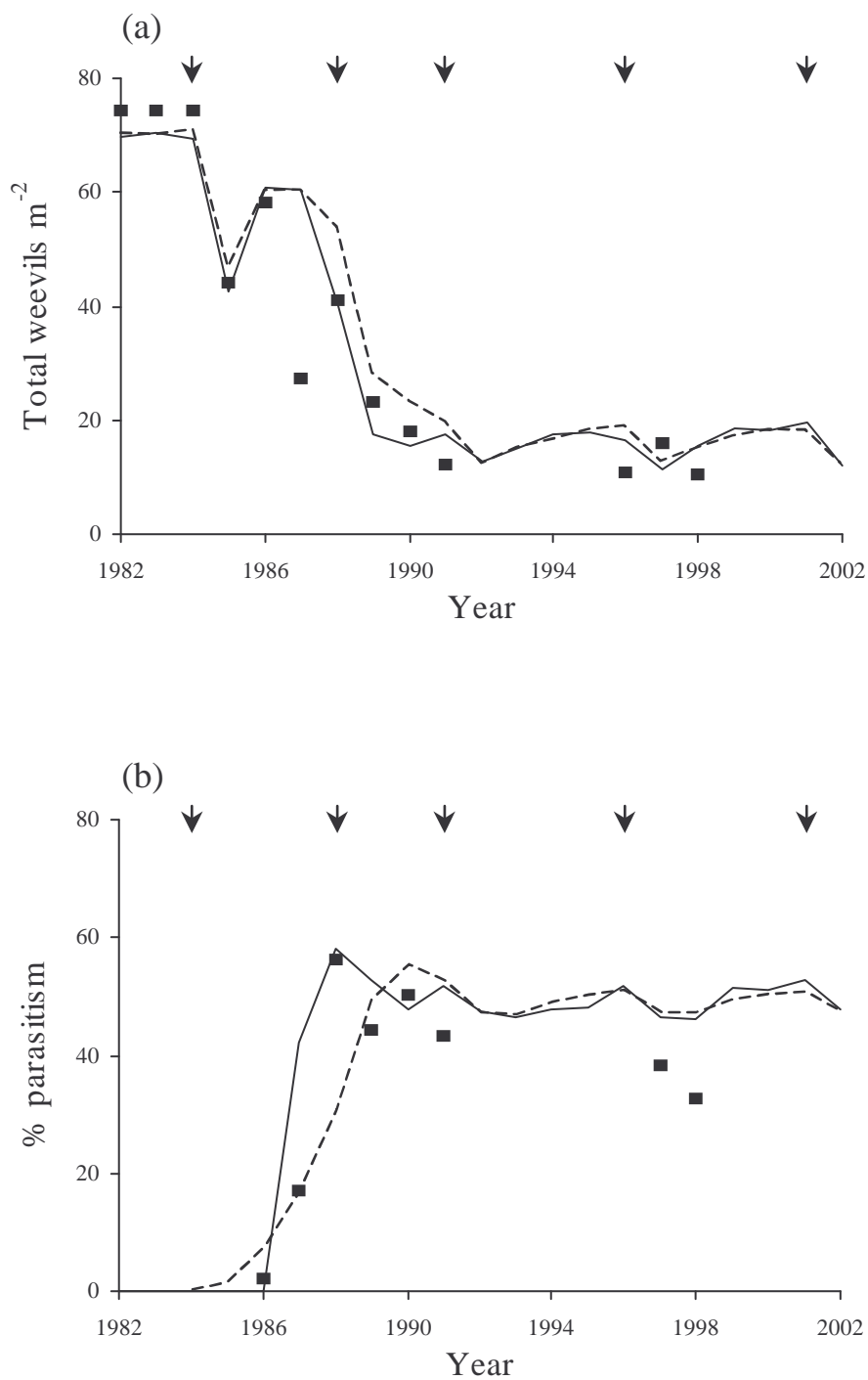


**Figure 5.4** Metapopulation model predictions as for figure 5.3. Solid lines: results for a single local population within a 30×30 lattice; dashed lines: overall mean results from 30×30 local populations; filled squares: observed values from Darfield.

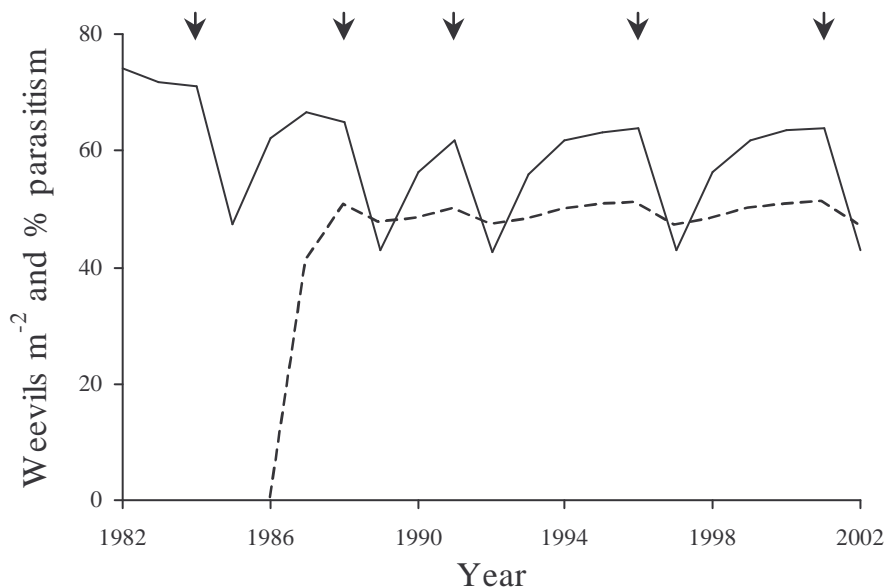


**Figure 5.5** Behaviour of the non-spatial Australian variant of the model in terms of autumn weevil densities (solid line) and parasitism levels (dashed lines) over time. Arrows indicate the timing of spring droughts. Actual parasitism values observed in Australia are 50 to 60%, but with little reduction in weevil densities (Hopkins 1989).

larval carrying capacity  $K_{max}$  had a large effect on weevil densities, but relatively little on suppression, since their influence was similar both before and after parasitoid introduction. Note that  $s_{larv}$  and  $K_{max}$  appear together in the model (equations 5.11 and 5.13), and therefore gave exactly the same results in the sensitivity analysis. Through its non-linear interaction with post-control weevil densities, the density-dependence factor  $w$  was important in determining both host density and suppression. The parameter for parasitoid survival in the crop over summer,  $s_{crop}$ , was estimated with the least certainty, but had little effect on the results. This was also the case for the probability of atypical development,  $p_{atyp}$ , and the probability of early immigration,  $p_{early}$ .

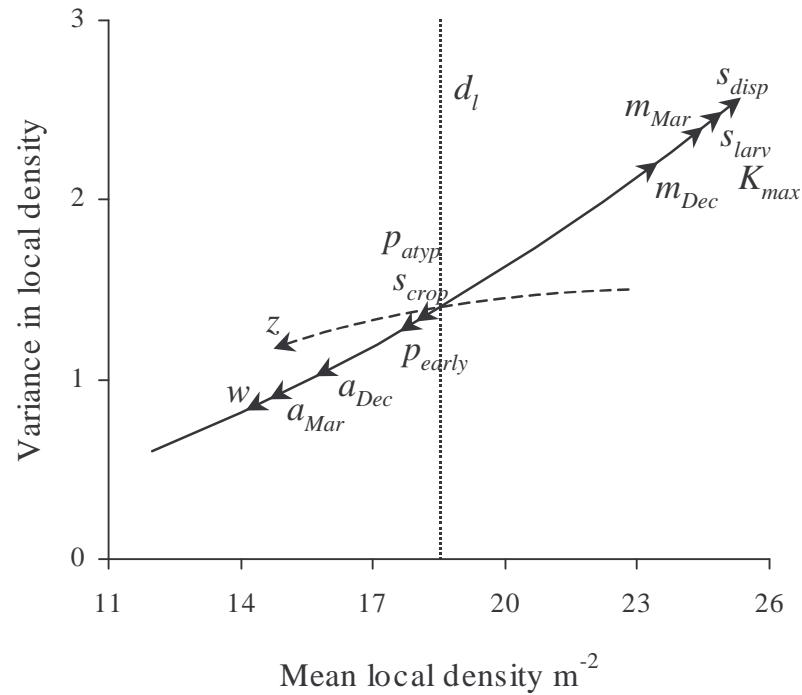


**Figure 5.6** Metapopulation model behaviour, in terms of mean and spatial variance of the local autumn weevil densities 40 years after parasitoid introduction. Individual parameters were varied between 80% and 120% of their default values (arrowheads indicate the results of multiplying each parameter by 120%), and all results lie along the solid line except those for the rate at which crop carrying capacity declines with age,  $z$ , which lie on the dashed line. Changing the dispersal range,  $d_l$ , affected only the variance, with results lying along the dotted line. Parameter definitions are listed in table 5.1.

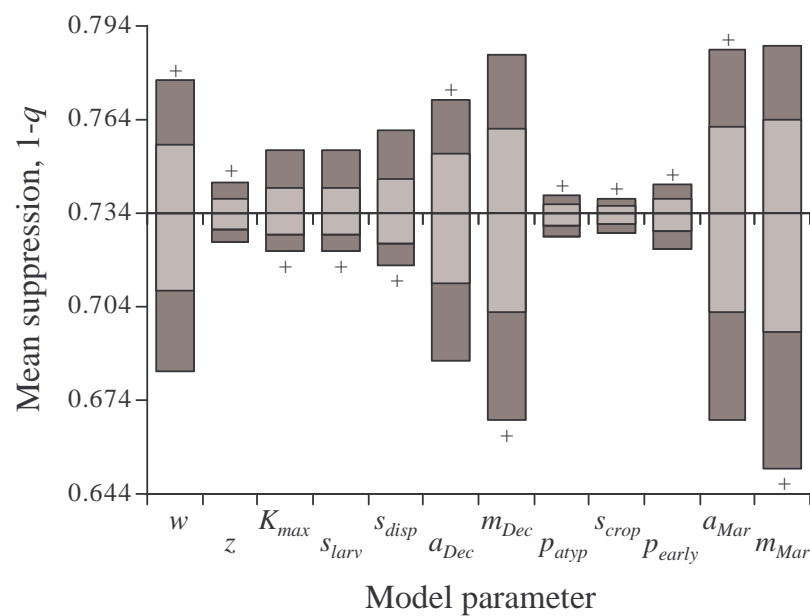


**Figure 5.7** Sensitivity of the metapopulation model, in terms of mean host suppression by the biocontrol agent, to changes of  $\pm 10\%$  (light bars) and  $\pm 20\%$  (dark bars) in individual model parameters (see table 5.1). Plus signs indicate the direction to which parameter increases result.

### 5.3.3 Effect of crop density on dispersal survival

As noted previously, the survival rate of dispersing weevils is very low:  $s_{disp} = 0.032$ . Part of this mortality is due to dispersing weevils failing to locate suitable lucerne stands, which in turn depends on the relative abundance of lucerne in the landscape. Lucerne crops made up 0.3% of total land use for the one area of Canterbury that has been studied in detail (Ian Lynn, unpublished data), though it may be higher around Darfield where the *S. discoideus* surveys were centred.

Based on Ward *et al.* (1998), weevil survival during dispersal may be modelled as

$$s_{disp} = s_{aest} [1 - \exp(-\varepsilon L)] \quad (5.14)$$

where  $\varepsilon$  determines the efficiency with which dispersing weevils locate suitable lucerne stands (analogous to searching efficiency in parasitoid-host models), and  $L$  is the relative abundance of lucerne in the environment. The rate of survival through aestivation, prior to dispersal, is included as the parameter  $s_{aest}$ . Its effect is to determine the maximum overall survival when crop abundance is large. When  $L$  is small, as it is for the *S. discoideus* system, the relationship (equation 5.14) may be approximated by the linear function  $s_{disp} = s_{aest} \varepsilon L$ , in which dispersal survival is directly proportional to crop abundance. The same approximation arises from a similar model by Dixon and Kindlmann (1990). Since dispersal survival plays an important part in determining *S. discoideus* densities, this suggests that the availability of the host crop may have an effect on the pest status of the weevil (figure 5.8).

## 5.4 Discussion

There is convincing evidence that spatial interactions at various scales may have a profound effect on population dynamics (Levin 1992; Chesson 1996; Duarte *et al.* 1998). However, there have been few attempts to assess their importance in real world case studies. Perhaps the most important question is whether detailed spatial models, such as that presented here, are necessary, rather than simpler models, like the B&G, which subsume spatial effects within an empirical fit to data.

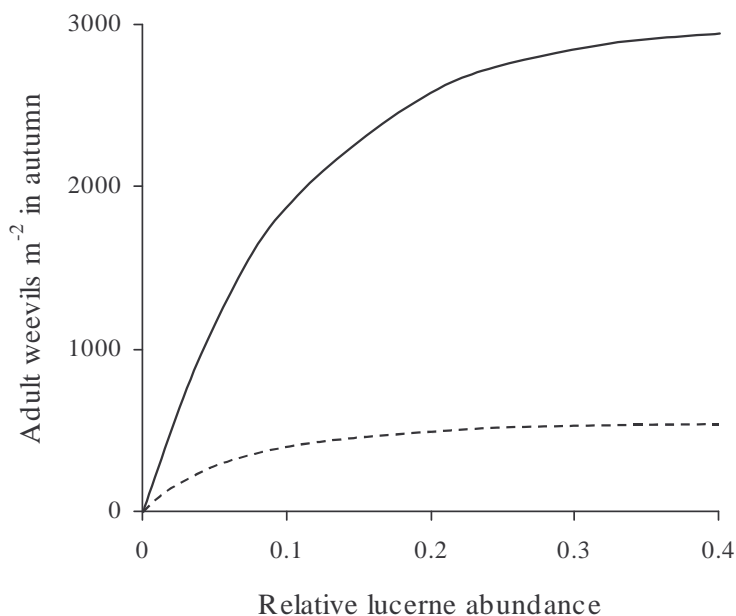


**Figure 5.8** Hypothesised relationship between lucerne abundance and weevil density in lucerne, brought about by dispersal mortality, with (dotted line) and without (solid line) *M. aethiopoulos*. Results are from the metapopulation model, plus equation 5.14 with search parameter  $\varepsilon = 10$  and aestivation survival rate  $s_{aest} = 1$  to fit apparent relative lucerne abundance  $L = 0.003$  and dispersal survival rate  $s_{disp} = 0.032$  at Darfield.

The metapopulation model behaved very similarly to the non-spatial B&G model. Host density-dependence and non-random parasitism attack behaviour regulate local population densities to such an extent that spatial interactions play a minor part in weevil population dynamics. Because of this local stability, metapopulation behaviour (figure 5.4) was equivalent to local population behaviour (figure 5.3) except in its transient responses to spatially heterogeneous perturbations such as the initial parasitoid release. The rate of initial build-up from a point release was slower for the overall metapopulation model than for a local model (figure 5.4(b)) because of the time lags involved in parasitoid dispersal. For predicting the long-term success of biological control, however, the detailed model performed no better or worse than the simpler B&G model. There was little spatial heterogeneity evident in the results from the detailed model, despite paddock renewal providing a substantial amount of local perturbation. It is clear that strong local density-dependence, coupled with homogenising dispersal (captured implicitly in equation 5.2 of the B&G model) make explicit consideration of spatial processes unnecessary in this system. In terms of

predicting the long-term outcome from biological control, the simple non-spatial model performed just as well as the more detailed spatial version.

When modified to mimic the Australian system, the model predicted 51% parasitism in autumn, but little effective suppression of the host, which is consistent with what is actually observed there (Hopkins 1989). As suggested by previous authors (Goldson *et al.* 1990; Barlow & Goldson 1993), the critical factors for the success of *M. aethiopoides* in New Zealand seem to be cooler autumn temperatures which ensure few weevil eggs are laid before spring, and atypical parasitoid development which allows higher parasitism rates to be achieved in summer weevils.

This system also demonstrates the effect that host crop abundance can have on the pest status of a herbivore. Dixon and Kindlmann (1990) showed that the proportional cover of the host plant can have a large effect on the abundance of an aphid, and this may be the reason why there are few species of aphids in highly heterogeneous habitats such as the tropics (Dixon *et al.* 1987). Leather *et al.* (1989) highlighted the abundance of primary host plants as being a major contributor to the pest status of the aphid *Rhopalosiphum padi* in Scandinavia but not in Britain, where only 0.6% of autumn migrants successfully find hosts (Ward *et al.* 1998). In the case of *S. discoideus*, it appears that only 3.2% of weevils survive summer aestivation and dispersal in the Darfield area, reflecting the relative scarcity of lucerne stands in the landscape. This analysis suggests that *S. discoideus* would be a considerably greater pest if its food crops were more abundant (figure 5.8), and this would be true even in the presence of a biological control agent. Though the relative suppression achieved by biological control remains approximately constant, pest densities may still be considerably larger when crop abundance is greater. In other words, success of biological control, as well as local pest density, may be a function of the abundance of pest habitat. These findings have general implications for agriculture, and there is considerable potential for further investigation in this area.

## 5.5 Summary

A published non-spatial model for the *Microctonus aethiopoies/Sitona discoideus* system was expanded to include dispersal in a coupled map lattice. Both models gave results consistent with observed data, mimicking the successful biological control of *S. discoideus* by the introduced parasitoid with a reduction in weevil density from 1984 to 1991 and a sustained suppression of around 75% thereafter.

The metapopulation model was locally stable because of strong host density dependence and a stabilising parasitoid attack function, so the contribution of spatial structure to local dynamics was only relevant when predicting transient behaviour, such as initial rates of parasitoid spread or the response to a local perturbation, and in determining overall weevil abundance.

Assuming that the observed low survival rate of weevils during dispersal (around 0.3%) was related to the relative scarcity of its host plant in the landscape, the model suggested that local weevil density could substantially increase with an increase in area of crop planted. The extent of biological control would be sustained in relative terms but increasing the crop abundance would still allow a substantial increase in absolute pest density.

With appropriate adjustment, the new model also simulated the unsuccessful biological control observed in Australia. Advancing weevil oviposition in autumn (reflecting warmer autumn temperatures in Australia) and reducing parasitism rates among aestivating weevils (reflecting a lack of summer development of parasitoids in Australia, compared with the atypical development of a proportion in New Zealand) resulted in parasitism being unable to substantially reduce modelled weevil populations.

## 6. Disease metapopulation dynamics in continuous time

### 6.1 Introduction

Previous chapters showed that metapopulation interactions enhance the persistence of otherwise unstable local dynamics, and catalogued the range of metapopulation patterns that may arise from various local stability types. These results, however, were derived for metapopulation interactions in discrete time. May (1973) demonstrated how the stability properties of non-spatial models differ between discrete and continuous time analogues. This chapter, therefore, investigates whether continuous-time metapopulations behave similarly to those in discrete time.

Within the field of pest management, continuous-time models have been most commonly applied to disease-host systems. Spatial effects are usually incorporated as ‘continuous space’, modelled as different forms of diffusion (Skellam 1951; Okubo 1980; Holmes *et al.* 1994). These typically focus on rate of spread and shape of a wave-front rather than local population dynamics. A related approach is to use cellular automata with individual animals occupying points in space and experiencing interactions from their nearest neighbours (e.g. Mollison & Kuulasmaa 1985; Barlow & Kean 1996). In this chapter, however, a simple metapopulation approach is adopted, enabling direct comparison with previous chapters.

In continuous-time models, zero-densities are approached asymptotically and so extinction may never occur. Models differ in the way in which they handle this problem. In some (e.g. Anderson *et al.* 1981; Murray *et al.* 1986; Louie *et al.* 1993), it is ignored, while others (e.g. Barlow & Kean 1998) implement a low threshold value below which extinction is assumed to occur. Individual-based models (e.g. Smith & Harris 1991; Barlow 1993; Wilson & Hassell 1997) side-step the problem completely, but in doing so become stochastic. Though the importance of these

assumptions is known (Mollison 1991), their effects have not previously been compared.

This chapter examines the qualitative dynamics of a range of disease-host metapopulation models, and demonstrates how disease persistence and spatial patterning depend on local stability characteristics and the density at which extinction is assumed to occur.

## 6.2 Models

Disease-host interactions may take a wide variety of different forms, and models for many of these have been well studied (Anderson & May 1979, 1980, 1981; May & Anderson 1979; Mollison 1984; Bowers *et al.* 1993; Louie *et al.* 1993; Barlow 1996). This chapter takes two of the most common forms to explore in a metapopulation context. Both assume direct transmission between infected and susceptible hosts, as well as density-dependent background mortality. The first model applies when some infected hosts recover to become immune to subsequent infection, while the second features an incubation stage for the disease.

### 6.2.1 SIR model

Disease models which assume some recovery and subsequent immunity are generally known as ‘SIR’ models. Here, the state variables refer to the densities of susceptible ( $S$ ), infectious ( $I$ ), and recovered ( $R$ ) individuals, respectively. One commonly-used SIR model is

$$\begin{aligned}\frac{dS}{dt} &= b(N - I) - (d + wN)S - \beta SI \\ \frac{dI}{dt} &= \beta SI - (d + wN)I - (\alpha + \nu)I \\ \frac{dR}{dt} &= \nu I - (d + wN)R\end{aligned}\tag{6.1}$$

where  $t$  denotes time, and total population density,  $S+I+R$ , is denoted  $N$ . Parameter  $b$  is the reproductive rate of non-infectious animals, while  $d$  is the minimum mortality

rate in the absence of disease, and is increased by density-dependent mortality acting through parameter  $w$ . The intrinsic rate of increase of the population,  $r$ , is given by  $b-d$ , while the carrying capacity (maximum population size possible),  $K$ , equals  $r/w$  (Barlow & Kean 1998).

For the disease,  $\beta$  is the transmission coefficient, which is related to the contact rate  $\beta K$  between animals at density  $K$ . The mortality rate due to disease is denoted  $\alpha$ , while  $\nu$  is the recovery rate. A useful statistic in disease models is the non-dimensional quantity  $R_0$ , the basic reproductive rate of the disease. This describes the number of new infections created in the lifetime of a single infectious animal introduced into a susceptible population at its carrying capacity. For the SIR model described above,

$$R_0 = \frac{\beta K}{(b + \alpha + \nu)} \quad (6.2)$$

(appendix 4.11). Another useful disease statistic is  $r_d$ , the intrinsic rate of increase of the disease, which is the specific rate of increase of infectious animals when the disease is first introduced to a host population at its carrying capacity (N.D. Barlow, personal communications). For this model (appendix 4.12),

$$r_d = \beta K - (b + \alpha + \nu) \quad (6.3)$$

Barlow & Kean (1998) used equations 6.1 to explore the possible impacts of rabbit calicivirus disease (RCD) on New Zealand rabbit (*Oryctolagus cuniculus*) populations. Their published parameter values (table 6.1) are used as defaults for model 6.1, though it is now thought that the Australian epidemic from which these were derived was an unusually severe one; subsequent epidemics in New Zealand suggest lower  $\beta$  and higher  $\nu$  (N.D. Barlow, unpublished data). Since the focus of this chapter is general disease dynamics, the published parameter values are used.

### 6.2.2 SEI model

Another useful class of disease models, generically termed ‘SEI’ models, applies to fatal diseases with no recovery, and features an implicit time lag between exposure and infectiousness. One such model is

$$\begin{aligned}\frac{dS}{dt} &= b(N - I) - (d + wN)S - \beta SI \\ \frac{dE}{dt} &= \beta SI - (d + wN)E - \sigma E \\ \frac{dI}{dt} &= \sigma E - (d + wN)I - \alpha I\end{aligned}\tag{6.4}$$

where the state variables refer to the densities of animals which are susceptible ( $S$ ), exposed but not yet infectious ( $E$ , sometimes called ‘latent’), or infectious ( $I$ ). Again, the total population density,  $S+E+I = N$ . All parameters are the same as described for the SIR model above, except that here  $\sigma$  denotes the inverse of the mean latent period (duration of state  $E$ ).  $R_0$  is obtained as before (appendix 4.11):

$$R_0 = \frac{\sigma\beta K}{(b + \alpha)(b + \sigma)}\tag{6.5}$$

The formula for  $r_d$  is more complicated. A suitable approximation (N.D. Barlow, personal communications, appendix 4.12) is

$$r_d \cong \frac{\sigma\beta K - (b + \alpha)(b + \sigma)}{2b + \alpha + \sigma}\tag{6.6}$$

Anderson *et al.* (1981) used equations 6.4 to model rabies in foxes (*Vulpes vulpes*), while a close variant was used by Barlow (1991) for modelling patches of bovine tuberculosis (*Mycobacterium bovis*, ‘Tb’) in New Zealand possums (*Trichosurus vulpecula*). The parameter values for these systems are given in table 6.1.

### 6.2.3 Metapopulation formulations

The models were replicated in space, using a 30×30 coupled map lattice (Kaneko 1989) with reflecting boundaries (figure 2.2). Dispersal was modelled as a proportion  $\mu$  of each disease class being redistributed among the nearest eight neighbouring subpopulations. The dispersal rate was assumed to be equal for all model classes, since in this case the disease is not free-living and can only disperse with its host. In this respect, the models are more similar to the *Sitona discoideus/Microctonus aethiopoidea* model of chapter 5 than to the host-parasitoid systems of chapter 3, where host and parasite dispersal rates differed from each other. The assumption of equal dispersal rates for all disease classes addresses the concern of Busenberg and

**Table 6.1** Default parameter values for disease/host systems discussed in the text.

Rabbit/RCD values from Barlow & Kean (1998), fox/rabies values from Anderson *et al.* (1981), possum/Tb values from Barlow (1991). Dispersal rates are arbitrary defaults.

		Rabbit/RCD	Fox/rabies	Possum/Tb
model type		SIR	SEI	SEI
time unit		day	month	year
area unit		ha	km <sup>2</sup>	ha
$b$	mean reproductive rate	0.00822	0.083	0.305
$d$	minimum background mortality	0.00460	0.042	0.105
$K$	carrying capacity	24	2.0	10
$\beta$	transmission coefficient	0.14	6.7	1.0
$\alpha$	mortality rate due to disease	0.6	6.1	4.0
$\nu$	rate of recovery from disease	0.04	-	-
$\sigma$	inverse of mean latent period	-	1.1	1.0
$R_0$	basic reproductive rate of disease	5.18	2.01	1.78
$r_d$	rate of increase of disease (yr <sup>-1</sup> )	990	12	0.78
$r$	rate of increase of host (yr <sup>-1</sup> )	1.3	0.5	0.2
$r_d/r$	disease dynamics relative to host	762	24	3.9
$\mu$	dispersal rate	0.01	0.02	0.1

Travis (1983) that net dispersal of each disease class should reflect the mechanism for dispersal of the whole population.

The models were solved numerically, using the fourth-order Runge-Kutta method (Kreyszig 1988) and ensuring that the timesteps used were short enough to have negligible effect on the local dynamics. In practice, this was achieved with 10 timesteps per day for the rabbit/RCD system, 30 per month for fox/rabies, and 52 per year for possums/Tb. Shorter timesteps added to the complications arising from the effects of very small densities, as discussed in section 1.3.3 below.

Four model variants were created, differing in the way in which they handled arbitrarily small densities. In the ‘no threshold’ formulation, local densities were allowed to become infinitely small, and since the models approach zero asymptotically, extinction was precluded. A ‘threshold’ formulation checked local densities at the end of each timestep, and any lower than an extinction threshold,  $K_L$ , were set to zero. This is essentially an ‘Allee effect’ (Allee *et al.* 1949; Murray 1993). In the ‘discrete dispersal’ variant, an extinction threshold at  $K_L$  was also implemented, but dispersal occurred as a discrete event just once each time unit (daily for RCD, monthly for rabies, and yearly for Tb). Finally, an ‘individual-based’ formulation defined  $K_L$  to represent the contribution by one individual to the local density. The maximum number of individual animals allowed in each subpopulation was therefore  $K/K_L$ . Here, all population processes (birth, death, disease transmission, recovery, becoming infectious, and dispersal) were made to refer to discrete individual animals, by applying a Binomial probability (using the algorithm of Kelton & Law 1991) to calculate the outcome.

Metapopulations were initialised in one of two ways. The first, corresponding to the ‘biocontrol’ initial condition of chapter 3, had all subpopulations disease-free and at their carrying capacity ( $S = K$ ,  $I = R = E = 0$ ), and infectious animals introduced into location (3,1) at a density of  $10 \times K_L$  (or  $K \times 10^{-5}$  for the no threshold formulation). A second ‘heterogeneous equilibrium’ initial configuration had all local densities initialised at their equilibrium values (table 6.2), except that local susceptible densities were drawn randomly from a uniform distribution between 0 and twice the equilibrium. This was used only for exploring emergent spatial patterns.

**Table 6.2** Behaviour of metapopulations with various local dynamics. Default parameters used except where indicated.

Model	Non-default parameters	Non-spatial equilibrium	Equilibrium stability	Metapopulation outcome
SIR, rabbit/RCD	-	$S_{eq} = 24$ $I_{eq} = 0$ $R_{eq} = 0$	boom-bust, non-persistent	non-persistent, homogeneous (figure 6.2(b))
SEI, fox/rabies	-	$S_{eq} = 0.98$ $E_{eq} = 0.019$ $I_{eq} = 0.003$	boom-bust, non-persistent	persistent, homogeneous (figure 6.2(b))
SEI, possum/Tb	-	$S_{eq} = 5.1$ $E_{eq} = 0.48$ $I_{eq} = 0.11$	converging oscillations, stable	persistent, homogeneous (figure 6.2(a))
SEI, possum/Tb	$w = 0$ $\sigma = 1.4$	$S_{eq} = 4.4$ $E_{eq} = 0.74$ $I_{eq} = 0.28$	stable limit cycles	persistent, heterogeneous (figure 6.2(c))
SIR, rabbit/RCD	$b = 0.82$ $d = 0.46$ $w = 0, v = 0$	$S_{eq} = 7.6$ $I_{eq} = 2.6$ $R_{eq} = 0$	neutral stability	persistent, heterogeneous (figure 6.2(d), (e))
SEI, possum/Tb	$w = 0$ only susceptibles reproduce	$S_{eq} = 4.5$ $E_{eq} = 0.82$ $I_{eq} = 0.20$	diverging oscillations, unstable	persistent, heterogeneous (figure 6.2(f))

## 6.3 Results

### 6.3.1 Model behaviour and spatial patterning

Anderson and May (1981) explored the properties and stability of a range of simple disease models, though the specific models of equations 6.1 and 6.4 were not examined. Nevertheless, similar models including recovery or latency were analysed in detail, and similar methods were applied here. Between them, the two disease models described above exhibit a range of local behaviour (table 6.2). Without dispersal, the dynamics of the SIR model (equations 6.1) are stable, except for fatal

diseases ( $v = 0$ ) in unbounded host populations ( $w = 0$ ), when the equations collapse to the neutrally stable Lotka-Volterra model (Lotka 1925; Volterra 1926; May 1973). The SEI model (equations 6.4) is generally stable for biologically realistic parameter values, but can exhibit limit cycle behaviour when the host carrying capacity is large ( $w \rightarrow 0$ , Anderson *et al.* 1981). Unstable oscillations arise in the SEI model if it is assumed that only susceptible animals reproduce successfully, so that the term  $b(N-I)$  in equations 6.4 is replaced by  $bS$ .

For the purposes of this chapter, it was necessary to define a special type of local model behaviour. ‘Boom-bust’ models were defined as those in which densities of disease classes drop below  $K_L$  at any time after an initialisation of  $I = 10 \times K_L$ ,  $S = K$ , and all other disease classes empty in the non-spatial model. This most commonly occurs when the intrinsic rate of increase of the disease ( $r_d$ ) is high in comparison with that for the host ( $r$ ). Local models could be stable, with the equilibrium state resistant to small perturbations, yet exhibit boom-bust dynamics when the disease is introduced at a low density into a wholly susceptible population at its carrying capacity.

Chapter 3 showed for discrete-time models that the stability of local populations in isolation determines the type of spatial patterning that emerges when these are linked in a metapopulation. Here, the same kind of effect was tested for in continuous-time metapopulations. Introducing disease into the metapopulations gave an initial pattern of ripple-like wave fronts radiating outward from the site of introduction (figure 6.1). In stable local models, this was eventually followed by homogeneity, with the disease either persisting at some equilibrium level (figure 6.2(a)), or, in the case of most boom-bust scenarios, going extinct (figure 6.2(b)). Like discrete-time models (chapter 3), limit cycle local dynamics gave regional homogeneity (figure 6.2(c)), and unstable local models gave heterogeneous ‘spatial chaos’ in the metapopulations (figure 6.2(d) to (f)). Neutrally stable local models also gave heterogeneous spatial patterns in a metapopulation, and this heterogeneity persisted even when the dispersal rate was high (figure 6.2(d) and (e)). Local oscillations were much greater for unstable local models than for neutrally stable or limit cycle models. Overall, recognisable spirals were not apparent in disease

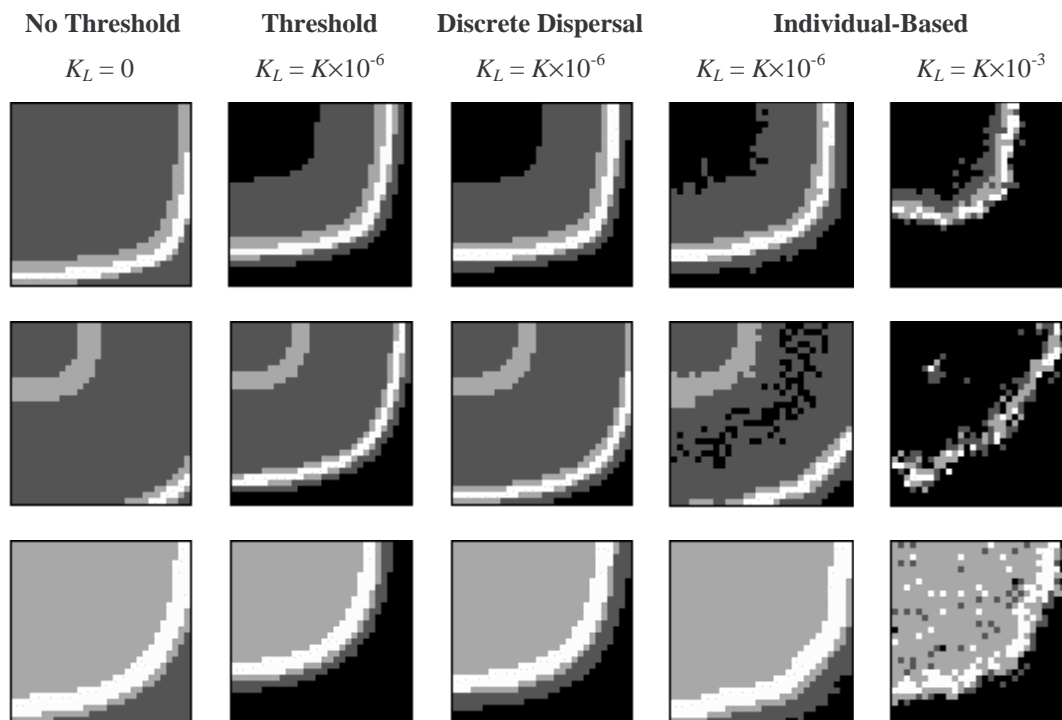


**Figure 6.1** Comparison of metapopulation simulations with different assumptions about very low densities and dispersal. ‘Biocontrol’ disease introduction at location (3,1) and parameter values as listed in table 6.1. The local density of infectious animals,  $I$ , is shown, with shading relative to the maximum local value in each metapopulation,  $I_{max}$ : black for  $I = 0$ ; dark grey for  $I \leq I_{max}/10$ ; light grey for  $I \leq I_{max}/2$ ; white for  $I > I_{max}/2$ . Long-term persistence is indicated by the presence of grey or white in the top left quadrant. Top: rabbit/RCD at  $t = 50$  days; middle: fox/rabies at  $t = 120$  months; bottom: possum/Tb at  $t = 80$  years.

metapopulations, which contrasts with host-parasitoid metapopulations where they formed the basis of most spatial patterns. Instead, patterns often consisted of interacting ‘arcs of infection’ (Mollison & Kuulasmaa 1985).

### 6.3.2 Effect of space on disease persistence

Metapopulation dynamics allowed persistence of otherwise unstable disease interactions. This includes local models that in isolation gave diverging oscillations, as well as many boom-bust scenarios. For example, the fox/rabies model with default parameters behaved in a boom-bust way when there was no dispersal, with infectious

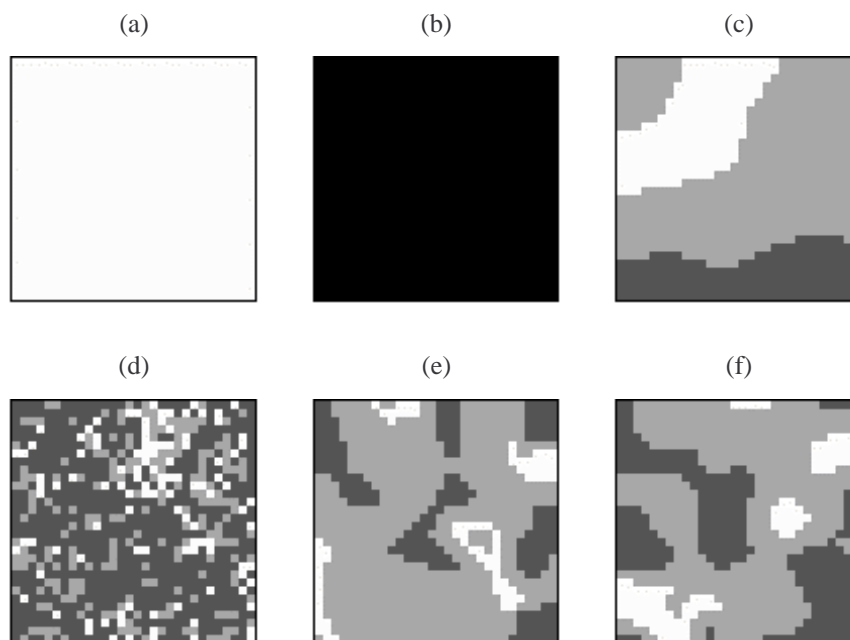


**Figure 6.2** Snapshots of metapopulation simulations under different local stability conditions (parameters as in table 6.2). Local infectious densities, shaded as for figure 6.1, shown after 500 time units after ‘heterogeneous equilibrium’ initialisation. (a) persistent, homogeneous; (b) non-persistent (extinct); (c) stable limit cycles; (d) neutral stability,  $\mu = 0.01$ ; (e) neutral stability,  $\mu = 0.1$ ; (f) diverging oscillations (unstable).

densities going as low as  $3 \times 10^{-7} \times K$  between the first and second disease outbreaks. However, with dispersal this minimum was substantially higher, allowing persistence with  $K_L = 10^{-6} \times K$  the arbitrary threshold for extinction in the model. Metapopulation dispersal acted to dampen the initial oscillations in local density, and though the effect was slight (figure 6.3), this was enough to keep densities above the imposed threshold for extinction. In individual-based versions, local extinctions were common, but always followed by recolonisation from elsewhere in the metapopulation. Here, overall persistence occurred, but local equilibrium was not attained (figure 6.3) due to demographic stochasticity (the randomness arising when demographic processes such as birth, death, disease transmission, and dispersal are applied to small numbers of discrete individuals). Metapopulation structure with low to medium dispersal rates always allowed persistence of the otherwise boom-bust rabies model for the range of scenarios tested.

In some cases, individual-based models allowed persistence via some infectious animals ‘breaking back’ across the post-epidemic trough behind a wave of disease. These then seeded subsequent epidemic waves once the densities of susceptible animals recovered sufficiently (figure 6.4).

### 6.3.3 Effects of assumptions about very low densities

Some difficulties were experienced while solving the models numerically. Specifically, the small timesteps needed for an accurate numerical solution sometimes generated very small densities of disease classes. In particular, dispersal of diseased animals into previously disease-free areas generated very small founding populations, which were often below the imposed threshold for extinction,  $K_L$ . Therefore, disease spread depended on infected animals behind the wave front increasing to sufficient numbers that these founding populations exceeded  $K_L$ . Meanwhile, unsuccessful founders acted as a drain for local disease, reducing its rate of local build-up and speed of spatial spread. It was even possible to use timesteps so short, or dispersal rates so low, that all founding populations were sub-threshold, and the disease failed to disperse at all. Careful selection of the model timestep helped to minimise these effects in the metapopulation results presented here.

The rate of movement of disease epidemics across a metapopulation varied depending on the model’s treatment of very low densities (Figure 6.1). The fastest rates of spread were observed in ‘no threshold’ ( $K_L = 0$ ) models, but were almost matched by those of individual-based models with many animals per subpopulation ( $K_L$  small). Extinction thresholds reduced the epidemic velocity, though this effect was less pronounced when dispersal was implemented at discrete intervals. The slowest, and least robust, wave fronts occurred in individual-based models with few individuals per subpopulation ( $K_L$  relatively large).

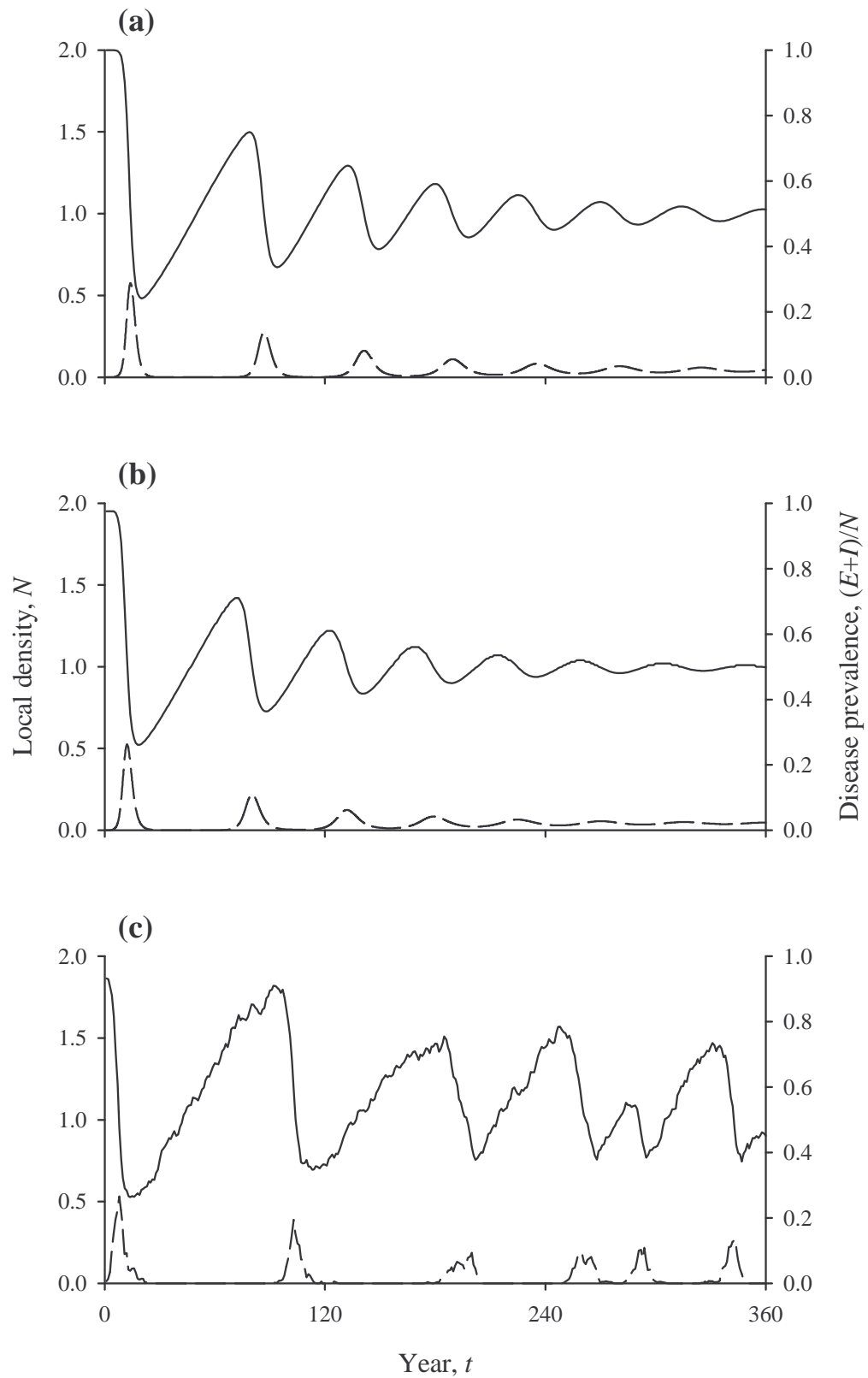


**Figure 6.3** Dynamics of a local population within the default fox/rabies model. Biocontrol initialisation; (a) non-spatial model; (b) metapopulation with continuous dispersal and extinction threshold  $K_L = 10^{-6}$ ; (c) individual-based model with  $K_L = 10^{-3}$ .

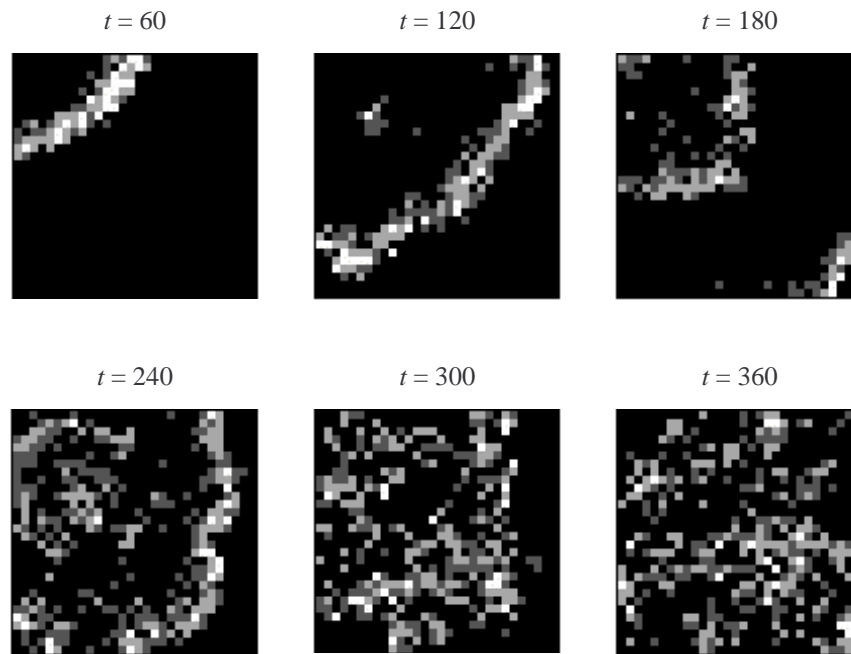


**Figure 6.4** Snapshots of an individual-based fox/rabies metapopulation at different times  $t$  after a ‘biocontrol’ disease introduction. Default parameters as in table 6.1, and  $K_L = K \times 10^{-3}$ . Local densities of infectious animals shown as for figure 6.1.

Long-term results, too, were found to be affected by a model’s assumptions about low densities (figure 6.5). When the assumed density of extinction,  $K_L$ , was low, and these densities were subsequently rare, then there was little qualitative difference between models with different assumptions. With a higher  $K_L$ , however, model assumptions about extinction became increasingly important, and there could be significant qualitative differences between model results (figure 6.5).

Local extinctions in the models acted as ‘symmetry breakers’, and appeared to be more important in the evolution of spatial patterns than the lattice edge effects which were the primary disrupters of symmetry in the discrete-time metapopulations of chapter 3. For example, figure 6.6 tracks mean disease prevalence in a metapopulation with unstable local dynamics (the diverging oscillations scenario of table 6.2, with extinction threshold  $K_L = 10^{-6}$ ). Over the first hundred years of simulation from a ‘heterogeneous equilibrium’ initialisation, local densities fluctuated largely in concert, and the dynamics of the metapopulation as a whole

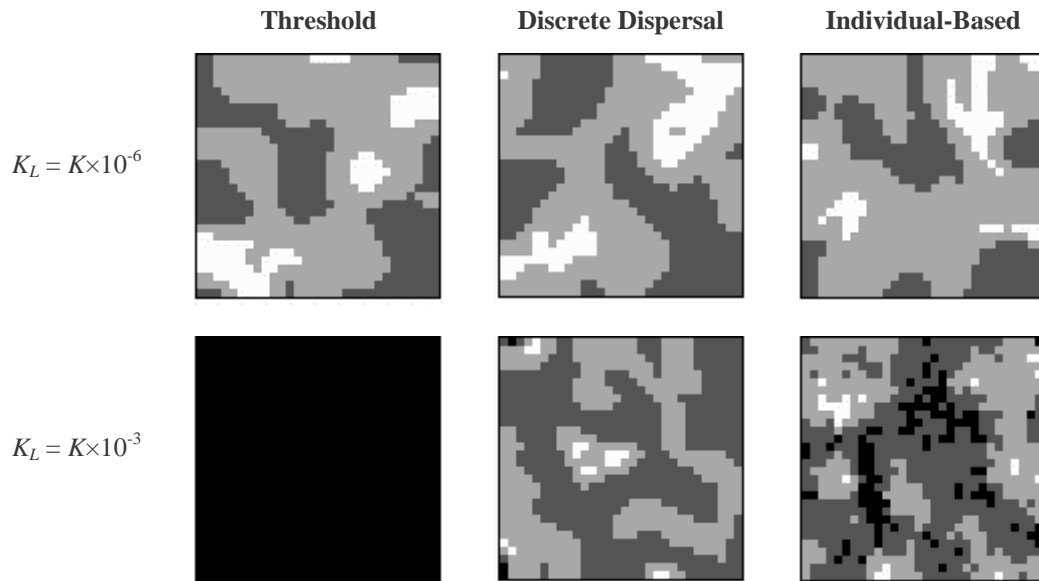


**Figure 6.5** Effect of low density assumptions on patterns emerging from unstable local models (possum/Tb model with  $c = 0$  and reproduction by susceptibles only, see table 6.2). Each simulation was initialised from the same ‘heterogeneous equilibrium’ state and run for 500 years. Infectious densities shown, shaded as for figure 6.1.

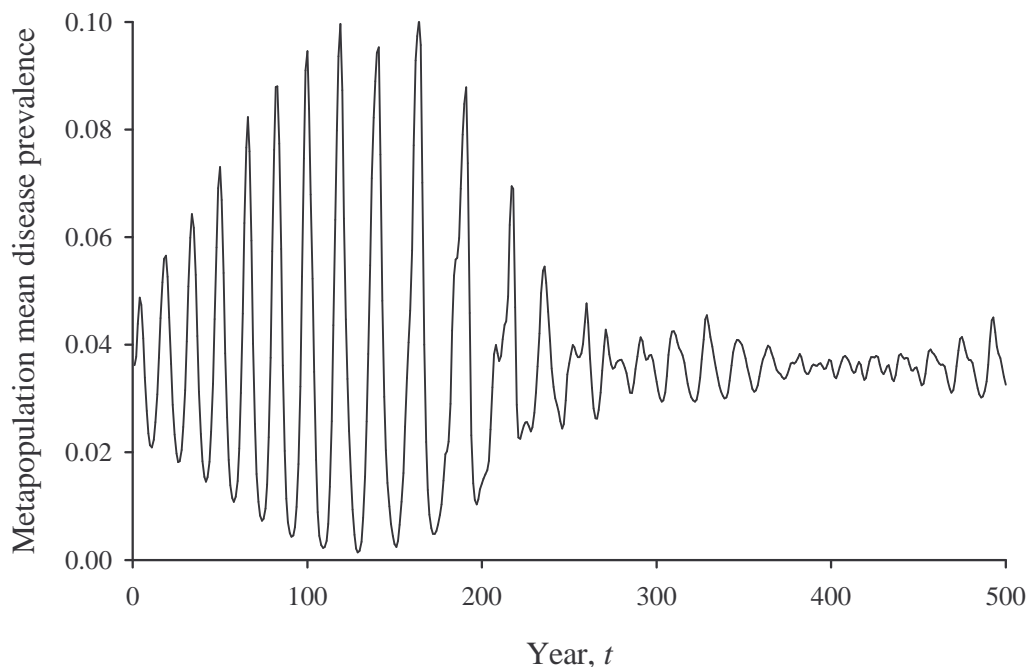


**Figure 6.6** Metapopulation mean disease prevalence in possum/Tb model with diverging oscillations (table 6.2), run from a ‘heterogeneous equilibrium’ initial condition. Final pattern is shown in figure 6.2(f).

showed diverging oscillations. Local extinctions began to occur at around year 150, causing the metapopulation dynamics to become less regular. Finally, whole regions of the metapopulation started going extinct; the delay in recolonising these areas resulted in full asynchrony across the metapopulation, and thereby more constant overall dynamics, at around year 200. Once this period of self-organisation was completed, local extinctions again became a rare event. A snapshot of this metapopulation after 500 years is shown in figure 6.2(f).

## 6.4 Discussion

To date, there have been few modelling studies on continuous-time processes in discrete space. Prior to the results presented in this chapter, none have examined the general dynamics of diseases in metapopulations with limited dispersal range, though Grenfell and Harwood (1997) pointed out that simple disease models may be regarded as metapopulations in the classical sense, with hosts acting as habitat patches for the disease.

The few explicit-space disease metapopulation models that have been published have all been targeted at some particular problem. Swinton *et al.* (1998) modelled a phocine distemper virus outbreak in North Sea harbour seals (*Phoca vitulina*) using a one-dimensional lattice model. Theirs was a boom-bust system and, like those explored here, a realistically-sized lattice was insufficient to allow disease persistence. Similar results emerge from the stochastic individual-based models that have been used to estimate the likely rate of spread of rabies in British foxes (e.g. Smith & Harris 1991; White *et al.* 1995).

Wood and Thomas (1996) used a continuous-time, discrete-space disease model to study a grasshopper biological control system. Their boom-bust model, however, contained relatively little within-generation mixing; the spatial dynamics were mainly driven by discrete between-generation global dispersal events. Disease persistence relied on global dispersal of the new generation of susceptible hosts at the start of each year, repopulating extinct locations behind the wave-front. When some populations events are discrete and regular, like global dispersal in their model, it is

possible to integrate the continuous-time disease dynamics between dispersal events, yielding a discrete-time model. White *et al.* (1996) used this approach to study a simple disease system, and the resulting discrete-time model with unstable local dynamics gave rise to a range of metapopulation patterns similar to those described in chapter 3.

The results presented in this chapter suggest that the principles for discrete-time metapopulation spatial patterning apply similarly to continuous-time models. Spatial patterning in disease-host metapopulations depended on the underlying stability of local populations in isolation. Stable local dynamics gave eventual metapopulation homogeneity: either global extinction for boom-bust models, or equilibrium densities equal throughout the metapopulation. As in discrete-time metapopulations (chapter 3), sustained heterogeneity required both unstable or undamped oscillatory local dynamics together with some heterogeneity in initial conditions. Local extinctions were found to be important as symmetry breakers in the evolution of spatial patterns. The patterns arising in these models (e.g. figures 6.2 and 6.5) tended not to show distinct spirals, but rather ‘arcs of infection’ similar to those noted by Mollison and Kuulasmaa (1985). Continuous local dispersal was insufficient to homogenise metapopulation densities in these cases.

The three case studies considered here span a wide range of disease characteristics. The intrinsic rate of increase of RCD is almost a thousand times greater than that of its rabbit host, while that for Tb is of the same order of magnitude as for possums (table 6.1). Between these extremes is rabies in foxes, which would have much more rapid dynamics if not for its latent period. The default rabies model gave particularly interesting metapopulation dynamics. Without dispersal, the minimum infectious density between outbreaks was less than the threshold value of  $K_L = 10^{-6}$ , resulting in its boom-bust characterisation. However, in a metapopulation context inter-epidemic densities remained above this threshold, and the disease persisted. The enhancement of local persistence by dispersal has been discussed elsewhere, such as in chapters 2 and 3. This result does, however, contrast with those from the diffusion model of Murray *et al.* (1986), where the density of infectious foxes became extremely low between outbreaks: of the order of  $10^{-18} \text{ km}^{-2}$ , termed the “atto-fox” by Mollison (1991). The reason for this appears to be that in their

model dispersal applied only to infectious animals, so that recovery of susceptible foxes after outbreaks was not aided by immigration. At such low densities, stochastic events become important. As Mollison (1991) suggested, it is dubious, therefore, to predict as Murray *et al.* (1986) do, not only that rabies persists in such situations, but also that it outbreaks at regular intervals of 3 to 5 years.

In the individual-based rabies model with  $K_L = 10^{-3}$ , small pockets of infection remained behind the main wave-front, seeding secondary outbreaks in the recovering population. It is this behaviour, with disease ‘breaking back’ over the post-epidemic trough, that allows rabies persistence in this model and probably in the field (Mollison 1991). The rabies model of Jelsch *et al.* (1997) used occasional long-range dispersal of infected animals to achieve a similar result. In contrast, persistence in diffusion models for rabies (Murray *et al.* 1986) relies on the viability of atto-fox densities, and subsequent epidemics always originate in exactly the same place as the first.

The atto-fox, where qualitative model behaviour depends critically on very low densities, arises because extinction in simple no-threshold continuous-time models is approached asymptotically and therefore never reached. This is particularly the case in disease-host models which feature latency (disease incubation before infectiousness) or explicit spatial processes. Often, as in the rabies models of Anderson *et al.* (1981) and Murray *et al.* (1986) or the Tb model of Louie *et al.* (1993), this effect has simply been ignored (corresponding to the ‘no threshold’ formulation above). In simulation experiments, however, an extinction threshold is often used (e.g. Comins *et al.* 1992; Barlow & Kean 1998), but this threshold is often arbitrary and the effects of its magnitude are rarely tested. This approach also has the disadvantage that it may add up to a substantial mortality, especially in spatial models where dispersing densities in each timestep decrease as the dispersal time interval gets smaller. Implementing dispersal less frequently mitigates this problem, but results in what is essentially a discrete-time model similar to those discussed in previous chapters. Individual-based models, on the other hand, side-step the problem of very low densities completely, and in this respect may be the most logical and least arbitrary choice of model formulation for spatial systems. For example, it has been noted that simulated travelling waves typically move much more slowly than their

analytical counterparts (Mollison 1991). This is because the edges of analytical travelling waves spread via unrealistically tiny densities.

It is clear from figure 6.1 that the assumptions made about low densities and dispersal may have quantitative, and sometimes qualitative, effects on model behaviour. With no threshold ( $K_L = 0$ ), the leading edge of a dispersing disease moves infinitely quickly and there is no such thing as disease extinction. The rate of spread of epidemic waves is affected considerably by a model's treatment of very low densities. At a very broad level, the results of this study suggest that wave speed is reduced by extinction thresholds removing infectious animals. Similarly, epidemic waves move faster in models with discrete dispersal than those with continuous dispersal, because discrete dispersal results in more individuals moving less often and therefore less loss through the threshold. Individual-based models may allow epidemic waves to travel as fast as zero-threshold models, but the longer the timestep for dispersal and the fewer the individuals per subpopulation, the more stochastic effects become important, and the slower the speed of the wave front. The observation that epidemic waves in individual-based models tend to travel more slowly than in their linear counterparts is well-known, though not well quantified (Mollison 1991).

## 6.5 Summary

Disease-host metapopulations are formulated in continuous time and discrete space. Parameter sets are described for three case studies: rabbit/RCD, fox/rabies, and possum/Tb. These models are used to examine the qualitative dynamics of disease metapopulations, and examine the effects of model assumptions about very low densities.

As in discrete-time metapopulations (chapter 3), the type of spatial heterogeneity and spatial patterns generated depend on the stability characteristics of the local models in the absence of dispersal. Stable local dynamics give homogeneous metapopulations, while different local stability may result in persistent heterogeneous metapopulations, given suitable initial conditions and symmetry-breaking local

extinctions. Spatial patterns tend to be composed of ‘arcs of infection’, rather than the distinctive spirals arising in discrete-time metapopulations.

Some stable models, however, show non-persistent ‘boom-bust’ dynamics, whereby disease classes fall to unrealistically low densities between initial epidemics. Boom-bust systems are usually non-persistent in a metapopulation, but some may persist if dispersal damps initial oscillations sufficiently.

The qualitative dynamics of continuous-time disease host models are critically dependent on assumptions about what happens to disease classes at very low densities. This is particularly true in metapopulations, where densities of dispersing animals may be very small. Models that assume no local extinction give the fastest rate of disease spread and guarantee disease persistence. The assumption of some non-zero extinction threshold ‘wastes’ sub-threshold densities, resulting in slower disease spread. This effect is minimised when dispersal events are implemented less frequently. Individual-based models with many animals per subpopulation give similar results to those with extinction thresholds, but also give epidemic wave speeds similar to ‘no threshold’ formulations. With fewer animals per subpopulation, individual-based models are more reliant on demographic stochasticity, and disease wave-fronts move slower. Disease persistence may, however, rely on infectious animals breaking back across the post-epidemic trough, rather than on the less realistic persistence of disease classes above an arbitrarily-defined threshold for extinction.

## 7. Conclusions

### 7.1 Metapopulation structure promotes persistence

There is nothing new in the observation that metapopulations promote persistence of otherwise unstable interactions. This effect is at its most extreme in the pioneering metapopulation model of Levins (1969), where local extinctions are balanced by recolonisation from other subpopulations. All of the models discussed in the previous chapters show the promotion of persistence in metapopulations, though the mode of instability differed: stochastic extinction in single-species models; deterministic instability in host-parasitoid models; and boom-bust non-persistence in disease models. In each case, metapopulation interactions allowed these interactions to persist for longer than they would otherwise have, and in some cases effectively forever.

This thesis has highlighted some of the conditions necessary for long-term metapopulation persistence. Chapter 2 showed that when local population dynamics are stochastic, some density-dependence is necessary for long-term metapopulation persistence. When the metapopulation is large, however, so little density-dependence may be required that this may not be detectable in population time series.

For host-parasitoid interactions, the persistence conferred by metapopulation processes allowed very high host suppression to be obtained, but this persistence depended on the initial conditions. For pest management, we are most interested in what happens when the parasitoid or disease is introduced at a low initial density at a single point in a metapopulation with hosts at their carrying capacity. A wave of parasitism or disease then spreads outward from this source. Depending on the local models, this wave could be followed by extinction of the interaction ('boom-bust') or persistence with further wave propagation. Because of the disparity in initial densities between host and parasitoid or disease, such 'biocontrol' introductions are the most likely to produce boom-bust waves and therefore are the least likely to persist. In

host-parasitoid metapopulations, models which gave high host suppression (where equilibrium mean host densities are small compared to the host carrying capacity) also tend to have boom-bust dynamics and extinction following a biocontrol initialisation. As a result, the maximum persistent host suppression possible in a biocontrol metapopulation was 84%. This compares to the 60% maximum suppression possible in simple non-spatial models, and the 90% or more often observed in the field. Metapopulation structure can provide only a partial answer, therefore, to how such high levels of control are achieved and sustained. This result was robust to spatial variation in habitat quality.

Local extinction may be an important feature of some metapopulations (Murdoch *et al.* 1985; Lei & Hanski 1997), especially those with boom-bust local dynamics. Chapter 6 demonstrated that model assumptions about very low densities and extinction can affect the qualitative behaviour of metapopulation models. This is especially true in models with continuous dispersal, where dispersing quantities may be very very small. All models need to clearly state their assumptions about how very low densities are handled so that readers can evaluate whether these are realistic or not.

## **7.2 Sometimes you don't need to know dynamics in space in order to understand and predict dynamics in time**

Dispersal between asynchronous populations can have important, though sometimes subtle, effects on local dynamics (e.g. appendix 3). However, there are cases where it is not necessary to know the spatial interactions affecting a population in order to understand its temporal dynamics. In particular, if subpopulation densities are homogeneous, for example in the equilibrium state for a metapopulation with stable local dynamics, then metapopulation dynamics match those of the subpopulations. A case in point is the *S. discoideus*/*M. aethiopoidea*s host-parasitoid system in Canterbury. Here, dispersal plays an important part in the population dynamics, especially through the very large mortality rate experienced by dispersing weevils. However, a modelling analysis (chapter 5) showed that for this particular system there was little difference in predicted population dynamics whether

metapopulation interactions were modelled or not. This result was due to stable density-dependent local dynamics leading rapidly to metapopulation homogeneity.

Whenever metapopulation homogeneity is broken, however, by local perturbation or spatial patterning, then the behaviour of local subpopulations will differ from each other and from that of the overall metapopulation mean. For example, initial parasitoid build-up was slower in the spatial *S. discoideus* metapopulation than in any particular local population (figure 5.3), but once the parasitoid became wide-spread, there was no difference between the behaviour of the metapopulation and that of the local populations.

In chapter 2, stochastic local behaviour combined to give approximately logistic metapopulation dynamics (figure 2.7). Fitting models to overall metapopulation dynamics often gave very different results from the known underlying dynamics. Similarly, fitting models to local dynamics within a metapopulation sometimes gave different results. In the latter case, including net immigration terms did not improve model fits, and in both cases the model for random (Nicholson-Bailey) parasitoid attack gave the most successful fit to both metapopulation and subpopulation dynamics (chapter 3). Parasitoid attack functions which mimic aggregated attack, such as May's (1978) negative binomial model, failed to capture this effect at the scale of a metapopulation. These results highlight the importance of sampling field populations at an appropriate scale when trying to model their dynamics; independent estimates for some population parameters, such as the carrying capacity, may be required.

### **7.3 Do self-organised spatial patterns occur in natural metapopulations?**

The demonstration of self-organised spatial patterning in model host-parasitoid metapopulations (Allen 1975; Hassell *et al.* 1991a) sparked much theory (e.g. Solé *et al.* 1992b; Rohani & Miramontes 1995; White *et al.* 1996), which has tended to focus on what may be possible in metapopulations rather than what is realistic. Chapters 3 to 6 show that these spiral-based patterns arise only when the local interactions are

unstable, a situation which may be rare in nature (Harrison & Taylor 1997). For example, the local dynamics of the *Sitona discoideus*/*Microctonus aethioides* system are stabilised by host density-dependence and heterogeneous parasitoid attack behaviour (chapter 4). Because of this local stability, metapopulation models added little to the understanding of the system (chapter 5).

Spatial patterning, in the form of epidemic waves, is a widely accepted feature of many disease-host systems (e.g. Mollison & Kuulasmaa 1985; White *et al.* 1995; Swinton *et al.* 1998). However, chapter 6 showed that these models either tend towards homogeneity (as in possum/Tb), or disease persistence is hard to achieve from a point introduction (as for rabbit/RCD). Though much of the qualitative behaviour of these models depends on how very low densities are treated, this finding did not so depend.

Rohani *et al.* (1997) argued that spatial self-organisation in ecology cannot be categorically dismissed on theoretical grounds. Neither can it be dismissed from empirical evidence without actively searching for such dynamics in all possible field systems. Spatial self-organisation was not evident in the *S. discoideus* system interrogated in chapter 4, but there is some evidence for it in at least two other host-parasitoid systems (Godfray & Hassell 1997). Overall, the previous chapters suggest that spatial self-organisation may be of limited general relevance for real metapopulations, since patterns only appear under certain special conditions. Firstly, they require unstable local dynamics; secondly, patterns arise in lattice models only through interactions with symmetry-breaking edge effects; and thirdly, they may be difficult to establish from realistic initial conditions.

#### **7.4 Metapopulation processes have not been important for the control of *Sitona discoideus* by *Microctonus aethioides***

The population dynamics of *S. discoideus* and its parasitoid *M. aethioides* were monitored over three seasons at several sites in Canterbury, New Zealand. This was one of the few field studies to be aimed specifically at testing the predictions of host-parasitoid metapopulation models. It confirmed that successful control of *S.*

*discoideus* has been achieved by *M. aethiopoides*. Though there was spatial heterogeneity in *S. discoideus* densities, this did not appear to be a function of metapopulation dynamics, but rather related to longitude, probably through soil type or perhaps crop abundance (chapter 4), and to stochastic or unexplained environmental effects. There was some evidence for density-dependent parasitism, and also for aggregation in parasitoid attacks within local populations. The scale of homogeneity of local populations was estimated at 12 km radius, giving some indication of effective dispersal distance.

A new, mechanistic model for the *S. discoideus*/*M. aethiopoides* system (chapter 5) gave similar results to a previous empirically-fitted model (Barlow & Goldson 1993), but was also able to predict the unsuccessful biological control of this system observed in Australia. When extended to a metapopulation, the new model performed very similarly to the non-spatial model overall, suggesting that metapopulation dynamics *per se* are of relatively minor importance in this system. Mortality during dispersal, however, was observed to have a big effect on *S. discoideus* densities. If related to habitat abundance, this suggests that the area of crop grown may alone affect the densities of dispersing pest species. A similar explanation has been proposed for the relative rarity of aphids in the tropics (Dixon & Kindlmann 1990).

## 7.5 Directions for further research

Though there is extensive and growing theory on metapopulation dynamics, much has little grounding in the real world. Too much time has been spent asking “what is possible in metapopulations?” when a more useful question, perhaps, is “what is probable?”. There is also a real need for field studies to test and refine the escalating body of metapopulation theory. In particular, the question of whether self-organising spatial population patterns are realistic needs further investigation. Detailed study of the *S. discoideus*/*M. aethiopoides* system found no evidence for intrinsically-generated spatial heterogeneity. New theory, however, has suggested the conditions under which patterns might occur, allowing a more informed search to be conducted.

Theoretical and field studies, including this thesis, repeatedly highlight the importance of sampling populations at an appropriate scale (Levin 1992; Chesson 1996). The scale at which metapopulation processes act is determined largely by dispersal range, yet this proves to be one of the most difficult parameters to measure in the field. Chapter 4 describes a rather unsophisticated spatial averaging technique to estimate the scale of homogeneity between local populations. However, improved methods of estimating animal dispersal ranges would be of great benefit, for both pest management and conservation.

The hypothesis, arising from chapter 5, that local density may be related through dispersal mortality to habitat abundance is intriguing and deserves closer examination. Similarly, the possibility that stochastic populations may persist at low overall density with little density-dependence (suggested by the models of chapter 2) is worthy of further investigation with respect to real rare species. Finally, it is suggested that further monitoring be carried out on the *S. discoideus*/*M. aethiopoidea* system at regular, though not necessarily frequent, intervals. This could provide a valuable long-term data set, and make this one of the first biocontrol systems to be monitored for any length of time after its inception.

## Acknowledgements

When embarking on this journey, three and a half years ago, I imagined the road ahead: a smooth straight highway to a golden horizon. But that dream didn't last beyond the first bend. I might still be lost among a tangle of false leads and dead ends, if not for the companions who showed the way and encouraged me forward.

Of my university supervisors, James Sneyd helped set my feet on the initial path, while Bruce Robson and Steve Wratten were there for the final hill. In between, valuable help was provided by a range of people at AgResearch: Steve Goldson gave generously of his data and expertise; much-appreciated technical assistance and occasional light relief was supplied by the Nasty Boys (Mark McNeill, John Proffitt, Craig Phillips, Simon Kelly, and Rachel Cane); Nick Caldwell assisted bravely in the field; Davids Baird and Saville advised on statistical analyses; and useful tips on computing and poultry production were provided by the indefatigable Ian Laurenson.

Valuable insights were gained from stimulating discussions with Mike Hassell, Charles Godfray, Mark Rees, and Tony Dixon. Roger Pech, Brian Manly, Ilkka Hanski, Graham Ruxton, Frederick Adler, and two anonymous referees made helpful suggestions on the manuscript. Continual support and encouragement was gratefully received from friends, family, and flatmates too numerous to name. Financial support was provided by the Marsden Fund.

Finally, I am especially grateful to the two people who have shared the whole journey, right from the very first step. To my best friend and office-mate, Shona Lamoureux, I owe an in-depth knowledge of cat behaviour, *Hieracium* counting, and chillies. Another great friend, and supervisor *par excellence* has been Nigel Barlow. Maybe one day I may be able to keep pace with his great footsteps and characteristic gait.

Together, and individually, these friends have accompanied me through some of the most eventful, enjoyable, and interesting years of my life. But the road goes ever on, and I hope we can share the way a while longer yet.

JMK.

*Comes jucundus in via pro vehiculo est*

A pleasant companion on a journey is as good as a carriage

– Publilius Syrus, *Maxims*, 1<sup>st</sup> century BC

## References

- Adler, F.R. (1993) Migration alone can produce persistence of host-parasitoid models. *American Naturalist*, **141**, 642-450.
- Allee, W.C., Emerson, A.E., Park, O., Park, T. & Schmidt, K.P. (1949) *Principles of Animal Ecology*. Saunders, Philadelphia.
- Allen, J.C. (1975) Mathematical models of species interactions in time and space. *American Naturalist*, **109**, 319-342.
- Allen, J.C., Schaffer, W.M. & Rosko, D. (1993) Chaos reduces species extinction by amplifying local population noise. *Nature*, **364**, 229-232.
- Amarasekare, P. (1998) Allee effects in metapopulation dynamics. *American Naturalist*, **152**, 298-302.
- Anderson, R.M., Jackson, H.C., May, R.M. & Smith, A.M. (1981) Population dynamics of fox rabies in Europe. *Nature*, **289**, 765-771.
- Anderson, R.M. & May, R.M. (1979) Population biology of infectious diseases: part I. *Nature*, **280**, 361-367.
- Anderson, R.M. & May, R.M. (1980) Infectious diseases and population cycles of forest insects. *Science*, **210**, 658-661.
- Anderson, R.M. & May, R.M. (1981) The population dynamics of microparasites and their invertebrate hosts. *Philosophical Transactions of the Royal Society of London, Series B*, **291**, 451-524.
- Andrewartha, H.G. & Birch, L.C. (1954) *The Distribution and Abundance of Animals*. University of Chicago Press, Chicago.

- Bailey, V.A., Nicholson, A.J. & Williams, E.J. (1962) Interaction between hosts and parasites when some host individuals are more difficult to find than others. *Journal of theoretical Biology*, **3**, 1-18.
- Bakker, K. (1964) Backgrounds of controversies about population theories and their terminologies. *Zeitschrift fur angewandte Entomologie*, **53**, 187-208.
- Barlow, N.D. (1991) A spatially aggregated disease/host model for bovine Tb in New Zealand possum populations. *Journal of Applied Ecology*, **28**, 777-793.
- Barlow, N.D. (1993) A model for the spread of bovine Tb in New Zealand possum populations. *Journal of Applied Ecology*, **30**, 156-164.
- Barlow, N.D. (1996) The ecology of wildlife disease control: simple models revisited. *Journal of Applied Ecology*, **33**, 303-314.
- Barlow, N.D. & Dixon, A.F.G. (1980) *Simulation of Lime Aphid Population Dynamics*. Pudoc, Wageningen.
- Barlow, N.D. & Goldson, S.L. (1993) A modelling analysis of the successful biological control of *Sitona discoideus* (Coleoptera: Curculionidae) by *Microtonus aethiopoidea* (Hymenoptera: Braconidae) in New Zealand. *Journal of Applied Ecology*, **30**, 165-178.
- Barlow, N.D. & Kean, J.M. (1996) Spatial models for tuberculosis in possums. *Tuberculosis in Wildlife and Domestic Animals*, (ed. F. Griffin & G. de Lisle), pp. 214-218. University of Otago Press, Dunedin.
- Barlow, N.D. & Kean, J.M. (1998) Simple models for the impact of rabbit calicivirus disease (RCD) on Australasian rabbits. *Ecological Modelling*, **109**, 225-241.
- Barlow, N.D. & Wratten, S.D. (1996) Ecology of predator-prey and parasitoid-host systems: progress since Nicholson. *Frontiers of Population Ecology*, (ed. R.B. Floyd, A.W. Sheppard & P.J. De Barro), pp. 217-243. CSIRO Publishing, Melbourne.

- Bascompte, J. & Solé, R.V. (1994) Spatially induced bifurcation in single-species population dynamics. *Journal of Animal Ecology*, **63**, 256-264.
- Beddington, J.R., Free, C.A. & Lawton, J.H. (1978) Characteristics of successful natural enemies in models of biological control of insect pests. *Nature*, **273**, 513-519.
- Boerlijst, M.C., Lamers, M.E. & Hogeweg, P. (1993) Evolutionary consequences of spiral waves in a host-parasitoid system. *Proceedings of the Royal Society of London, Series B*, **253**, 15-18.
- Bonsall, M.B., Jones, T.H. & Perry, J.N. (1998) Determinants of dynamics: population size, stability and persistence. *Trends in Ecology and Evolution*, **13**, 174-176.
- Bowers, R.G., Begon, M. & Hodgkinson, D.E. (1993) Host-pathogen population cycle in forest insects? Lessons from simple models reconsidered. *Oikos*, **67**, 529-538.
- Busenberg, S.N. & Travis, C.C. (1983) Epidemic models with spatial spread due to population migration. *Journal of Mathematical Biology*, **16**, 181-198.
- Chesson, P.L. (1996) Matters of scale in the dynamics of populations and communities. *Frontiers of Population Ecology*, (ed. R.B. Floyd, A.W. Sheppard & P.J. De Barro), pp. 353-368. CSIRO Publishing, Melbourne.
- Chesson, P.L. & Murdoch, W.W. (1986) Aggregation of risk: relationships among host-parasitoid models. *American Naturalist*, **127**, 696-715.
- Comins, H.N. & Hassell, M.P. (1996) Persistence of multi-species host-parasitoid interactions in spatially distributed models with local dispersal. *Journal of theoretical Biology*, **183**, 19-28.
- Comins, H.N., Hassell, M.P. & May, R.M. (1992) The spatial dynamics of host-parasitoid systems. *Journal of Animal Ecology*, **61**, 735-748.

- Crowley, P.H. (1981) Dispersal and the stability of predator-prey interactions. *The American Naturalist*, **118**, 673-701.
- Cullen, J.M. & Hopkins, D.C. (1982) Rearing, release and recovery of *Microctonus aethiopoidea* Loan (Hymenoptera: Braconidae) imported for the control of *Sitona discoidea* Gyllenhal (Coleoptera: Curculionidae). *Journal of the Australian Entomological Society*, **21**, 279-284.
- Czárán, T. & Bartha, S. (1992) Spatiotemporal dynamic models of plant populations and communities. *Trends in Ecology and Evolution*, **7**, 38-42.
- den Boer, P.J. (1968) Spreading of risk and stabilisation of animal numbers. *Acta Biotheoretica*, **18**, 165-194.
- den Boer, P.J. (1981) On the survival of populations in a heterogeneous and variable environment. *Oecologia*, **50**, 39-53.
- den Boer, P.J. (1991) Seeing the trees for the wood: random walks or bounded fluctuations of population size? *Oecologia*, **86**, 484-491.
- den Boer, P.J. & Reddingius, J. (1989) On the stabilisation of animal numbers. Problems of testing. II. Confrontation with data from the field. *Oecologia*, **79**, 143-149.
- Dixon, A.F.G. & Kindlmann, P. (1990) Role of plant abundance in determining the abundance of herbivorous insects. *Oecologia*, **83**, 281-283.
- Dixon, A.F.G., Kindlmann, P., Leps, J. & Holman, J. (1987) Why there are so few species of aphids, especially in the tropics. *American Naturalist*, **129**, 580-592.
- Duarte, L.C., Boldrini, J.L. & dos Reis, S.F. (1998) Scaling phenomena and ecological interactions in space: cutting to the core. *Trends in Ecology and Evolution*, **13**, 176-177.
- Edelstein-Keshet, L. (1988) *Mathematical Models in Biology*. McGraw-Hill, Inc., New York.

- Ferguson, C.M., Roberts, G.M., Barratt, B.I.P. & Evans, A.A. (1994) The distribution of the parasitoid *Microctonus aethioides* Loan (Hymenoptera: Braconidae) in southern South Island *Sitona discoideus* Gyllenhal (Coleoptera: Curculionidae) populations. *Proceedings of the 47th New Zealand Plant Protection Conference*, pp. 261-265.
- Fisher, R.A. (1937) The wave of advance of advantageous genes. *Annals of Eugenics*, **7**, 255-369.
- Foley, P. (1994) Predicting extinction times from environmental stochasticity and carrying capacity. *Conservation Biology*, **8**, 124-137.
- Foley, P. (1997) Extinction models for local populations. *Metapopulation Biology: Ecology, Genetics, and Evolution*, (ed. I. Hanski & M.E. Gilpin), pp. 215-246. Academic Press, London.
- Free, C.A., Beddington, J.R. & Lawton, J.H. (1977) On the inadequacy of simple models of mutual interference for parasitism and predation. *Journal of Animal Ecology*, **46**, 543-554.
- Fusco, R.A. & Hower, A.A., Jr. (1973) Host influence on laboratory production of the parasitoid, *Microctonus aethiops* (Nees). *Environmental Entomology*, **2**, 971-975.
- Gardner, M. (1970) The fantastic combinations of John Conway's new solitaire game "life". *Scientific American*, **223**, 120-123.
- Gause, G.F. (1934) *The Struggle for Existence*. Williams and Wilkins, Baltimore.
- Genstat 5 Committee (1993) *Genstat 5 Release 3 Reference Manual*. Clarendon Press, Oxford.
- Gilbert, F.S. (1980) The equilibrium theory of island biogeography: fact or fiction? *Journal of Biogeography*, **7**, 209-235.
- Godfray, H.C.J. & Hassell, M.P. (1997) Hosts and parasitoids in space. *Nature*, **386**, 660-661.

- Godfray, H.C.J. & Pacala, S.W. (1992) Aggregation and the population dynamics of parasitoids and predators. *American Naturalist*, **140**, 30-40.
- Goldson, S.L., Frampton, E.R., Barratt, B.I.P. & Ferguson, C.M. (1984) The seasonal biology of *Sitona discoideus* Gyllenhal (Coleoptera: Curculionidae), an introduced pest of New Zealand lucerne. *Bulletin of Entomological Research*, **74**, 249-259.
- Goldson, S.L., Frampton, E.R. & Proffitt, J.R. (1988) Population dynamics and larval establishment of *Sitona discoideus* (Coleoptera: Curculionidae) in New Zealand lucerne. *Journal of Applied Ecology*, **25**, 177-195.
- Goldson, S.L. & French, R.A. (1983) Age-related susceptibility of lucerne to sitona weevil, *Sitona discoideus* Gyllenhal (Coleoptera: Curculionidae), larvae and the associated patterns of adult infestation. *New Zealand Journal of Agricultural Research*, **26**, 251-255.
- Goldson, S.L. & Muscroft-Taylor, K.E. (1988) Interseasonal variation in *Sitona discoideus* Gyllenhal (Coleoptera: Curculionidae) larval damage to lucerne in Canterbury and the economics of insecticidal control. *New Zealand Journal of Agricultural Research*, **31**, 399-346.
- Goldson, S.L., Proffitt, J.R. & McNeill, M.R. (1990) Seasonal biology and ecology in New Zealand of *Microtonus aethiopoides* (Hymenoptera: Braconidae), a parasitoid of *Sitona* spp. (Coleoptera: Curculionidae), with special emphasis on atypical behaviour. *Journal of Applied Ecology*, **27**, 703-722.
- Grenfell, B.T. & Harwood, J. (1997) (Meta)population dynamics of infectious diseases. *Trends in Ecology and Evolution*, **12**, 395-399.
- Gyllenberg, M., Söderbacka, G. & Ericsson, S. (1993) Does migration stabilise local population dynamics? Analysis of a discrete metapopulation model. *Mathematical Biosciences*, **118**, 25-49.
- Hanski, I. (1990) Density dependence, regulation and variability in animal populations. *Philosophical Transactions of the Royal Society of London, Series B*, **330**, 141-150.

- Hanski, I. (1994a) Patch-occupancy dynamics in fragmented landscapes. *Trends in Ecology and Evolution*, **9**, 131-135.
- Hanski, I. (1994b) A practical model of metapopulation dynamics. *Journal of Animal Ecology*, **63**, 151-162.
- Hanski, I. (1998) Metapopulation dynamics. *Nature*, **396**, 41-49.
- Hanski, I., Foley, P. & Hassell, M.P. (1996) Random walks in a metapopulation: how much density dependence is necessary for long-term persistence? *Journal of Animal Ecology*, **65**, 274-282.
- Hanski, I. & Gilpin, M. (1991) Metapopulation dynamics: brief history and conceptual domain. *Biological Journal of the Linnean Society*, **42**, 3-16.
- Hanski, I. & Gilpin, M.E. (1997) *Metapopulation Biology: Ecology, Genetics, and Evolution*. Academic Press, London.
- Hanski, I., Pöyry, J., Pakkala, T. & Kuussaari, M. (1995) Multiple equilibria in metapopulation dynamics. *Nature*, **377**, 618-621.
- Hanski, I. & Simberloff, D. (1997) The metapopulation approach, its history, conceptual domain, and application to conservation. *Metapopulation Biology: Ecology, Genetics, and Evolution*, (ed. I. Hanski & M.E. Gilpin), pp. 5-26. Academic Press, London.
- Hanski, I. & Thomas, C.D. (1994) Metapopulation dynamics and conservation: a spatially explicit model applied to butterflies. *Biological Conservation*, **68**, 167-180.
- Harrison, S. (1994) Metapopulations and conservation. *Large-scale ecology and conservation biology*, (ed. P.J. Edwards, R.M. May & N. Webb), pp.111-128. Blackwell, Oxford.
- Harrison, S. & Taylor, A.D. (1997) Empirical evidence for metapopulation dynamics. *Metapopulation Biology: Ecology, Genetics, and Evolution*, (ed. I. Hanski & M.E. Gilpin), pp. 27-42. Academic Press, London.

- Harrison, S.P. (1997) Persistent, localized outbreaks in the western tussock moth *Orgyia vetusta*: the roles of resource quality, predation and poor dispersal. *Ecological Entomology*, **22**, 158-166.
- Hassell, M.P. (1980) Foraging strategies, population models and biological control: a case study. *Journal of Animal Ecology*, **49**, 603-628.
- Hassell, M.P., Comins, H.N. & May, R.M. (1991a) Spatial structure and chaos in insect population dynamics. *Nature*, **353**, 255-258.
- Hassell, M.P., Comins, H.N. & May, R.M. (1994) Species coexistence and self-organizing spatial dynamics. *Nature*, **370**, 290-292.
- Hassell, M.P., Godfray, H.C.J. & Comins, H.N. (1993) Effects of global change on the dynamics of insect host-parasitoid interactions. *Biotic Interactions and Global Change*, (ed. P.M. Kareiva, J.G. Kingsolver & R.B. Huey), pp. 402-423. Sinauer Association, Sunderland, MA.
- Hassell, M.P. & May, R.M. (1973) Stability in insect host-parasite models. *Journal of Animal Ecology*, **42**, 693-726.
- Hassell, M.P. & May, R.M. (1974) Aggregation of predators and insect parasites and its effect on stability. *Journal of Animal Ecology*, **43**, 567-594.
- Hassell, M.P. & May, R.M. (1988) Spatial heterogeneity and the dynamics of parasitoid-host systems. *Annales Zoologici Fennici*, **25**, 55-61.
- Hassell, M.P., May, R.M., Pacala, S.W. & Chesson, P.L. (1991b) The persistence of host-parasitoid associations in patchy environments. I. A general criterion. *American Naturalist*, **138**, 568-583.
- Hassell, M.P., Miramontes, O., Rohani, P. & May, R.M. (1995) Appropriate formulations for dispersal in spatially structured models: comments on Bascombe & Solé. *Journal of Animal Ecology*, **64**, 662-664.

- Hassell, M.P. & Pacala, S.W. (1990) Heterogeneity and the dynamics of host-parasitoid interactions. *Philosophical Transactions of the Royal Society of London, Series B*, **330**, 203-220.
- Hassell, M.P. & Varley, G.C. (1969) New inductive population model for insect parasites and its bearing on biological control. *Nature*, **223**, 1133-1137.
- Hawkins, B.A. & Cornell, H.V. (1994) Maximum parasitism rates and successful biological control. *Science*, **266**, 1886.
- Hilborn, R. (1975) The effect of spatial heterogeneity on the persistence of predator-prey interactions. *Theoretical Population Biology*, **8**, 346-355.
- Hochberg, M.E. & Lawton, J.H. (1990) Spatial heterogeneities in parasitism and population dynamics. *Oikos*, **59**, 9-14.
- Holling, C.S. (1959) Some characteristics of simple types of predation and parasitism. *Canadian Entomologist*, **91**, 385-398.
- Holmes, E.E., Lewis, M.A., Banks, J.E. & Veit, R.R. (1994) Partial differential equations in ecology: spatial interactions and population dynamics. *Ecology*, **75**, 17-29.
- Hopkins, D. (1981) Establishment and spread of the sitona weevil parasite *Microtonus aethiopoides* in South Australia. *Proceedings of the 3rd Australian Conference on Grassland Invertebrate Ecology*, Adelaide, pp. 177-182.
- Hopkins, D.C. (1989) Widespread establishment of the sitona weevil parasite, *Microctonus aethiopoides* and its effectiveness as a control agent in South Australia. *Proceedings of the 5th Australasian Conference on Grassland Invertebrate Ecology*, Melbourne (ed. P.P. Stahle), pp. 49-53.
- Hopper, K.R., Powell, J.E. & King, E.G. (1991) Spatial density dependence in parasitism of *Heliothis virescens* (Lepidoptera: Noctuidae) by *Microplitis croceipes* (Hymenoptera: Braconidae) in the field. *Environmental Entomology*, **20**, 292-302.

- Howard, L.O. & Fiske, W.F. (1911) The importation into the United States of the parasites of the gipsy-moth and the brown-tail moth. *Bulletin of the Bureau of Entomology, United States Department of Agriculture*, **91**, 1-312.
- Huffaker, C.B. (1958) Experimental studies on predation: dispersion factors and predator-prey oscillations. *Hilgardia*, **27**, 343-383.
- Ives, A.R. (1992) Continuous-time models of host-parasitoid interactions. *American Naturalist*, **140**, 1-29.
- Jeltsch, F., Müller, M.S., Grimm, V., Wissel, C. & Brandl, R. (1997) Pattern formation triggered by rare events: lessons from the spread of rabies. *Proceedings of the Royal Society of London, Series B*, **264**, 495-503.
- Kaneko, K. (1989) Spatiotemporal chaos in one- and two-dimensional coupled map lattices. *Physica D*, **37**, 60-82.
- Kelton, W.D. & Law, A.M. (1991) *Simulation Modelling and Analysis, 2 edition*. McGraw-Hill, Inc., New York.
- Kingsland, S.E. (1996) Evolutionary theory and the foundations of population ecology: the work of A.J. Nicholson (1895-1969). *Frontiers of Population Ecology*, (ed. R.B. Floyd, A.W. Sheppard & P.J. De Barro), pp. 13-25. CSIRO Publishing, Melbourne.
- Krebs, C.J. (1994) *Ecology: the Experimental Analysis of Distribution and Abundance, 4th edition*. HarperCollins College Publishers, New York.
- Kreyszig, E. (1988) *Advanced Engineering Mathematics, 7th edition*. John Wiley & Sons, New York.
- Kuno, E. (1981) Dispersal and the persistence of populations in unstable habitats: a theoretical note. *Oecologia*, **49**, 123-126.
- Leather, S.R., Walters, K.F.A. & Dixon, A.F.G. (1989) Factors determining the pest status of the bird cherry-oat aphid, *Rhopalosiphum padi* (L.) (Hemiptera:

- Aphididae), in Europe: a study and review. *Bulletin of Entomological Research*, **79**, 345-360.
- Lei, G.-C. & Hanski, I. (1997) Metapopulation structure of *Cotesia melitaerum*, a specialist parasitoid of the butterfly *Melitaea cinxia*. *Oikos*, **78**, 91-100.
- Lei, G.-C. & Hanski, I. (1998) Spatial dynamics of two competing specialist parasitoids in a host metapopulation. *Journal of Animal Ecology*, **67**, 422-433.
- Levin, S.A. (1992) The problem of scale in ecology. *Ecology*, **73**, 1943-1967.
- Levins, R.A. (1969) Some demographic and genetic consequences of environmental heterogeneity for biological control. *Bulletin of the Entomological Society of America*, **15**, 237-240.
- Lindenmayer, D.B., McCarthy, M.A. & Pope, M.L. (1999) Arboreal marsupial incidence in eucalypt patches in south-eastern Australia: a test of Hanski's incidence function metapopulation model for patch occupancy. *Oikos*, **84**, 99-109.
- Lotka, A.J. (1925) *Elements of Physical Biology*. Williams and Wilkins, Baltimore.
- Louie, K., Roberts, M.G. & Wake, G.C. (1993) Thresholds and stability analysis of models for the spatial spread of a fatal disease. *IMA Journal of Mathematics Applied in Medicine and Biology*, **10**, 207-226.
- MacArthur, R.H. (1960) Population studies: animal ecology and demography. *Quarterly Review of Biology*, **35**, 82-83.
- MacArthur, R.H. & Wilson, E.O. (1967) *The Theory of Island Biogeography*. Princeton University Press, Princeton.
- Mackerras, I. (1970) Alexander John Nicholson. *Records of the Australian Academy of Science*, **2**, 66-81.
- Maron, J.L. & Harrison, S. (1997) Spatial pattern formation in an insect host-parasitoid system. *Science*, **278**, 1619-1621.

- May, R.M. (1973) On relationships among various types of population models. *American Naturalist*, **107**, 46-57.
- May, R.M. (1978) Host-parasitoid systems in patchy environments: a phenomenological model. *Journal of Animal Ecology*, **47**, 833-843.
- May, R.M. & Anderson, R.M. (1979) Population biology of infectious diseases: part II. *Nature*, **280**, 455-461.
- May, R.M. & Hassell, M.P. (1988) Population dynamics and biological control. *Philosophical Transactions of the Royal Society of London, Series B*, **318**, 129-169.
- May, R.M., Hassell, M.P., Anderson, R.M. & Tonkyn, D.W. (1981) Density dependence in host-parasitoid models. *Journal of Animal Ecology*, **50**, 855-865.
- May, R.M. & Oster, G.F. (1976) Bifurcations and dynamic complexity in simple ecological models. *American Naturalist*, **110**, 573-599.
- Maynard Smith, J. (1974) *Models in Ecology*. Cambridge University Press, New York.
- Moilanen, A., Smith, A.T. & Hanski, I. (1998) Long-term dynamics in a metapopulation of the American pika. *American Naturalist*, **152**, 530-542.
- Mollison, D. (1984) Simplifying simple epidemic models. *Nature*, **310**, 224-225.
- Mollison, D. (1991) Dependence of epidemic and population velocities on basic parameters. *Mathematical Biosciences*, **107**, 255-287.
- Mollison, D. & Kuulasmaa, K. (1985) Spatial epidemic models: theory and simulations. *Population Dynamics of Rabies in Wildlife*, (ed. P.J. Bacon), pp. 291-309. Academic Press, London.
- Morrison, G. & Strong, D.R. (1980) Spatial variations in host density and the intensity of parasitism: some empirical examples. *Environmental Entomology*, **9**, 149-152.

- Murdoch, W.W. (1990) The relevance of pest-enemy models to biological control. *Critical Issues in Biological Control*, (ed. M. Mackauer, L.E. Ehler & J. Roland), pp. 1-24. Intercept Ltd., Andover.
- Murdoch, W.W., Chesson, J. & Chesson, P.L. (1985) Biological control in theory and practice. *American Naturalist*, **125**, 344-366.
- Murdoch, W.W. & Stewart-Oaten, A. (1989) Aggregation by parasitoids and predators: effects on equilibrium and stability. *American Naturalist*, **134**, 288-310.
- Murray, B.G., Jr. (1999) Can the population regulation controversy be buried and forgotten? *Oikos*, **84**, 148-152.
- Murray, J.D. (1993) *Mathematical Biology, 2nd edition*. Springer-Verlag, Berlin.
- Murray, J.D., Stanley, E.A. & Brown, D.L. (1986) On the spatial spread of rabies among foxes. *Proceedings of the Royal Society of London, Series B*, **229**, 111-150.
- New Zealand Meteorological Service (1981) Summaries of climatological observations to 1980. *New Zealand Meteorological Service Miscellaneous Publication*, **177**, 120.
- Nicholson, A.J. (1954) An outline of the dynamics of animal populations. *Australian Journal of Zoology*, **2**, 9-65.
- Nicholson, A.J. & Bailey, V.A. (1935) The balance of animal populations. *Proceedings of the Zoological Society of London*, **1935**, 551-598.
- Okubo, A. (1980) *Diffusion and Ecological Problems: Mathematical Models*. Springer-Verlag, Berlin.
- Pacala, S.W. & Hassell, M.P. (1991) The persistence of host-parasitoid associations in patchy environments. II. Evaluation of field data. *American Naturalist*, **138**, 584-605.
- Ranta, E., Kaitala, V. & Lundberg, P. (1997) The spatial dimension in population fluctuations. *Science*, **278**, 1621-1623.

- Reddingius, J. & den Boer, P.J. (1970) Simulation experiments illustrating stabilization of animal numbers by spreading of risk. *Oecologia*, **5**, 240-284.
- Reeve, J.D. (1988) Environmental variability, migration, and persistence in host-parasitoid systems. *American Naturalist*, **132**, 810-836.
- Reeve, J.D. (1990) Stability, variability, and persistence in host-parasitoid systems. *Ecology*, **71**, 422-426.
- Ricker, W.E. (1954) Stock and recruitment. *Journal of the Fisheries Research Board of Canada*, **11**, 559-623.
- Roff, D.A. (1974) Spatial heterogeneity and the persistence of populations. *Oecologia*, **15**, 245-258.
- Rohani, P., Godfray, H.C.J. & Hassell, M.P. (1994) Aggregation and the dynamics of host-parasitoid systems: a discrete-generation model with within-generation redistribution. *American Naturalist*, **144**, 491-509.
- Rohani, P., Lewis, T.J., Grünbaum, D. & Ruxton, G.D. (1997) Spatial self-organisation in ecology: pretty patterns or robust reality? *Trends in Ecology and Evolution*, **12**, 70-74.
- Rohani, P., May, R.M. & Hassell, M.P. (1996) Metapopulations and equilibrium stability: the effects of spatial structure. *Journal of theoretical Biology*, **181**, 97-109.
- Rohani, P. & Miramontes, O. (1995) Host-parasitoid metapopulations: the consequences of parasitoid aggregation on spatial dynamics and searching efficiency. *Proceedings of the Royal Society of London, Series B*, **260**, 335-342.
- Rohani, P. & Ruxton, G.D. (1999) Dispersal-induced instabilities in host-parasitoid metapopulations. *Theoretical Population Biology*, **55**, 23-36.
- Ruxton, G.D. (1993) Linked populations can still be chaotic. *Oikos*, **68**, 347-348.

- Ruxton, G.D. (1994) Low levels of immigration between chaotic populations can reduce system extinctions by inducing asynchronous regular cycles. *Proceedings of the Royal Society of London, Series B*, **256**, 189-193.
- Ruxton, G.D. & Doebeli, M. (1996) Spatial self-organisation and persistence of transients in a metapopulation model. *Proceedings of the Royal Society of London, Series B*, **263**, 1153-1158.
- Ruxton, G.D., González-Andujar, J.L. & Perry, J.N. (1997) Mortality during dispersal stabilizes local population fluctuations. *Journal of Animal Ecology*, **66**, 289-292.
- Ruxton, G.D. & Rohani, P. (1996) The consequences of stochasticity for self-organised spatial dynamics, persistence and coexistence in spatially extended host-parasitoid communities. *Proceedings of the Royal Society of London, Series B*, **263**, 625-631.
- Savill, N.J., Rohani, P. & Hogeweg, P. (1997) Self-reinforcing spatial patterns enslave evolution in a host-parasitoid system. *Journal of theoretical Biology*, **188**, 11-20.
- Sherratt, J.A., Eagan, B.T. & Lewis, M.A. (1997) Oscillations and chaos behind predator-prey invasion: mathematical artifact or ecological reality? *Philosophical Transactions of the Royal Society of London, Series B*, **352**, 21-37.
- Skellam, J.G. (1951) Random dispersal in theoretical populations. *Biometrika*, **38**, 196-218.
- Smith, G.C. & Harris, S. (1991) Rabies in urban foxes (*Vulpes vulpes*) in Britain: the use of a spatial stochastic simulation model to examine the pattern of spread and evaluate the efficacy of different control regimes. *Philosophical Transactions of the Royal Society of London, Series B*, **334**, 459-479.
- Smith, H.S. (1935) The role of biotic factors in the determination of population densities. *Journal of Economic Entomology*, **28**, 873-898.

- Solé, R.V., Bascompte, J. & Valls, J. (1992a) Stability and complexity in spatially extended two-species competition. *Journal of theoretical Biology*, **159**, 469-480.
- Solé, R.V., Valls, J. & Bascompte, J. (1992b) Spiral waves, chaos and multiple attractors in lattice models of interacting populations. *Physics Letters A*, **166**, 123-128.
- Soulé, M.E. & Simberloff, D. (1986) What do genetics and ecology tell us about the design of nature reserves? *Biological Conservation*, **35**, 19-40.
- Stiling, P. (1987) The frequency of density-dependence in insect host-parasitoid systems. *Ecology*, **68**, 844-856.
- Stone, L. (1993) Period-doubling reversals and chaos in simple ecological models. *Nature*, **365**, 617-620.
- Strong, D.R. (1986) Density-vague population change. *Trends in Ecology and Evolution*, **1**, 39-42.
- Stufkens, M.A.W., Farrell, J.A. & Goldson, S.L. (1987) Establishment of *Microctonus aethiopoides*, a parasitoid of the sitona weevil in New Zealand. *Proceedings of the 40th New Zealand Weed and Pest Control Conference*, Nelson, New Zealand, (ed. A.J. Popay), pp.31-32.
- Swinton, J., Harwood, J., Grenfell, B.T. & Gilligan, C.A. (1998) Persistence thresholds for phocine distemper virus infection in harbour seal *Phoca vitulina* metapopulations. *Journal of Animal Ecology*, **67**, 54-68.
- Taylor, A.D. (1993) Heterogeneity in host-parasitoid interactions: 'aggregation of risk' and the ' $CV^2 > 1$  rule'. *Trends in Ecology and Evolution*, **8**, 400-405.
- Thompson, W.R. (1924) La theorie mathematique de l'action des parasites entomophages et le facteur du hasard. *Annales - Faculté des Sciences de Marseille Serie 2*, **2**, 69-89.
- Turchin, P. (1999) Population regulation: a synthetic view. *Oikos*, **84**, 153-159.

- Vance, R.R. (1984) The effect of dispersal on population stability in one-species, discrete-space population growth models. *American Naturalist*, **123**, 230-254.
- Varley, G.C. (1947) The natural control of population balance in the knapweed gall-fly (*Urophera jaceana*). *Journal of Animal Ecology*, **16**, 139-187.
- Volterra, V. (1926) Variazioni e fluttuazioni del numero d'individui in specie animali conviventi. *Memoria della Regia Accademia Nazionale dei Lincei, Series 6*, **2**, 31-113.
- Waage, J.K. (1990) Ecological theory and the selection of biological control agents. *Critical Issues in Biological Control*, (ed. M. Mackauer, L.E. Ehler & J. Roland), pp.135-157. Intercept Ltd., Andover.
- Walde, S.J. & Murdoch, W.W. (1988) Spatial density dependence in parasitoids. *Annual Review of Entomology*, **33**, 441-466.
- Ward, S.A., Leather, S.R., Pickup, J. & Harrington, R. (1998) Mortality during dispersal and the cost of host-specificity in parasites: how many aphids find hosts? *Journal of Animal Ecology*, **67**, 763-773.
- White, A., Begon, M. & Bowers, R.G. (1996) Host-pathogen systems in a spatially patchy environment. *Proceedings of the Royal Society of London, Series B*, **263**, 325-332.
- White, P.C., Harris, S. & Smith, G.C. (1995) Fox contact behaviour and rabies spread: a model for the estimation of contact probabilities between urban foxes at different population densities and its implications for rabies control in Britain. *Journal of Applied Ecology*, **32**, 693-706.
- Williamson, M.H. (1989) The MacArthur and Wilson theory today: true but trivial. *Journal of Biogeography*, **16**, 3-4.
- Wilson, H.B. & Hassell, M.P. (1997) Host-parasitoid spatial models: the interplay of demographic stochasticity and dynamics. *Proceedings of the Royal Society of London, Series B*, **264**, 1189-1195.

Wilson, W.G., Harrison, S.P., Hastings, A. & McCann, K. (1999) Exploring stable pattern formation in models of tussock moth populations. *Journal of Animal Ecology*, **68**, 94-107.

Wood, S.N. & Thomas, M.B. (1996) Space, time and persistence of virulent pathogens. *Proceedings of the Royal Society of London, Series B*, **263**, 673-680.

# Appendices

## Appendix 1: Glossary of terms

The following definitions are used throughout the thesis. Other technical terms are defined at their first usage.

**absorbing boundaries:** animals dispersing over the edge of a lattice model are assumed to be lost to the system. There is no immigration from outside the lattice.

**aestivation:** summer dormancy.

**carrying capacity:** the maximum population size or density that can be supported in an area, typically assumed to be determined by resource requirements.

**cellular automaton:** a spatially-explicit model formulation in which entities (e.g. subpopulations) are arranged on a grid, and each entity may exist in one of a small finite number of different of states. Changes in local state are determined by the states of nearby entities, and may be stochastic.

**continuous-time model:** a model in which processes occur continuously and rates of change are related to the current state through differential equations.

**coupled map lattice:** a spatially-explicit model formulation in which subpopulations are arranged on a grid, local densities are modelled explicitly as continuous variables, and local dispersal occurs.

**density:** number of animals per unit area.

**density-dependence:** a form of population regulation in which the *per capita* rate of change of the population is a function of density (and may include a time delay).

**density-independence:** population regulation in which the *per capita* rate of change is independent of population density.

**discrete-time model:** a model in which the measure of time advances in discrete units, and the current state of the system at the end of each time unit is related to that at the beginning using difference equations.

**dispersal:** movement of animals between habitat patches.

**equilibrium:** model state at which densities remain constant, usually implying also that model densities are non-zero ('non-trivial').

**global:** involving all subpopulations within a metapopulation.

**heterogeneity:** difference (e.g. between local densities in a metapopulation).

**homogeneity:** uniformity.

**host:** species which is attacked by a particular disease or parasitoid.

**incidence function model:** metapopulation model in which the probability of a particular habitat patch being occupied is related, through colonisation and extinction functions, to its spatial characteristics.

**individual-based model:** a model in which population numbers are integer values representing discrete individual animals.

**metapopulation:** a set of potential local populations between which dispersal may occur.

**neutral stability:** describing the behaviour of a model which is at a point equilibrium or undergoes cycles of a magnitude dependent on the initial densities, but which shows no tendency to return to the equilibrium when disturbed.

**oscillation:** regular or semi-regular fluctuation.

**parasitoid:** an insect species, the larvae of which feed exclusively on the body of another insect, eventually killing it.

**patch model:** a simple metapopulation model which predicts the proportion of available habitat patches occupied depending on colonisation and extinction rates.

**perturbation:** a disturbance (externally imposed change) in model densities.

**periodic boundaries:** animals dispersing beyond the edge of a lattice are assumed to be balanced by equal immigration at the opposite edge.

**persistence:** continued presence of a species, or group of interacting species, in one or more patches of a metapopulation.

**population:** group of individuals of the same species which form a breeding unit in a particular area of habitat at a particular time.

**population dynamics:** changes in population densities over time.

**reflecting boundaries:** animals are prevented from dispersing beyond the edge of a lattice by 'bouncing back' from the lattice edge.

**searching efficiency:** a characteristic 'area of discovery' to which a parasitoid's ability to find hosts is often assumed to be limited.

**stability:** the behaviour of a model when disturbed from equilibrium.

**stable:** describing an equilibrium state to which the model will return after a small disturbance.

**stable limit cycle:** a regular oscillation in densities with no underlying trend, to which the model will return when disturbed.

**stochastic:** random.

**subpopulation:** group of individuals which share a habitat patch and interact with each other.

**teneral:** describing a newly-emerged adult insect which is not yet capable of flight.

**univoltine:** having one generation per year in the field.

**unstable:** describing an equilibrium state from which the model will diverge if disturbed.

## Appendix 2: List of symbols used

### A2.1 General symbols used throughout the thesis

- $a$  parasitoid searching efficiency
- $B$  boundary condition of a coupled map lattice
- $c$  number of neighbouring subpopulations within dispersal range in a coupled map lattice
- $e$  base of natural logarithms, 2.71828
- $\exp(n)$   $e$  raised to the power of  $n$
- $H$  total number of subpopulations in a metapopulation
- $K$  carrying capacity of a local population
- $\ln$  (natural) logarithm to base  $e$
- $\lambda$  number of offspring produced by each non-parasitised host
- $m$  metres
- $m$  coefficient for pseudo-interference between searching parasitoids
- $\mu$  dispersal rate, proportion of a local population dispersing each model time unit
- $N$  local population size (or density)
- $P$  local number (or density) of searching parasitoids
- $Q$  proportion of hosts parasitised
- $r$  per capita reproductive rate
- $w$  density-dependence coefficient (for parasitoid attack in chapter 3, weevil larval survival in chapter 5, or host mortality in chapter 6)

#### *Subscripts:*

- $i$  a variable used for counting
- $imm$  net immigration of quantity
- $j$  a variable used for counting
- $p$  quantity averaged over the entire metapopulation
- $t$  quantity at a particular time (or generation)
- $t+1$  quantity in the following generation
- $eq$  quantity at equilibrium

$x$  referring to a particular subpopulation or habitat patch (chapter 1), or its position (other chapters)

$y$  referring to the position of a particular subpopulation or habitat patch

0 initial quantity at time zero

## A2.2 Statistical and mathematical abbreviations

$CV^2$  coefficient of variation squared of searching parasitoids per host

*d.f.* degrees of freedom

$n$  number of data points in a statistical test

$p$  probability that an observed relationship is due to chance alone

$R^2$  coefficient of correlation for a regression

*s.e.* standard error of an estimate

$\infty$  infinity

$\rightarrow$  approaches

$\Sigma$  sum of

$\cong$  is approximately equal to

## A2.3 Additional symbols used in *Sitona discoideus* models and analysis

$A$  age of lucerne stand

$C$  autumn density of unparasitised weevils

$C_w$  weighted average of the densities of unparasitised weevils at all sites

$d_x$  distance to site  $x$

$d_l$  some characteristic distance (chapter 4) or the lattice distance determining dispersal range (chapter 5)

$^{\circ}C$  degrees Celsius

$^{\circ}D$  degree-days

$\varepsilon$  lucerne locating efficiency for dispersing weevils

$K_{max}$  maximum carrying capacity of lucerne

$L$  relative abundance of lucerne in the environment

$p_{atyp}$  proportion of parasitised teneral weevils showing atypical (non-dispersing) behaviour

$p_{early}$  proportion of immigrating weevils that arrive during March

- $s$  proportion of weevils surviving through some stage
- $s_{disp}$  proportion of weevils surviving aestivation and dispersal
- $s_{larv}$  proportion of peak weevil larvae surviving to eclose in early summer
- $v$  weevil density-dependence parameter
- $W$  local density of parasitised weevils
- $w_x$  weighting to be applied to autumn density of unparasitised weevils in site  $x$
- $z$  rate at which crop carrying capacity declines with age

*Subscripts:*

- $aest$  quantity in aestivation in summer
- $aut$  quantity in autumn of the current season
- $crop$  quantity in the crop over summer
- $Dec$  quantity in early summer (December)
- $Mar$  quantity in autumn (March)
- $next$  quantity in autumn of the following season
- $spr$  quantity in spring, at time of peak weevil larval density
- $wait$  quantity in the crop at the end of summer

#### **A2.4 Other symbols used**

- $\alpha$  mortality rate due to disease (chapter 6)
- $b$  density-independent reproductive rate (chapter 6)
- $\beta$  disease transmission coefficient (chapter 6)
- $C$  overall colonisation rate of empty patches (chapter 1)
- $C'$  colonisation rate of empty patches per occupied patch (chapter 1)
- $D$  diffusion coefficient (appendix 3)
- $d$  density-independent mortality rate (chapters 3 and 6)
- $E$  extinction rate of occupied patches (chapter 1), or density of disease-latent (incubating) animals (chapter 6)
- $f(N,P)$  the proportion of  $N$  host larvae surviving parasitism by  $P$  searching parasitoids (chapter 3)
- $g(N)$  the proportion of  $N$  host larvae surviving density-dependent mortality (chapter 3)

- $h$  handling time, the proportion of the total available parasitoid searching time that is spent handling (parasitising) each prey encountered (chapter 3)
- $I$  density of infectious animals (chapter 6)
- $J$  occupancy of habitat patches (chapter 1)
- $K_L$  threshold for extinction (chapter 6)
- $k$  negative binomial parameter describing the degree of aggregation (chapter 3)
- $p(0)$  proportion of metapopulation simulations going extinct (chapter 2)
- $p(K)$  mean incidence of density-dependence per subpopulation per generation (chapter 2)
- $p(t_{1000})$  proportion of metapopulation simulations persisting for 1000 generations (chapter 2)
- $q$  equilibrium host density as a fraction of host carrying capacity (chapter 3)
- $R$  density of recovered, immune animals (chapter 6)
- $R_0$  basic reproductive rate of disease (chapter 6)
- $r_d$  intrinsic rate of increase of disease (chapter 6)
- $r_m$  mean of the normal distribution from which local realised per capita reproductive rates are drawn (chapter 2)
- $S$  density of susceptible animals (chapter 6)
- $\sigma$  inverse of mean latent time (chapter 6)
- $t_p$  mean persistence time (chapter 2)
- $v$  weevil density-dependence parameter (chapter 5), or rate of recovery from disease (chapter 6)
- $v_r$  variance of the normal distribution from which local realised per capita reproductive rates are drawn (chapter 2)

### Appendix 3: Effects of dispersal on local dynamics

Much of the literature on dispersal and biological invasions is based on diffusion models. The main appeal of diffusion equations is that the rate of spread and shape of the wave-front of invading organisms may be investigated analytically. In doing so, however, information about the population dynamics of a particular site is lost, yet this may be of the greatest ecological interest. For example, a key issue in biological invasions (especially managed invasions like biocontrol releases) is how fast local populations grow, given that dispersal may be playing a key role in determining the local dynamics.

The invasion case study studied in detail in this thesis (chapters 4 and 5) tells us little about population dynamics at an invasion release site, because the rate of increase was so rapid (figure 5.3(b)). Therefore, this simple diffusion modelling approach is adopted to address the issue. In addition, diffusion equations arise as an instantaneous-time approximation to the types of dispersal employed in the models of this thesis. In this appendix, diffusion is modelled numerically, since it is not easy to investigate temporal dynamics under diffusion using analytical methods.

A one-dimensional coupled map lattice is used to model local population dynamics influenced by dispersal. Local population increase is assumed to be density-dependent, with maximum rate of increase  $r$ , and density expressed relative to the carrying capacity. In addition, a proportion  $\mu$  of each local population is assumed to disperse each timestep, being reallocated equally between the two immediately neighbouring subpopulations. This gives the model

$$\Delta N_x = rN_x(1 - N_x) - \mu \left[ N_x - \frac{(N_{x-1} + N_{x+1})}{2} \right] \quad (\text{A3.1})$$

where  $\Delta N_x$  is the net change in the density of subpopulation  $x$ , and the densities of the two neighbouring populations are denoted  $N_{x-1}$  and  $N_{x+1}$ . With Taylor expansion, and letting space and time increments tend to zero, the model becomes the one-dimensional version of the well-known ‘Fisher equation’ (Fisher 1937) for logistic increase plus diffusion:

$$\frac{\partial N}{\partial t} = rN(1 - N) + D \frac{\partial^2 N}{\partial x^2} \quad (\text{A3.2})$$

where  $t$  is time,  $x$  is space, and  $D$  is the ‘diffusion coefficient’ given by  $\mu/2$  when  $t$  and  $x$  are very small. Analytical treatment of equation A3.2 suggests that the invasion wave front travels at a speed of at least  $2(rD)^{0.5}$ , and that this is true for both exponential and logistic local growth models (Okubo 1980), as well as for spread in one or two dimensions (given that  $D$  has a slightly different meaning and value in both cases), provided that the wave has spread sufficiently far from the site of introduction.

Local population dynamics, governed by equation A3.1, were tallied at two particular lattice locations, the first being the site of introduction (at an initial density of 0.01), and the second a site 50 subpopulations from this through which the wave of invasion subsequently spreads. The lattice was extended for a further 50 locations each side of these sites. Boundary conditions were irrelevant because simulations were always halted before the boundaries were reached. A range of parameter values were investigated:  $r$  from 0.03 to 0.3 (default value 0.1), and  $\mu$  from 0.01 to 0.9 (default 0.1). Since the units for time and space were arbitrary, the main interest was in the relative magnitudes of  $r$  and  $\mu$ , rather than their actual values.

Figure A3.1 shows the spread outward from the source for three parameter combinations. The rate of spread was affected by both  $r$  and  $\mu$ , and depended on their product, as predicted by the diffusion approximation (equation A3.2). The realised rate of local increase in both introduction and invaded sites differed from that expected from non-spatial models (figures A3.2 to A3.4). Increase was slower than expected in the site of introduction (dashed lines in the figures), because there dispersal acts only to remove individuals. The effect of dispersal retarding local increase at the introduction site was most pronounced when dispersal rates were high, as would be expected. There, net immigration was never positive (figure A3.3), and the overall effect of dispersal was simply to reduce proportionally the realised local rate of increase (figure A3.4(a)). This reduction in  $r$  averaged around 10% for the

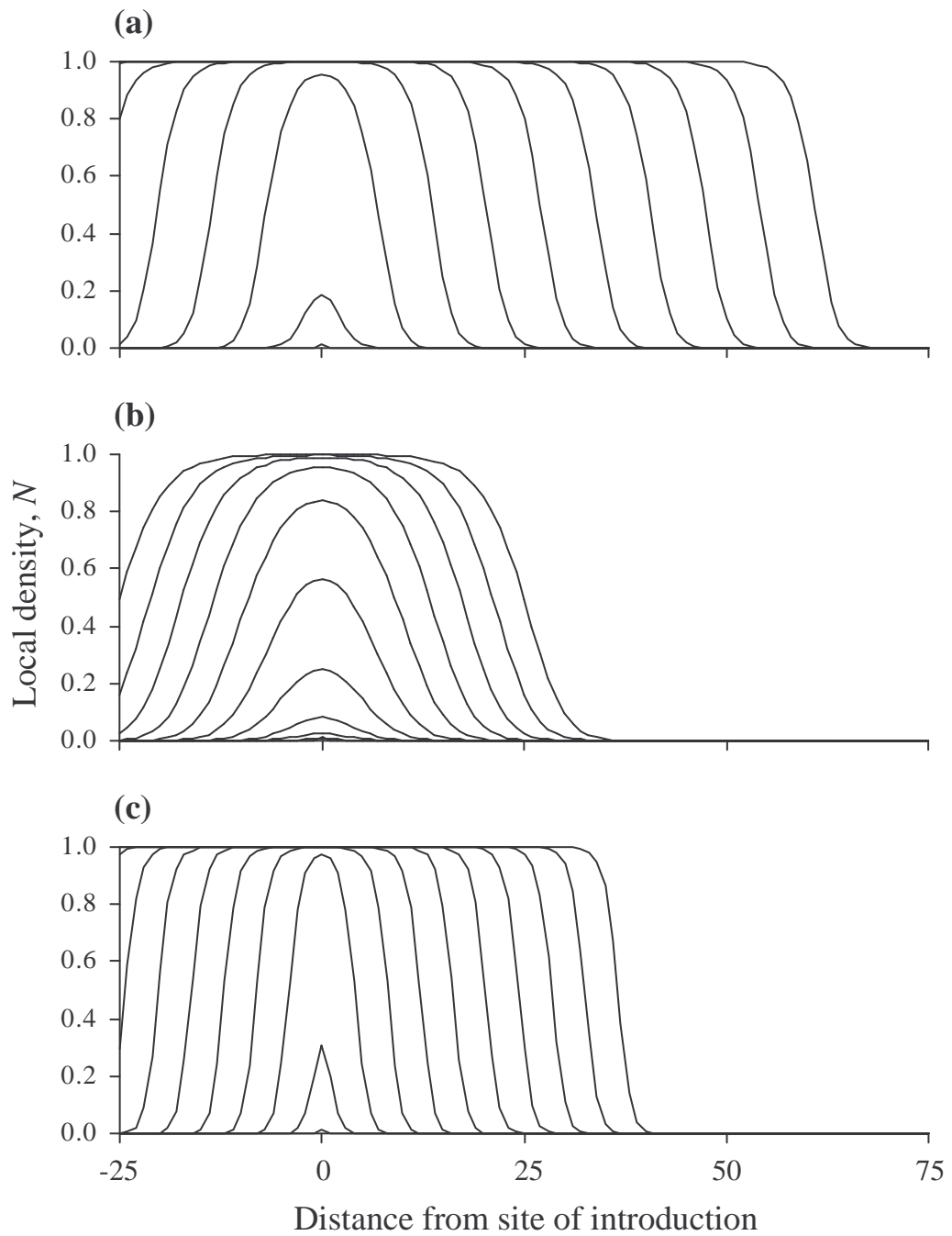


**Figure A3.1** Spread of a density-dependent population from a local introduction at density 0.01. Local densities are shown at intervals of 50 time units. (a) local intrinsic rate of increase  $r=0.1$ , proportion dispersing  $\mu=0.1$ ; (b)  $r=0.03$ ,  $\mu=0.1$ ; (c)  $r=0.1$ ,  $\mu=0.03$ .

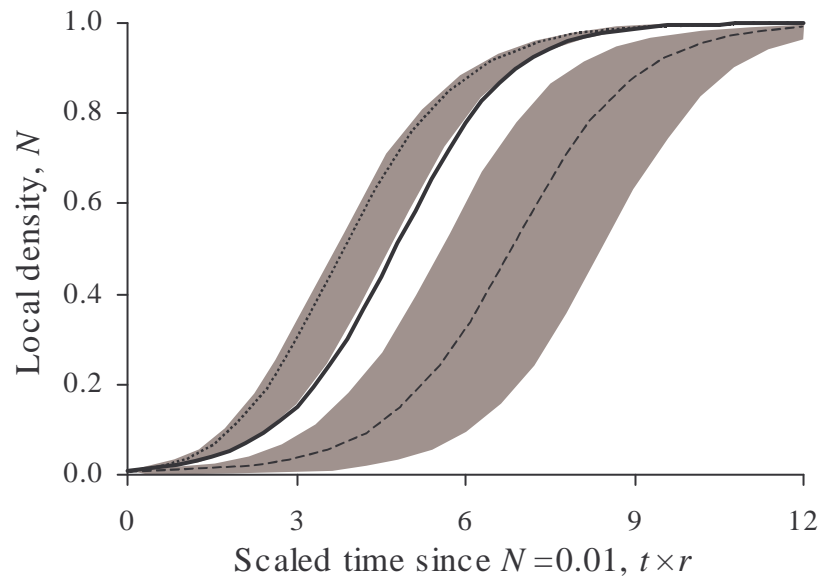


**Figure A3.2** Temporal dynamics of two sites in a density-dependent population with dispersal. Note that the time axis has been scaled by  $r$  to allow comparison between a range of simulations. Results are shown for non-spatial logistic growth (solid line), introduction site in a spatial model (dashed line), and an invaded site (dotted line). Shaded areas indicate the range of responses observed for  $0.03 \leq r \leq 0.3$  and  $0.01 \leq \mu \leq 0.9$ .

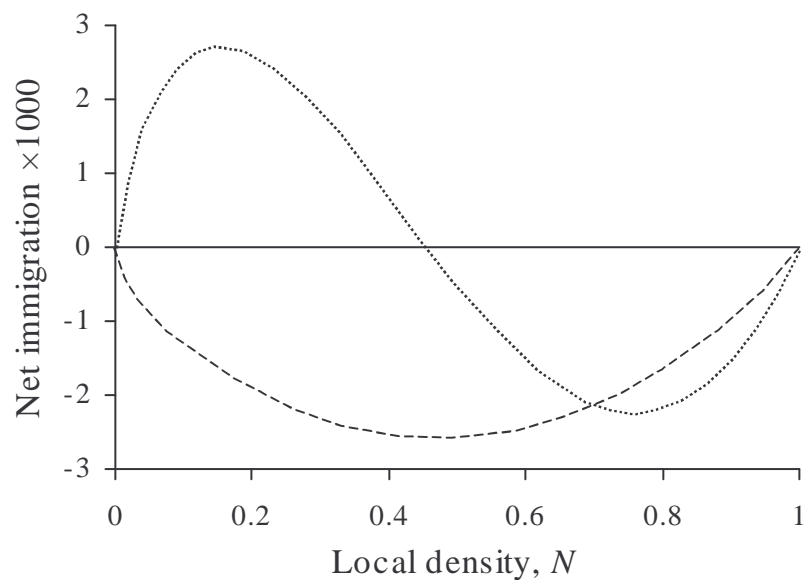


**Figure A3.3** Net immigration observed locally in a density-dependent spatial population, with  $r = 0.1$  and  $\mu = 0.1$ . Results shown for the site of introduction (dashed line) and an invaded site (dotted line).

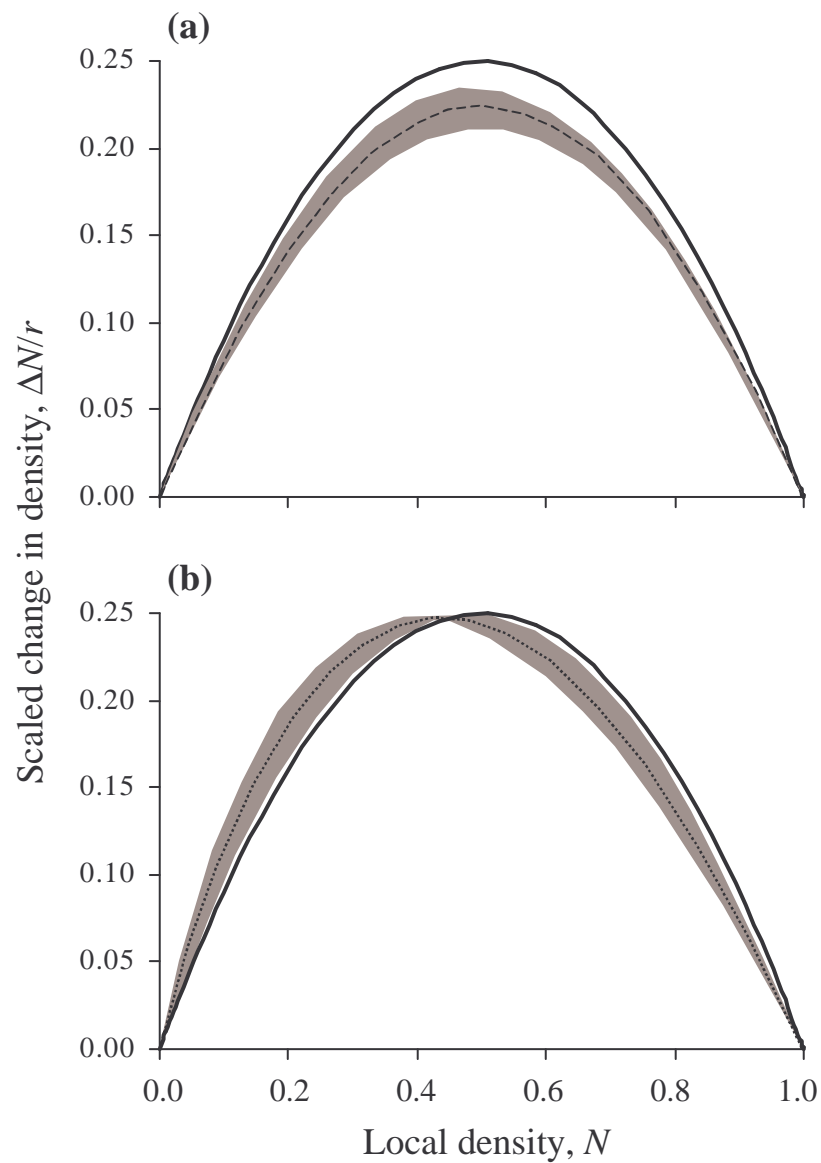


**Figure A3.4** Local growth responses of two sites in a density-dependent population with dispersal. Change in density has been scaled by  $1/r$  to allow comparison across a range of simulations. Results are shown for logistic density-dependence in the absence of dispersal (solid line), and realised responses (broken lines) in a one-dimensional spatial model at (a) introduction site; (b) invaded site. Shaded areas indicate the range of results observed for  $0.03 \leq r \leq 0.3$  and  $0.01 \leq \mu \leq 0.9$ .

range of scenarios tried here, implying that estimates of local increase of an invader at its release site may underestimate by around this order its true potential for population increase.

At the site of invasion, however, dispersal initially boosted local density as the site was first colonised, but later slowed local increase as net immigration became negative (figure A3.3). The overall effect of dispersal on an invaded site was to skew the realised growth curve to the left (figure A3.4(b)).

Overall, the effect of dispersal on local population increase was relatively minor at an invaded site, where it accelerates the initial increase but hinders later population growth. Dispersal has a greater overall effect at the site of introduction, where it proportionally reduces the realised rate of increase at all densities, acting effectively as a density-dependent mortality. These effects may only be measurable in the field when dispersal rate is very high, otherwise they are likely to be concealed by random variation caused by extrinsic factors.

## Appendix 4: Supporting material

### A4.1 Derivation of general host-parasitoid models

General host-parasitoid models (equations 3.1 to 3.3) may be derived by considering four critical processes in the life cycle of the host: density-dependent mortality, parasitoid attack, death of parasitised hosts, and reproduction. Host reproduction must be the last of these processes to occur, since  $N_t$  is defined as the initial density of host larvae in generation  $t$ . Three general models are possible as different orderings of the remaining processes. The proportions of hosts unaffected by density-dependence or parasitism are described by the functions  $g(N)$  and  $f(N,P)$ , respectively. Host *per capita* reproductive rate,  $\lambda$ , is assumed to be independent of density. Subdividing each generation into four steps and using fractional subscripts to denote these, model 1 (equations 3.1) may be derived as:

- |                               |   |                               |
|-------------------------------|---|-------------------------------|
| a) parasitism of host         | $N_{t+1/4} = f(N_t, P_t) \times N_t$        | $P_{t+1/4} = N_t - N_{t+1/4}$ |
| b) death of parasitised hosts |   | $P_{t+1} = P_{t+1/4}$         |
| c) host density-dependence    | $N_{t+3/4} = g(N_{t+1/4}) \times N_{t+1/4}$ |                               |
| d) host reproduction          | $N_{t+1} = N_{t+3/4} \times \lambda$        |                               |

In the first step,  $N_t$  hosts are attacked by  $P_t$  parasitoids, and the fraction escaping parasitism is given by  $f(N_t, P_t)$ . Next, the parasitised hosts are killed to produce the next generation of adult parasitoids,  $P_{t+1}$ . In the third step, the remaining hosts experience density-dependent mortality, the proportion  $g(N_{t+1/4})$  of which survive to reproduce in the final step.

For model 2 (equations 3.2), density-dependence acts before parasitism:

- |                               |  |                                     |
|-------------------------------|--|-------------------------------------|
| a) host density-dependence    | $N_{t+1/4} = g(N_t) \times N_t$                  |                                     |
| b) parasitism of host         | $N_{t+1/2} = f(N_{t+1/4}, P_t) \times N_{t+1/4}$ | $P_{t+1/2} = N_{t+1/4} - N_{t+1/2}$ |
| c) death of parasitised hosts |  | $P_{t+1} = P_{t+1/2}$               |
| d) host reproduction          | $N_{t+1} = N_{t+1/2} \times \lambda$             |                                     |

Finally, in model 3 (equations 3.3) density-dependence acts before parasitised hosts are killed, with the result that parasitised hosts contribute to total host density-dependence and are themselves subject to that mortality:

$$\begin{aligned}
 \text{a) parasitism of host} & \quad N_{t+1/4} = f(N_t, P_t) \times N_t & \quad P_{t+1/4} = N_t - N_{t+1/4} \\
 \text{b) host density-dependence} & \quad N_{t+1/2} = g(N_{t+1/4} + P_{t+1/4}) \times N_{t+1/4} & \quad P_{t+1/2} = g(N_{t+1/4} + P_{t+1/4}) \times P_{t+1/4} \\
 & \quad = g(N_t) \times N_{t+1/4} & \quad = g(N_t) \times P_{t+1/4} \\
 \text{c) death of parasitised hosts} & & \quad P_{t+1} = P_{t+1/2} \\
 \text{d) host reproduction} & \quad N_{t+1} = N_{t+1/2} \times \lambda
 \end{aligned}$$

#### A4.2 Derivation of default host-parasitoid model parameter values

The default model parameter values were chosen to scale the equilibrium host and parasitoid densities for the Nicholson-Bailey model (Nicholson & Bailey 1935) to  $N_{eq} = 1.0$  and  $P_{eq} = 0.5$ . The model is given by equations 3.4 with  $f(N,P) = e^{-aP}$ :

$$\begin{aligned}
 N_{t+1} &= \lambda N_t e^{-aP_t} \\
 P_{t+1} &= N_t (1 - e^{-aP_t})
 \end{aligned} \tag{A4.1}$$

At equilibrium,  $N_{t+1} = N_t = N_{eq}$  and  $P_{t+1} = P_t = P_{eq}$ . Substituting into equations A4.1 gives  $P_{eq} = r/a$  and  $N_{eq} = P_{eq} \times \lambda / (\lambda - 1)$ . To get  $N_{eq} = 2 \times P_{eq}$  requires  $\lambda = 2$ . Since, by definition,  $r = \ln(\lambda)$ , then  $r = \ln(2) = 0.693$ . Finally, to get  $P_{eq} = 0.5$  requires  $a = 2 \ln(2) = 1.386$ .

#### A4.3 Derivation of the proportion of hosts parasitised at equilibrium

At equilibrium, denoted by the subscript  $eq$ , the assumption that each parasitised host gives rise to exactly one searching adult parasitoid in the following generation means that  $Q_{eq} = P_{eq}/N_{eq}$ . Using this, the host equation of model 1 (equations 3.1) at equilibrium may be rewritten

$$N_{eq} = \lambda N_{eq} (1 - Q_{eq}) g(N_{eq} - P_{eq}) \tag{A4.2}$$

and on rearrangement gives equation 3.6. Similarly, the host equations of both models 2 and 3 (equations 3.2 and 3.3) at equilibrium give

$$N_{eq} = \lambda N_{eq} g(N_{eq}) (1 - Q_{eq}) \quad (\text{A4.3})$$

which rearranges to equation 3.7.

#### A4.4 Relationships between parasitism and host suppression at equilibrium

For models 2 and 3, the relationship between the proportion parasitised at equilibrium,  $Q_{eq}$ , and host suppression,  $1-q$ , requires the host density-dependence function,  $g(N)$  to be specified. Remembering that  $\lambda = e^r$ , equation 3.7 may be rewritten as

$$\ln(1 - Q_{eq}) = -r - \ln[g(N_{eq})] \quad (\text{A4.4})$$

by taking natural logarithms of both sides. With Ricker density-dependence, at equilibrium  $g(N_{eq}) = \exp(-rN_{eq}/K) = \exp(-rq)$  where  $q = N_{eq}/K$ . Substituting into equation A4.4 gives

$$\ln(1 - Q_{eq}) = -r + rq \quad (\text{A4.5})$$

which may be rearranged to equation 3.8.

By the same method, equation 3.6 for model 1 may be rewritten

$$\ln(1 - Q_{eq}) = -r - \ln[g(N_{eq} - P_{eq})] \quad (\text{A4.6})$$

and the Ricker function suggests  $g(N_{eq} - P_{eq}) = \exp[-r(N_{eq} - P_{eq})/K] = \exp(-rq + rP_{eq}/K)$ .  $P_{eq}$  may be obtained from the parasitism function evaluated at equilibrium, and noting that this equals  $1 - Q_{eq}$ . For random parasitoid attack (table 3.1),  $f(N_{eq}, P_{eq}) = \exp(-aP_{eq}) = 1 - Q_{eq}$ , therefore  $P_{eq} = -\ln(1 - Q_{eq})/a$ . Now equation A4.6 becomes

$$\ln(1 - Q_{eq}) = -r + rq + \frac{r}{aK} \ln(1 - Q_{eq}) \quad (\text{A4.7})$$

and this rearranges to equation 3.9.

#### A4.5 Host-parasitoid models with Ricker host density-dependence and random parasitoid attack

With random parasitoid attack and Ricker host density-dependence, host-parasitoid model 1 (equations 3.1) becomes

$$N_{t+1} = N_t \exp \left[ r \left( 1 - \frac{N_t e^{-aP_t}}{K} \right) - aP_t \right] \quad P_{t+1} = N_t (1 - e^{-aP_t}) \quad (\text{A4.8})$$

while models 2 and 3 (equations 3.2 and 3.3) become

$$N_{t+1} = N_t \exp \left[ r \left( 1 - \frac{N_t}{K} \right) - aP_t \right] \quad P_{t+1} = N_t \exp \left[ -\frac{rN_t}{K} \right] (1 - e^{-aP_t}) \quad (\text{A4.9})$$

#### A4.6 CV<sup>2</sup> in host-parasitoid metapopulations

Hassell & May (1988) suggested that a host-parasitoid equilibrium should be stable if the squared coefficient of variation of searching parasitoids per host is greater than unity:  $CV^2 > 1$ . For a host-parasitoid metapopulation, the number of parasitoids in each subpopulation must be weighted by the number of hosts. If  $N_x$  and  $P_x$  refer to the number of hosts and parasitoids respectively in subpopulation  $x$ , and sums are over all populations, then the appropriate statistics are given by

$$\begin{aligned} \text{mean} &= \frac{\sum N_x P_x}{\sum N_x} \\ \text{variance} &= \frac{\sum N_x P_x^2}{\sum N_x} - \left( \frac{\sum N_x P_x}{\sum N_x} \right)^2 \\ CV^2 &= \frac{\text{variance}}{(\text{mean})^2} = \frac{\sum N_x \sum N_x P_x^2}{(\sum N_x P_x)^2} - 1 \end{aligned} \quad (\text{A4.10})$$

#### A4.7 Results from fitting models to metapopulation mean dynamics

Below are some representative results obtained by fitting the models of table 3.1 to the mean dynamics of various host-parasitoid metapopulations.

**Table A4.1** Results from fitting models to metapopulation mean dynamics. Parameters as for the ‘homogeneous’ pattern in table 3.3, and 80% global reduction in densities every 100 generations.

Parasitism function			Host density-dependence		
Model	$R^2$	Parameter estimates	Model	$R^2$	Parameter estimates
random	100%	$a = 1.386$	density-ind.	34%	$\lambda = 1.439$
			Ricker	100%	$r = 0.693$ $K = 1.5$
neg. binomial	100%	$k = 10^4$ <sup>†</sup>		as above	
dd. neg. bin.	100%	$w = 10^5$ <sup>†</sup>		as above	
pseudo-int.	100%	$m = 0$ <sup>†</sup>		as above	

<sup>†</sup>model not significantly different from random parasitism

**Table A4.2** Results as for table A4.1, but from the ‘regionally synchronised’ pattern of table 3.3.

Parasitism function			Host density-dependence		
Model	$R^2$	Parameter estimates	Model	$R^2$	Parameter estimates
random	98%	$a = 1.12$	density-ind.	95%	$\lambda = 1.32$
			Ricker	99%	$r = 0.58$ $K = 2.6$
neg. binomial	98%	$k = 18.5$ <sup>†</sup>		as above	
dd. neg. bin.	98%	$w = 183.3$ <sup>†</sup>		as above	
pseudo-int.	98%	$m = 0.069$ <sup>†</sup>		as above	

<sup>†</sup>model not significantly different from random parasitism

**Table A4.3** Results as for table A4.1, but from the ‘large spiral’ pattern of table 3.3.

Parasitism function			Host density-dependence		
Model	$R^2$	Parameter estimates	Model	$R^2$	Parameter estimates
random	73%	$a = 0.69$	density-ind.	96%	$\lambda = 1.56$
			Ricker	96%	$K \rightarrow \infty^\ddagger$
neg. binomial	unsuccessful fit				
dd. neg. bin.	73%	$w = 540.4^\dagger$		as above	
pseudo-int.	68%	$a = 0.59$	density-ind.	96%	$\lambda = 1.58$
		$m = 0.42$	Ricker	96%	$K \rightarrow \infty^\ddagger$

<sup>†</sup>model not significantly different from random parasitism

<sup>‡</sup>model not significantly different from density-independent host increase

**Table A4.4** Results as for table A4.1, but from the ‘spatial chaos’ pattern of table 3.3.

Parasitism function			Host density-dependence		
Model	$R^2$	Parameter estimates	Model	$R^2$	Parameter estimates
random	76%	$a = 0.83$	density-ind.	92%	$\lambda = 1.55$
			Ricker	92%	$K \rightarrow \infty^\ddagger$
neg. binomial	unsuccessful fit				
dd. neg. bin.	76%	$w = 122.9^\dagger$		as above	
pseudo-int.	62%	$a = 0.70$	density-ind.	92%	$\lambda = 1.69$
		$m = 0.52$	Ricker	92%	$K \rightarrow \infty^\ddagger$

<sup>†</sup>model not significantly different from random parasitism

<sup>‡</sup>model not significantly different from density-independent host increase

#### A4.8 Results from fitting models to emergent subpopulation dynamics

Below are some representative results obtained by fitting the models of table 3.1, plus immigration terms, to the dynamics of a subpopulation within a host-parasitoid metapopulation.

**Table A4.5** Results from fitting models to dynamics of a local population within a metapopulation. Parameters as for the 'homogeneous' pattern in table 3.3, and 100% local reduction in densities every 100 generations.

Parasitism function			Host density-dependence			
Model	$R^2$	Parameter estimates	Model	$R^2$	Parameter estimates	
random	99%	$a = 1.393$	density-ind.	99%	$\lambda = 1.53$	
			di. + imm.	99%	$\lambda = 0.72$ $N_{imm} = 0.47$	
			Ricker	92%	$r = 1.09$ $K = 0.95$	
			Ricker + imm.	92%	$r = 0.29$ $K = 0.76$ $N_{imm} = 0.27$	
			density-ind.	93%	$\lambda = 1.53$	
			di. + imm.	93%	$\lambda = 0.52$ $N_{imm} = 0.58$	
random + imm.	99%	$a = 0.73$ $P_{imm} = 0.13$	Ricker	67%	$r = 1.43$ $K = 0.83$	
			Ricker + imm.	unsuccessful fit		
			neg. binomial	unsuccessful fit		
dd. neg. bin.	unsuccessful fit					
pseudo-int.	85%	$a = 0.48$ $m = 0.90$	density-ind.	85%	$\lambda = 1.53$	
			di. + imm.	85%	$\lambda = 0.57$ $N_{imm} = 0.56$	
			Ricker	74%	$r = 1.36$ $K = 0.84$	
			Ricker + imm.	unsuccessful fit		

**Table A4.6** Results as for table A4.5, but from the ‘spatial chaos’ pattern of table 3.3.

Parasitism function			Host density-dependence		
Model	$R^2$	Parameter estimates	Model	$R^2$	Parameter estimates
random	97%	$a = 1.53$	density-ind.	99%	$\lambda = 1.78$
			di. + imm.	99%	$\lambda = 1.72$
					$N_{imm} = 0.09$
			Ricker	100%	$r = 0.76$
					$K = 7.51$
			Ricker + imm.	100%	$r = 0.74$
					$K = 7.94$
					$N_{imm} = 0.02$
random + imm.	96%	$a = 1.48$			as above
		$P_{imm} = 0.01$			
neg. binomial	unsuccessful fit				
dd. neg. bin.	96%	$w = 10^{4\dagger}$			as above
pseudo-int.	98%	$a = 1.03$	density-ind.	96%	$\lambda = 1.77$
		$m = 0.41$	di. + imm.	96%	$\lambda = 1.79$
					$N_{imm} = -0.02$
			Ricker	96%	$K \rightarrow \infty^\ddagger$
			Ricker + imm.	96%	$r = 0.59$
					$K = 144$
					$N_{imm} = -0.02$

<sup>†</sup>model not significantly different from random parasitism

<sup>‡</sup>model not significantly different from density-independent host increase

**Table A4.7** Results as for table A4.5, but from a metapopulation in which local populations experience negative-binomial aggregated parasitism with  $K = 20$ ,  $k = 1.2$ , and all parameters as for table 3.2, which gives local dynamics which are just unstable in the absence of dispersal.

Parasitism function			Host density-dependence		
Model	$R^2$	Parameter estimates	Model	$R^2$	Parameter estimates
random	99%	$a = 1.00$	density-ind.	95%	$\lambda = 1.85$
			di. + imm.	97%	$\lambda = 1.65$
					$N_{imm} = 0.26$
			Ricker	96%	$r = 0.76$
					$K = 8.66$
			Ricker + imm.	unsuccessful fit	
random + imm.	99%	$a = 0.93$	as above		
		$P_{imm} = 0.05$			
neg. binomial	unsuccessful fit				
dd. neg. bin.	100%	$a = 1.11$	density-ind.	96%	$\lambda = 1.89$
			di. + imm.	97%	$\lambda = 1.74$
					$N_{imm} = 0.19$
			Ricker	97%	$r = 0.76$
					$K = 10.1$
			Ricker + imm.	97%	$r = 0.64$
					$K = 17.6$
					$N_{imm} = 0.12$
pseudo-int.	100%	$a = 0.90$	density-ind.	99%	$\lambda = 1.89$
			di. + imm.	100%	$\lambda = 1.80$
					$N_{imm} = 0.11$
			Ricker	100%	$r = 0.71$
					$K = 14.5$
			Ricker + imm.	100%	$r = 0.67$
					$K = 19.9$
					$N_{imm} = 0.05$

#### A4.9 Derivation of *Sitona discoideus* model parameters

The tables below show how several parameters were derived for the *Sitona discoideus*/*Microctonus aethiopoidea* model.

**Table A4.8** Calculation of *S. discoideus* survival parameters  $s_{larv}$ ,  $s_{disp}$ , and  $s_{crop}$ , from Darfield data (three sites, three years). All values, except those for  $Q_{aest}$ , are  $m^{-2}$ .

Autumn		Spring		Aestivation and dispersal			Atypicals in crop		Autumn	
$N_{aut}^1$	$W_{aut}^1$	$N_{spr}^2$	$N_{ten}^3$	$Q_{aest}^1$	$N_{aest}^4$	$N_{imm}^5$	$W_{crop}^6$	$W_{wait}^7$	$W_{Mar}^8$	$N_{next}^1$
12.1	4.4	743.2	174.4	0.207	173.3	9.6	1.1	2.1	3.3	7.6
7.6	4.8	146.8	111.8	0.131	111.3	5.2	0.5	-0.3	0.1	4.5
4.5	1.2	177.7	100.4	0.206	99.8	4.2	0.6	2.3	2.8	3.3
20.2	4.1	1256.6	1096.0	0.252	1087.5	49.6	8.5	-1.7	5.5	37.1
37.1	20.4	602.3	345.8	0.197	343.7	28.3	2.1	-1.3	1.9	22.7
22.7	10.6	507.8	1008.4	0.095	1005.4	20.2	3.0	7.0	8.1	18.3
63.3	10.6	2243.1	1690.6	0.336	1673.2	34.9	17.4	4.9	11.7	23.2
23.2	12.5	446.0	263.0	0.249	261.0	25.3	2.0	-1.9	1.8	19.0
19.0	10.1	406.1	1064.0	0.205	1057.3	10.1	6.7	3.2	4.4	8.0
<i>Sums:</i>		$6529.4^9$	$5854.4^9$		$5812.6^{10}$	$187.3^{10}$	$41.8^{11}$	$14.3^{11}$		

<sup>1</sup>Actual data (S. Goldson, unpublished data).

<sup>2</sup>Calculated from  $N_{aut}$  and  $W_{aut}$  using equation 5.4, itself an empirical fit of earlier Darfield data (Barlow & Goldson 1993). Includes effects of actual droughts and stand age.

<sup>3</sup>Total density of teneral adults emerging in November to January, actual data (S. Goldson, unpublished data).

<sup>4</sup>From equation 5.6, using  $N_{ten}$ ,  $Q_{aest}$ , and  $p_{atyp} = 0.03$  (Goldson *et al.* 1990).

<sup>5</sup>Density of total immigrants, given by  $N_{next}/(1-Q_{aest})$ , a rearrangement of equation 5.9.

<sup>6</sup>From equation 5.7, or  $N_{ten} - N_{aest}$ .

<sup>7</sup>Density of non-immigrant parasitised weevils in March, resulting from atypicals remaining in the crop over summer, given by  $W_{Mar} - p_{early} W_{imm}$ , or  $W_{Mar} - p_{early} (N_{imm} - N_{next})$  from equation 5.9, where  $p_{early} = 0.58$ .

<sup>8</sup>Total density of parasitised weevils in the crop in March, actual data (S. Goldson, unpublished data).

<sup>9</sup>Larval survival,  $s_{larv}$ , estimated from  $\sum N_{ten}/\sum N_{spr} = 0.90$ .

<sup>10</sup>Survival through aestivation and dispersal,  $s_{disp}$ , estimated from  $\sum N_{imm}/\sum N_{aest} = 0.032$ .

<sup>11</sup>Summer increase in parasitised weevils in crop,  $s_{crop}$ , estimated from  $\sum W_{wait}/\sum W_{crop} = 0.34$ , including negative values estimated for  $W_{wait}$ . Excluding these negatives gives  $s_{crop} = 0.47$ , which has little effect on the model results (figures 5.5 and 5.6).

**Table A4.9** Flight trap catches for two Darfield sites, 29 February to 16 May 1988 (S. Goldson, unpublished data).

	Before mid-March	After mid-March
Total <i>S. discoideus</i>	48	75
Proportion of total	39%	61%
Parasitised <i>S. discoideus</i>	23	17
Proportion of total	58%	42%

**Table A4.10** Day-degree calculation results for autumn parasitoids.

	March	April	May
Mean daily maximum <sup>†</sup>	20.6	17.3	13.3
Mean daily minimum <sup>†</sup>	8.7	6.0	3.1
Daily mean <sup>†</sup>	14.7	11.7	8.2
Larval development rate <sup>‡</sup>	5.15	2.83	0.88
Pupal development rate <sup>‡</sup>	6.48	4.03	1.28
Days to develop from instar II to pupa <sup>‡</sup>	14	26	83
Days to develop from pupa to adult <sup>‡</sup>	19	31	98

<sup>†</sup>All in °C. Monthly means for Darfield weather station, 1939 to 1980 (New Zealand Meteorological Service 1981).

<sup>‡</sup>Calculated using day-degree relationships published by Goldson *et al.* (1990). Maximum and minimum temperatures weighted by 0.25, mean weighted by 0.5, as detailed in Barlow and Dixon (1980).

#### A4.10 Derivation of dispersal radius for the *Sitona discoideus* model

Lucerne crops made up 0.3% of total land use for the one area of Canterbury that has been studied in detail (Ian Lynn, unpublished data). Assuming a mean lucerne stand size of 5 ha = 0.05 km<sup>2</sup>, this suggests a lucerne density of 1 stand per 0.05/0.003 = 16.7 km<sup>2</sup> total land area. If lucerne stands are spaced approximately evenly as on a square grid, then the mean distance between stands is  $\sqrt{16.7} \cong 4$  km. In chapter 4, weevil dispersal distance was estimated as approximately 12 km, which suggests  $d_l = 12/4 = 3$  for the metapopulation model of chapter 5.

#### A4.11 Derivation of disease basic reproductive rate, $R_0$

The basic reproductive rate of a disease,  $R_0$ , is the number of new infections created in the lifetime of a single infectious animal introduced into a susceptible population at its carrying capacity. For the SIR model of equations 6.1, it can be seen that the rate of creation of new infections is  $\beta SI$ . Expressed per infectious host, this is simply  $\beta S$ . The expected duration of the infectious state is given by the inverse of the sum of all the outflow rates,  $1/(d+wN+\alpha+\nu)$ . Since hosts are at their carrying capacity,  $N = K$ , so  $d+wN = d+wK = b$ . Now, remembering that  $R_0$  applies to a new infection introduced into a wholly susceptible population,  $S \rightarrow K$ . Including this, and multiplying new infections per host by the duration of infectiousness gives  $R_0 = \beta K/(b+\alpha+\nu)$ , as in equation 6.2.

Derivation of  $R_0$  for the SEI model (equations 6.4) is complicated by the intermediate latent stage. In this case, each infectious host gives rise to new latent infections at a rate  $\beta S$ , but only a proportion of these survive to become infectious. This proportion is given by the rate of maturation to infectiousness divided by the total outflow rate from the latent stage:  $\sigma/(d+wN+\sigma)$ . Therefore, the rate of production of new infectious hosts per infectious host is given by  $\sigma\beta S/(d+wN+\sigma)$ . The expected duration of the infectious state is  $1/(d+wN+\alpha)$  for this model. Using  $N = K$  and  $S \rightarrow K$ , then  $R_0 = \sigma\beta K/(b+\alpha)(b+\sigma)$  as in equation 6.5.

#### A4.12 Derivation of disease intrinsic rate of increase, $r_d$

The intrinsic rate of increase of a disease,  $r_d$ , is derived as  $(dI/dt)/I$ , when  $I \rightarrow 0$  and  $S \rightarrow K$ . For the SIR model (equations 6.1),  $(dI/dt)/I = \beta S - (d+wN+\alpha+\nu)$ . If  $N = K$ , then  $d+wN = b$ . Now, with  $S \rightarrow K$ ,  $r_d = \beta K - (b+\alpha+\nu)$ .

The latent stage in the SEI model (equations 6.4) adds considerable difficulties to the derivation of  $r_d$  in this case. The main steps are laid out below; further details are presented in a forthcoming publication (N.D. Barlow, in preparation). First, the relevant parts of the model are rewritten when  $N = K$  and  $S \rightarrow K$ :

$$\begin{aligned}\frac{dE}{dt} &= \beta KI - (b + \sigma)E \\ \frac{dI}{dt} &= \sigma E - (b + \alpha)I\end{aligned}\tag{A4.11}$$

This is then expressed as a second-order differential equation in terms of  $I$ ,

$$\frac{d^2I}{dt^2} + \frac{dI}{dt} [2b + \alpha + \sigma] + I[(b + \alpha)(b + \sigma) - \sigma\beta K] = 0\tag{A4.12}$$

which has solutions of the form  $I(t) = c \times \exp(r_d \times t)$  where  $c$  is a constant. Solving equation A4.12 gives the positive root

$$r_d = \frac{2b + \alpha + \sigma}{2} \left[ \sqrt{1 + \frac{4(\sigma\beta K - (b + \alpha)(b + \sigma))}{(2b + \alpha + \sigma)^2}} - 1 \right]\tag{A4.13}$$

Finally, performing a Taylor series expansion on the square root term in equation A4.13, and discarding terms of order 2 and above, the approximation of equation 6.6 is arrived at.